

TIME-RESOLVED MEASUREMENT OF INSULIN SECRETION FROM SINGLE
PANCREATIC BETA-CELLS

BY

LAN HUANG

A DISSERTATION PRESENTED TO THE GRADUATE SCHOOL
OF THE UNIVERSITY OF FLORIDA IN PARTIAL FULFILLMENT
OF THE REQUIREMENTS FOR THE DEGREE OF
DOCTOR OF PHILOSOPHY

UNIVERSITY OF FLORIDA

1995

UNIVERSITY OF FLORIDA LIBRARIES

To my wonderful parents, my lovely daughter and my dear husband

ACKNOWLEDGMENTS

I would like to sincerely thank my advisor, Dr. Robert T. Kennedy for his support, help and guidance during my stay at the University of Florida. I would like to thank all the members of the Kennedy group, past and present, for their help during my time spent at the University of Florida.

I would like to thank my wonderful parents for their constant selfless support, encouragement and love during all these years.

Finally, I would like to thank my dear husband for his love, support, thoughtfulness and encouragement.

TABLE OF CONTENTS

	<u>pages</u>
ACKNOWLEDGMENTS.....	iii
ABSTRACT.....	vi
CHAPTERS	
1 INTRODUCTION.....	1
Secretion of Neurotransmitters and Hormones.....	1
Pancreatic Islets.....	3
Insulin.....	4
Insulin Biosynthesis	7
Control of Insulin Secretion.....	10
Measurements of Insulin Secretion from β -cells.....	14
Electrochemistry at Microelectrodes.....	17
2 ELECTRODE DEVELOPMENT AND CHARACTERIZATION..	27
Introduction.....	27
Experimental.....	31
Results and Discussion.....	37
3 DETECTION OF INSULIN SECRETION AT SINGLE β -CELLS..	52
Introduction.....	52
Experimental.....	54
Results and Discussion.....	65
4 COMPARISON OF 5-HYDROXYTRAPTAMINE AND INSULIN SECRETION.....	96
Introduction.....	96
Experimental.....	98
Results and Discussion.....	100

5	EFFECTS OF EXTRACELLULAR pH ON INSULIN SECRETION.....	126
	Introduction.....	126
	Experimental.....	129
	Results and Discussion.....	130
6	CONCLUSIONS AND FUTURE WORK.....	151
APPENDIX		
	SPECIAL CARES DURING RAT ISLET ISOLATION AND CELL DISPERSION.....	156
	REFERENCES.....	158
	BIOGRAPHIC SKETCH.....	167

Abstract of Dissertation Presented to the Graduate School
of the University of Florida in Partial Fulfillment of the
Requirements for the Degree of Doctor of Philosophy

TIME-RESOLVED MEASUREMENT OF INSULIN SECRETION FROM
SINGLE PANCREATIC BETA-CELLS

By

Lan Huang

December 1995

Chairman: Robert T. Kennedy
Major Department: Chemistry

An amperometric method for measuring insulin secretion from individual pancreatic beta-cells (β -cells) was developed and tested. The electrode used was a carbon-fiber microelectrode modified with a composite of ruthenium oxide/cyanoruthenate film. The chemically modified electrode allowed anodic detection of insulin under physiological conditions with a detection limit of 0.5 μ M. When the electrode was positioned 1 μ m away from a β -cell stimulated with insulin secretagogues glucose, K^+ , or tolbutamide, a series of randomly occurring current spikes were measured. Chromatography and flow injection analysis showed that the primary secreted substance detected by the electrode was insulin. It was concluded that spikes were due to detection of concentration pulses of insulin secreted by exocytosis.

Because of instability of the modified electrode, secretion of a substance co-secreted with insulin was investigated for studying insulin secretion. Bare carbon microelectrodes which do not detect insulin, were used to monitor chemical secretions from single β -cells loaded with 5-hydroxytryptamine (5-HT). When glucose or tolbutamide were applied to loaded β -cells, a series of current spikes were observed. The pattern of 5-HT release from loaded cells was similar to that of insulin secretion from unloaded cells. However, the shapes of insulin and 5-HT current spikes were different, suggesting different mechanisms of their clearance from the vesicles. Although 5-HT is a good marker of secretory activity of β -cells, it is not a useful substitute for studying the dynamics of insulin clearance from vesicles.

The effects of extracellular pH on release of insulin from β -cells was investigated. Insulin is stored in a solid granule as a complex with Zn in secretory vesicles of pancreatic β -cells. The modified electrodes do not detect insulin in the presence of excess Zn^{2+} , suggesting that they only detect free insulin uncomplexed with Zn^{2+} . Insulin secretion was detected as a series of current spikes at extracellular pH 7.4, but not at pH 6.4. The release of 5-HT was detected regardless of pH, indicating that vesicle fusion and opening occurs at both pH's. Therefore, it was concluded that extracellular pH is required by rapid release of insulin during exocytosis. This conclusion was also supported by the results obtained from Ca^{2+} -induced secretion at digitonin-permeabilized β -cells.

CHAPTER 1 INTRODUCTION

Secretion of neurotransmitters and hormones

Secretion of neurotransmitters and hormones is a complex process that is central to many important biological functions, including memory, learning, growth and metabolism. Peptides represent acting as neurotransmitters and hormones a major class of biochemical messengers. Defects in the regulation of secreted peptides are implicated in many diseases including Alzheimer's and diabetes mellitus. A better understanding of these processes and diseases is critically dependent on understanding the regulation and function of the peptides involved. Regulation of a peptide messenger can encompass control of its synthesis, degradation, mass transport and secretion. These processes are dynamic, therefore time-resolved measurements of the peptides are critical. In addition, the rapid determination of peptides may be useful in clinical settings or for monitoring biotechnological production of proteins and peptides. In spite of the potential utility of sensors for peptides, little work has been done on their development. This probably stems from the difficulty involved. Peptide messengers are especially difficult to monitor because they tend to be potent in their actions and therefore present in trace concentrations at their site of action (1).

Among many types of neurotransmitters and hormones secretion, one of the most significant systems is secretion of insulin from β -cells of the pancreas. β -cells synthesize

insulin and store it in vesicles of approximately 350 nm diameter (2). Insulin is secreted from β -cells in response to elevated glucose levels. Secreted insulin enters the blood stream and induces glucose consumption in target cells. In this way, the body maintains glucose concentration in a narrow range.

The physiological deficiency of insulin action impairs the body's ability to transport glucose into the cells. As a result, glucose accumulates in the blood, leading to diabetes. Diabetes mellitus is characterized by the inability to secrete or utilize insulin in response to elevated glucose. Uncontrolled, diabetes can have devastating consequences on the eyes, kidneys and blood vessels, and it severely reduces life expectancy. Type I and type II diabetes are the major groups in the clinical cases (over 90%) (3). Type I diabetes, frequently called juvenile diabetes, is caused by autoimmune destruction of the β -cells of the pancreatic islets, which results in deficiency and finally total loss of insulin secretion. This type of diabetes is also called insulin-dependent diabetes. Type II diabetes, called adult onset diabetes, is associated with impaired β -cell function due to inefficient peripheral tissue glucose utilization and impaired basal and stimulated insulin secretion. This type of diabetes is also called insulin-independent diabetes. It has been suggested that the fundamental cause of these two types of diabetes is impairment of insulin secretion by the pancreatic β -cells (3,4).

Therefore, it is of medical interest to gain a great understanding of insulin secretion. However, many of the steps that are involved in insulin secretion are not understood at the chemical level (5-7). The ability to measure insulin secretion with temporal resolution is important in the study of insulin secretion mechanisms and

ultimately in developing a greater understanding of diabetes. The overall objective of this research is to develop a new method to detect insulin secretion at single cell level with high temporal and spatial resolution.

Pancreatic Islets

Insulin is synthesized and stored in pancreatic β -cells, which are localized in pancreatic islets (1,2). Pancreatic islets or the islets of Langerhans are clusters of endocrine cells scattered throughout the exocrine pancreas in all vertebrates higher in evolution than teleosts (bony fish). In adult mammals, islets make up 1-4% of the pancreas in volume. There are 800,000-1,200,000 islets found in human pancreas and 2,000-3,000 in most lab rodents (8, 9). Islets range in size from a clump of only a few cells less than 40 μm in diameter to oblate spheroids 400 μm in diameter composed of about 3,000 cells (10).

Each islet is a complex microorgan composed of several endocrine cell types, nerves, and blood vessels. Approximately 70-80% of the cells within an islet are β -cells (2, 11). There are three other primary types of cells which secrete hormones that regulate insulin secretion. The endocrine cells are arranged in a nonrandom distribution with the insulin-producing β -cells forming a central core surrounded by a discontinuous mantle of the non- β -cells (glucagon-producing α -cells, somatostatin-producing δ -cells, and pancreatic polypeptide-producing PP-cells) as shown in Figure 1-1 (12-14). The endocrine cell types found in the islets are listed in Table 1-1 with their frequency and hormone content (15). The cell types are best distinguished either ultrastructurally or immunocytochemically. Within the pancreas there is a regional heterogeneity of the

islets based on the presence of either α - or PP-cells (16). The regional distribution of either glucagon-rich islets or pancreatic polypeptide-rich islets is based on the embryological development of the pancreas. The frequency of a cell type varies with species to some extent. Usually, the population of β -cells varies with species in the range of 70% (rats) to 90% (ob/ob mice) of total number of cells in islets (2, 15). However, the frequency of other cell types changes more with age than species.

Table 1-1. Endocrine Cells Found in Islets of Langerhans

Cell type	Average relative abundance(%)	Hormonal content	Cells more abundant in	
			Islet	Pancreatic region
β (or B)	~70	Insulin	Center	ND
α (or A)	~24	Glucagon	Periphery	Dorsal
PP	~2	Pancreatic polypeptide	ND	Ventral
δ (or D)	~4	Somatostatin	Periphery	ND

ND = no difference.

Insulin

In order to find a way to detect insulin, it is important to know the structure and properties of insulin. All known insulins contain two dissimilar peptide chains, A and B. The shorter chain, called the A chain, is composed of 21 amino acids. The second chain, or B chain, consists of 29-31 amino acids dependent on the species, with 30 being the most common number (17). The chains are held together by two disulfide bonds, which connect positions A-7 to B-7 and A-20 to B-19 (shown for human insulin in Figure 1-2). The A-chain, which becomes more acidic than the B-chain after oxidative cleavage of -S-S- bonds, also has an internal disulfide bond bridging position A-6 to A-11 that forms a six-amino-acid loop. In mammalian insulins, all three disulfide bonds are invariant, suggesting that secondary and tertiary structure of this acidic (isoelectric point is

approximately pH 5.3), globular protein has been strictly conserved during evolution. Human insulin has a molecular weight of 5734 Da, and most other mammalian insulin species are similar-sized molecules (17, 18).

The differences in structural features of the insulins involved in this work are represented in Table 1-2. All residues are the same as those for human insulin except those indicated (18). It is interesting to note that the rat is the only mammal known to produce 2 forms of insulin, differing from each other at position 29 on the B-chain; this is not uncommon to lower vertebrates such as fishes, however. It is also interesting to note that the variations of amino acids in other species are mostly located in or near the region known as the A loop, A8, A9, and A10, in the 3-D structure of the molecule.

Table 1-2. Variants in Insulin Structure

Species	A4	A8	A9	A10	B3	B9	B29	B30
Human	Glu	Thr	Ser	Ilu	Asn	Ser	Lys	Thr
Bovine	-	Ala	-	Val	-	-	-	Ala
Rat1	Asp	-	-	-	Lys	Pro	-	Ser
Rat2	Asp	-	-	-	Lys	-	Met	Ser
Dog	-	-	-	-	-	-	-	Ala

As mentioned above, the insulins used in this work are human, rat, dog and bovine. The bovine insulin was used as a standard analyte for testing our insulin sensor. Standard rat I and rat II insulin were used for chromatographic analysis of islet releasates. Finally, insulin secretions from human, rat and dog β -cells were detected.

Insulin is probably a monomeric protein under physiologic conditions and concentrations (15, 19). However, at higher concentrations (such as found in cellular storage granules), insulin tends to self-associate. Important variables for self-association

of mammalian insulins include pH, ionic strength, and zinc concentration (15, 20-23). Low ionic strength has been found to lessen the degree of association either in acidic or alkaline situations (22, 23), increased ionic strength favors aggregation of molecules (21). When conditions favor self-association, dimers readily form by hydrophobic bonding between the side chains of two monomers and hydrogen bonding between B-24 and B-26 on two adjacent insulin monomers (24). The dimerization is inhibited when the solvents have low dielectric constants, which destabilize the hydrophobic interactions between the two monomers (25). Two dimers can associate to form tetramers. One dimer and one tetramer can further aggregate side by side to form a hexamer. The reported values for the dimerization constant ($K_D = [I_D]/[I_M]^2$; I_D and I_M are insulin dimer and monomer, respectively) are in the range of 10^4 - 10^6 M^{-1} ; values for the association constant for formation of the tetramer from two dimers in the absence of zinc are in the range of 20-100 M^{-1} ; values for association constants of formation of the hexamer from the dimer and the tetramer in the absence of zinc are in the range of 200-1000 M^{-1} (25-29). Recently capillary electrophoresis was used to measure insulin self-association constants (30). It was found that the dimerization constant of insulin at pH 8.4 ($6 (\pm 1) \times 10^3$ M^{-1}) is larger than that at pH 10.0 ($4.7 (\pm 0.5) \times 10^2$ M^{-1}), which indicates that the aggregation of insulin molecules decreases as the pH increases. Formation of the tetramer and hexamer of insulin (but not dimer) is enhanced in the presence of zinc (21). Insulin binds zinc to form Zn-insulin hexamer at the level of zinc as low as 0.35% in the range of pH 4.5 to pH 8.0. Zinc is not bound to insulin at all below the pH range 3.5-4.5. Dissociation increases with increasing pH above 8.0 even in the presence of high level zinc (21). Two

zinc molecules binding at the centrally located B-10 histidines of six porcine insulins formed the classic unit crystal used for X-ray crystallography (31). However, zinc-insulin hexamers do not form with some insulins, which have amino acids other than histidine at the B-10 position (15). Formation of two-zinc insulin hexamer is important for cellular storage of large amounts of insulin, and such zinc-insulin complexes stabilize the newly synthesized hormone. Electron microscopy confirms such an arrangement since secretory granules have an electron-dense core of condensed insulin with a crystallographic structure which is consistent with a hexameric form of a Zn-insulin complex (32-34). Crystalline insulin usually contains 0.5% zinc and is relatively insoluble in the pH range of 4.0-7.0 (35).

Insulin Biosynthesis

Insulin is produced in quantity only in pancreatic β -cells. Insulin biosynthesis is the important step before insulin secretion. Most of the chemicals which are co-stored and co-secrete with insulin are produced during insulin biosynthesis process. Therefore, the information about insulin biosynthesis will help to understand the localization of produced insulin and the complicated microenvironment around it in β -cells.

Briefly, the steps of insulin biosynthesis are illustrated in Figure 1-3 (35-37). First, insulin is synthesized in the form of preproinsulin (molecular weight-approximately 13,000) in the rough endoplasmic reticulum (RER). The signal portion of this molecule is quickly deleted, leaving a molecule of proinsulin. Second, proinsulin is transferred to the cisternae of the RER and transported to the periphery of the Golgi complex via smooth microvesicles. The transport to the Golgi apparatus takes about 10 min. Between

10 and 20 min after synthesis the proteins are found in the Golgi region. The condensing vacuoles of the Golgi complex are then transformed to immature, clathrin-coated secretory vesicles, where the new proteins begin to accumulate after 40 min. The maturation of the secretory vesicles with the loss of their clathrin coat coincides with the proteolytic cleavage of connecting peptide (C-peptide) from the proinsulin yielding a molecule of insulin. The mature secretory granules store insulin and eventually insulin molecules along with other molecules stored in secretory granules are discharged into the blood stream by exocytosis (35). There are several steps involved in exocytosis: 1) adhesion of vesicle to the interior of the cell membrane; 2) fusion of vesicle with the cell membrane; 3) expanding of initial fusion point; and 4) extrusion of the granular contents. This process has been viewed by electron microscopy (2). The remarkable aspect of the membrane fusion is that it allows insulin to be secreted while maintaining the continuity of the β -cell membrane at all times.

As depicted in Figure 1-3, there are at least two different types of secretory granule. The majority have a dense core surrounded by a pale or clear halo and the minority are clathrin-coated, lack a dense core, and are found near the trans Golgi. The former granules are sites of storage of condensed insulin. The latter are sites for all or most of proinsulin-to-insulin conversion. During or after conversion, coated granules eventually lose their coat and become the more acidic, dense-cored secretory granules with intravascular pH around 5.5 to 6 (38, 39). Then the non-coated, mature granules undergoes exocytosis.

As described above, proinsulin, insulin, and C-peptide are major components stored in secretory granules, totaling about 95 % of whole granular components. They are contained in the approximate molar ratios of 2-5% proinsulin to 95-98% insulin or connecting peptide (15). Proinsulin is a biosynthetic precursor of insulin (shown for human proinsulin structure in Figure 1-4). Proinsulin, a 9,000 Dalton single peptide (40), includes the entire insulin dipeptide plus a C-peptide, which usually is linked by -arg-arg- to the COOH-terminus of insulin's B-chain and by lys-arg- to the NH₂-terminus of A-chain. Proinsulin fulfills a clear biosynthetic need for the correct formation of the disulfide bonds within the insulin molecule, which is accomplished by the folding of the single chain polypeptide. C-peptide assures the correct folding of the parts of the molecule with proper positioning of the disulfide bonds. The sequence of the C-peptide varies to a great extent between different species, differing at up to 50% of the residues (18). There is also a variation in length from 26-31 residues. Despite these considerable structural differences, the C-peptides exhibit some homology which might be important for their function to facilitate the formation of the native structure of insulin. In all C-peptides studied to this point there are no aromatic, histidine or cysteine residues. At either end of the connecting peptide are regions with a high proportion of polar residues and in the center of the peptides high concentrations of glycine residues surrounded by residues which are largely nonpolar (41).

Besides these three major components, i.e. insulin, proinsulin and C-peptide, there are some other components co-stored in the granules, such as adenine nucleotides (ATP, ADP, AMP, and C-AMP) (42, 43), zinc, calcium, inorganic phosphate, enzymes

(including proinsulin converting enzymes, Ca^{2+} and Mg^{2+} dependent ATPase, acid phosphatase and protein kinase) (44-46), and some peptides ranging in size from 5-60 kD (47, 48). All these substances are co-secreted with insulin by exocytosis when β -cells respond to elevated level of glucose. Overall, insulin and C-peptide are the most abundant substances stored in the secretory granule. Therefore, it is obvious that insulin and C-peptide are the primary secreted chemicals from β -cells.

Control of Insulin Secretion

Insulin secretion from β -cells is induced by insulin secretagogues. Besides glucose, there are other kinds of chemicals, such as amino acids, potassium, and sulfonylureas, which also cause insulin secretion by exocytosis. In this work, glucose, potassium and tolbutamide were used as stimuli for the study of insulin secretion from single β -cells.

Among all these secretagogues, glucose is the most important. There are three reasons. First, insulin is the major regulation of carbohydrate metabolism. Second, physiological levels of glucose stimulate insulin release through most of insulin physiologic range. Finally, since glucose plays a central role in β -cell metabolism, glucose can influence the insulin responses to other secretagogues and to subsequent stimulation (15).

The whole process of insulin secretion induced by glucose is very complex. The main steps involved in glucose-stimulated insulin secretion are illustrated in Figure 1-5. The overview of the whole secretion process is described as follows. When blood glucose levels are high, glucose is transported through a glucose transporter to the interior

of the cell and metabolized. Increasing glucose metabolism changes the levels of metabolic products such as ATP, ADP, and pyridine nucleotides. It has been suggested that one of its metabolites, ATP, closes the ATP-regulated K^+ channel, reduces β -cell K^+ permeability and leads to depolarization of the cell, which allows extracellular Ca^{2+} to enter the cell through voltage-dependent Ca^{2+} channels. Increasing intracellular Ca^{2+} triggers exocytosis and results in insulin release (49). The details involved in each step are discussed below.

Glucose regulates insulin secretion by controlling the membrane potential of β -cells (50). The membrane potential of β -cells is controlled by ion concentration gradients across the membrane, which changes with the ion efflux or influx through the ion channels located at the cell membrane. Ion channels are macromolecular pores that transverse cellular membranes. There are many ion channels that produce and transduce electrical signals within excitable cells such as nerve, muscle, and pancreatic β -cells (5). In β -cells, the resting membrane potential is approximately -70 mV. Membrane potential is maintained by the selective permeability of the plasma membrane to K^+ and is regulated by conductance through K^+ channels. Two types of K^+ channels, the ATP-sensitive K^+ channels and the Ca^{2+} -activated K^+ channel, are considered to be primary regulators of membrane potential in β -cells (5, 51). In addition, the ATP-sensitive K^+ channel appears to be the primary target for both glucose and the sulfonylureas during stimulation for insulin secretion (52).

At low glucose level, ATP-sensitive K^+ channels are open and allow positively charged K^+ ions to leave the cell and thus hold the membrane at resting potential. At high

glucose level, increasing ATP level causes the ATP-sensitive K^+ channels to close, the efflux of positive K^+ ions is reduced, and the membrane potential becomes less negative (i.e. depolarizes, typically -30 to -50 mV) and reaches a threshold at which voltage-gated Ca^{2+} channels are activated. As the membrane potential shifts from -50 mV to +50 mV, more Ca^{2+} -channels are activated. The voltage-dependent Ca^{2+} channels open transiently when the cells are depolarized, allowing Ca^{2+} to enter the cell along the electrochemical gradient. In β -cells, normally the cytosolic free- Ca^{2+} level ($[Ca^{2+}]_i$) is finely regulated at ~ 100 nM despite the 10,000-fold higher concentration of Ca^{2+} present outside the cell. Therefore, small changes in membrane permeability to Ca^{2+} can produce a large increase in $[Ca^{2+}]_i$, which is a key regulator of insulin secretion. Increasing the cytosolic free Ca^{2+} level triggers insulin secretion by exocytosis (5, 53).

It is now clear that $[Ca^{2+}]_i$ is the primary intracellular signal that transmits the secretory signal into the biochemical events of exocytosis (53). However, the mode of action of Ca^{2+} on the secretory mechanism is unknown, although it is likely to involve the direct interaction of Ca^{2+} with functional components of the release mechanism. In addition, Ca^{2+} may also regulate the activity of protein kinases enzymes in the β -cells. While Ca^{2+} may interact directly with certain protein kinases enzymes, the activation of most protein kinases by Ca^{2+} involves the Ca^{2+} -binding protein calmodulin. Calmodulin is present in the β -cells and a Ca^{2+} -calmodulin complex is formed in the presence of Ca^{2+} , which activates the protein kinase. Thus the degree of phosphorylation of protein components of the secretory machinery, regulated by the intracellular concentrations of Ca^{2+} , may control the activity of secretory process (54).

Adenosine-3',5'-cyclic monophosphate (cAMP) has also been considered to play a role in glucose-stimulated insulin secretion (55, 56). It has been determined that cAMP level increases during glucose stimulation, but inhibition of adenylate cyclase or cAMP-dependent protein kinase does not affect insulin secretion in a consistent manner (55). However, addition of agents, such as forskolin (a direct activator of adenylate cyclase), which raises cytosolic cAMP concentration greatly, enhances electrical activity of β -cells and insulin secretion induced by glucose or other secretagogues (56, 57). It is suggested that cAMP acts in insulin secretory sequences by: 1) tightly linking Ca^{2+} entry to the process of insulin granule exocytosis, which may be accomplished by either modulating the permeability of Ca^{2+} -channels and facilitating Ca^{2+} influx in β -cells or causing an intracellular redistribution of Ca^{2+} to favor the cytosolic accumulation of Ca^{2+} ; 2) tightening the link between glucose metabolism and depolarization (55,56).

In general, Ca^{2+} and cAMP both play an important role in stimulus-secretion coupling. Ca^{2+} appears to be the primary signal responsible for activating secretory process and cAMP appears to modulate the size of the secretory response (54).

Tolbutamide, a sulfonylurea, is used as an antidiabetic drug (52). This drug, in micromolar range, can directly inhibit the electrical activity of ATP-sensitive K^+ channels and K^+ efflux through these channels. Similar to glucose-stimulated insulin secretion, inactivation of the ATP-sensitive K^+ channel results in an increase in the resting membrane potential, cell depolarization, and influx of extracellular Ca^{2+} through the voltage-dependent Ca^{2+} channel. The rise in intracellular free Ca^{2+} level triggers exocytosis. Although tolbutamide and glucose both inhibit the ATP-sensitive K^+

channel, they act at different sites. Tolbutamide elicits its effects directly by binding with the sulfonylurea receptor located on the outer surface of the plasma membrane associated with ATP-K⁺ channel as shown in Figure 1-5. In contrast, the glucose metabolite ATP acts on the cytoplasmic surface of the membrane.

In addition to glucose and tolbutamide, potassium can also be used as a stimulus for insulin secretion. When a β -cell is at resting potential, the intracellular concentration of potassium is 140 mM, while extracellular concentration is 5 mM (5). Increasing the extracellular potassium concentration to 60 mM alters cell membrane potential, inhibits the efflux of potassium and causes cell depolarized directly, which induces Ca²⁺ influx and triggers exocytosis.

Measurements of Insulin Secretion from β -cells

Spatial and temporal resolution are both important in measuring secretion. Measurement of concentration pulses resulting from exocytosis requires the detection of around 10⁶ molecules in the vicinity of a single cell with millisecond time resolution. The temporal pattern of hormone release is important in evaluating dynamics of the process, therefore high time resolution is desired. Spatial resolution sufficient to monitor secretion from single cells, cell clusters, and whole pancreas may also be useful. Measurements from single, isolated cells may be especially advantageous in determining how β -cells interact with each other and how the behavior of individual cells add together to generate observed in vivo insulin patterns (57, 58).

Available methods for measuring insulin secretion have limited temporal and spatial resolution. In the past, insulin secretion has been measured from populations of

pancreatic islet β -cells by whole pancreas perfusion or isolated islet perfusion. Recently, Insulin secretion from cell clusters and whole plate single cells has been measured using a reversed hemolytic plaque assay (57,58). This immunological technique requires a development procedure and is not suitable for dynamic measurements. Dynamic measurements are usually performed by holding the tissue of interest in a flow system and collecting fractions. The amount of insulin in the fractions is determined by radioimmunoassay. Insulin secretion from as few as 150,000 β -cells has been evaluated with 30 s time resolution using this technique (59). Other techniques include monitoring release in extracellular space of a fluorescence dye (e.g. quinacrine) previously loaded into vesicles (60), and monitoring incorporation of vesicle membrane into the plasma membrane by the tracking of membrane capacitance changes (the smallest measurable steps in capacitance are 1.0-1.5 fF, which roughly corresponds to that expected from the fusion of a granule with 200 nm in diameter) after depolarization of the β -cells induced by insulin secretagogues (61, 62). The capacitance measurement technique monitors stimulus-induced vesicle fusion without detecting any chemicals secreted from cells.

As stated above, the majority of studies on cells have been performed on populations of cells because of experimental limitations. However, techniques are now available which allow for analysis at the level of the single cell. For example, microcolumn liquid chromatography and capillary zone electrophoresis provide a means to precisely sample the contents of individual cells (63-67). Capillary chromatographic resolution is high and injection volumes required are only a few nanoliters, which makes this technique suitable for single-cell analysis. However, these methods lack sufficient

time resolution to monitor a dynamic event such as exocytosis (67). More recently, optical microscopy with native fluorescence detection was used to image neurotransmitter at single cell level (68). The temporal resolution of this detection system (CCD) is suggested to be 50 ms and the spatial resolution is diffraction limited. This technique may have a potential for monitoring release of neurotransmitter from single cells, however, it is limited to use for secreted substances with native fluorescence.

As mentioned before, the objective of this research is to develop a method for the time-resolved measurement of insulin secreted from single, living β -cells. The approach is to use a microvoltammetric electrode as a sensor. Sensors of this type have been widely used for in vivo measurements of easily oxidized neurotransmitters (69-71). More recently, several groups have begun to study the possible utility of electrochemical sensors for probing the chemical environment within and around single cells (72-80). Amperometry at carbon fiber microelectrodes has proven useful for these types of measurements (75-80). Carbon fiber microelectrodes enable measurements of very small amounts of biologically important compounds. This type of electrode has been used extensively for the detection of easily oxidizable compounds such as catecholamines and 5-hydroxytryptamine (5-HT), which serve as chemical messengers in biological systems. Amperometry was first applied to observation of exocytosis by detecting catecholamine release from single adrenal chromaffin cells (75, 76). The time resolution of the method was limited only by diffusion of released catecholamine from cell to electrode. The millisecond time resolution allowed the observation that catecholamine concentration fluctuated rapidly near the cell following stimulation of secretion. The secretion was

observed in the form of a rapid succession of current spikes of variable amplitude which have a duration of a few milliseconds (76). In the meanwhile, the use of cyclic voltammetry has established that catecholamines are only electroactive substances secreted from individual cultured adrenal chromaffin cells when stimulated under a variety of conditions (76, 82). However, much greater time resolution can be obtained with the electrode in the amperometric mode. The current spikes obtained by amperometry were demonstrated to be the consequence of exocytosis of individual vesicles, thus the method provide a powerful new tool for the study of stimulus-secretion coupling in those cells (82). Since then, amperometry has been successfully applied to measurement of secretion from PC-12 cells (72-74, 80), mast cells (79), neurons (83), and melanotrophs (84).

These results demonstrate that amperometry can be very useful in the study of exocytosis of easily oxidized substances. Unfortunately, many substances, including insulin, are oxidized so slowly at common electrode materials that they are not detectable. To apply amperometry to detection of substances with slow oxidation kinetics requires an electrode that can catalyze oxidations better than the carbon fiber microelectrode. Chemical modification of electrodes has proven to be a powerful approach to enhancing the catalytic activity of the electrode surface and for facilitation of electrochemical detection (85, 86).

Electrochemistry at Microelectrodes

Microvoltammetric electrodes are suitable for measurement secretion at single cells due to its unique size. Besides that, the currents at these electrodes are extremely

small, the electrodes can be used in solutions of very high resistance, and experiments can be performed in two-electrode system (87).

In principal, experiments using microelectrodes are similar to those using conventional electrodes. A stationary working electrode immersed in an unstirred electrolytic solution is given either a constant potential or one that changes linearly over time. Provided there is an electroactive substance, that is, one that can undergo oxidation or reduction, in the electrolytic solution, a heterogeneous charge transfer will occur at the solid/liquid interface, during which, electrons will be transferred. At the same time, the concentrations at the electrode surface start to change, which sets off diffusive mass transport to and from the electrode. In the situation of microelectrode, the diffusion process becomes dependent on the size and geometry of the electrode (87). Electroactive species transport to the microelectrode surface through linear (perpendicular) and radial diffusion (87, 88). In this work, three electrochemical methods have been used: they are cyclic voltammetry, chronoamperometry and amperometry.

In cyclic voltammetry, the potential changes linearly over time. Starting from an initial potential E_p , a linear potential sweep (potential ramp) is applied to the electrode. After reaching a switching potential E_s , the sweep is reversed and the potential returns linearly to its initial value (87). The experimental time scale is determined by the potential scan rate $v = \Delta E / \Delta t$. The resulting current from the redox processes is plotted as a function of potential. Initially the cyclic voltammograms at "high" v values (e.g. 10 V s^{-1} or higher) are peak-shaped. As electrolysis of the compound decreases its concentration at the electrode surface, the current returns toward the baseline after

reaching a maximum. This occurs because the electrolysis rate greatly exceeds the rate at which the species can diffuse to the electrode surface. At these rapid time scales, the majority of the diffusion is perpendicular to the electrode surface. As v declines, the voltammogram becomes sigmoid-shaped. The steady-state current arises because the electrolysis rate is approximately equal to the rate of diffusion of molecules to the electrode surface. At the slower scan rate, radial diffusion to the edges of the surface of the disk-shaped electrode as well as diffusion perpendicular to the surface becomes important. The resulting voltammogram is related to the chemical identity of the redox species (position and shape of the current wave on the potential axis) and on its concentration (magnitude of the current at a given potential) (88).

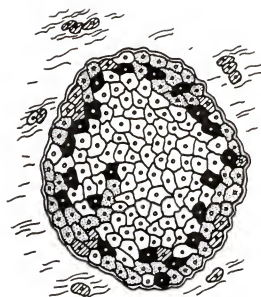
In chronoamperometry (89), the potential is initially held at a sufficiently low level where no oxidation occurs. A short square pulse is applied for between 100 ms to couple of seconds to a value beyond the peak potential for the particular substrate of interest and the current is sampled close to the end of the pulse where the ratio of faradaic to charging current is large. For disk microelectrode, the steady-state current $i_{ss} = 4r_0 n F D C^*$, where r_0 (cm) is the radius of the electrode, n is the number of electron transferred, F (C/equiv) is Faraday constant, D (cm^2/s) is the diffusion coefficient, and C^* (mole/ml) is the concentration of the analyte (87). One advantage of chronoamperometry over cyclic voltammetry is that the current throughout the entire interval of the potential step is proportional to the concentration of the species electrolyzed. Thus, more data can be averaged and, in theory, signal-to-noise ratios can be improved. The chief disadvantage is that one can no longer tell the origin of the current. Any species that is

electrolyzed in the potential range of the step as well as the residue current will contribute to the observed current. Because the residue current decays exponentially with time, whereas the faradaic current decays with the square root of time, current measurements are usually made at times near the end of the step. In this project, chronoamperometry has been used to determine the number of electrons transferred during the electrochemical reaction on the electrode.

In amperometry, the current is monitored continuously at a fixed potential sufficient to completely reduce or oxidize the substrate of interest at the electrode surface. The current recorded is proportional to the concentration detected at the electrode surface. The redox reactions are governed by Faraday's law, i.e. the amount of charge passed is proportional to the amount of the analyte oxidized or reduced, which is $Q = nNF$, where Q (C) is the charge, n (#/mole) is the number of electrons per mole transferred on the electrode, N (mole) is the number of moles of chemical detected and F is Faraday's constant. In amperometric mode, current spikes will be observed when concentration pulses of the analyte are rapidly detected at the electrode surface. Therefore, the area of the current spike measured, which has units of coulombs, represents the charge passed to oxidize the compound(s) detected. The charge passed is directly proportional to the number of moles oxidized according to Faraday's law. In order to calculate the amount of the analyte oxidized on the electrode using Faraday's law, the number of electrons transferred per mole needs to be determined, which will be described in chapter 2.

This technique has been used for single cell measurement because of its high time resolution, but applications are limited to the situations where the oxidation of only one

substrate can be demonstrated with some certainty in a complex biological system, since it is unable to differentiate between compounds with similar oxidation potentials.



- | | |
|----------------------------|---|
| ⊗ Glucagon
(A-Cell) | ⊙ Insulin (B-Cell) |
| ● Somatostatin
(D-Cell) | ⊘ Pancreatic
Polypeptide
(F-Cell) |

Figure 1-1. Schematic location of 4 different types of cells in rat pancreatic islet. (ref. 14)

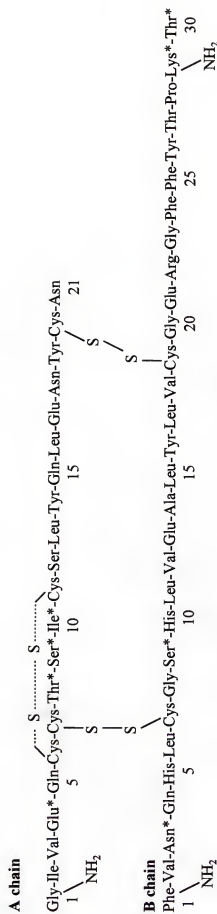


Figure 1-2. Amino acid sequence of human insulin. Inter- and Intra- chain disulfides are as indicated. An amino acid labeled with an asterick (*) indicates a location for variation among the species used in this work.

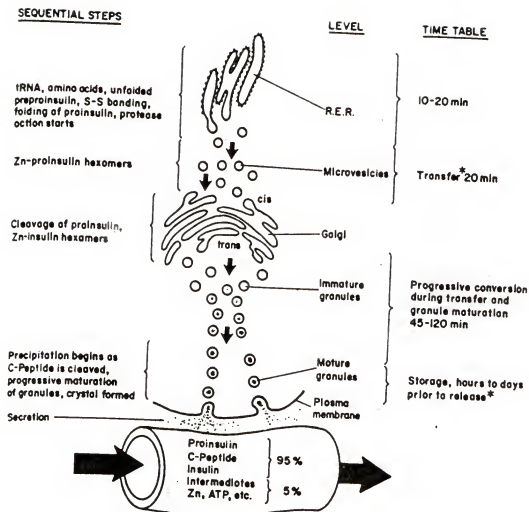


Figure 1-3. Schematic illustration of biochemical sequence of insulin biosynthesis and release (ref. 34)

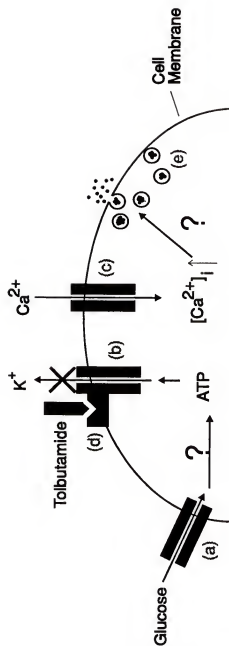


Figure 1-5. Schematic diagram of insulin secretion processes involved in glucose and tolbutamide stimulation on β -cells. (a)-glucose transporter; (b)-ATP-sensitive K^+ channel; (c)-Voltage-gated Ca^{2+} channel; (d)-Sulfonylureas receptor; (e)-insulin-containing granule. The question marks indicate the details involved in these steps are not well understood.

CHAPTER 2 ELECTRODE DEVELOPMENT AND CHARACTERIZATION

Introduction

The goal of this work is to develop an electrochemical method to characterize the pattern of insulin release from isolated β -cells grown in culture with the highest possible temporal and spatial resolution. Therefore, the first and key step to this project is the development of a microelectrode which can detect insulin rapidly and sensitively with reasonable stability under physiological conditions. This microelectrode must be small enough, around 10 μm at the tip, that it may be precisely placed near individual β -cells which are typically 12 μm in diameter(10).

Direct electrochemical detection of insulin seems to be the best basis for a sufficiently fast and sensitive sensor. Although insulin has several functionalities that may be electroactive, the most studied have been its three disulfide bonds (90). The X-ray crystallographic structure shows that the A7-B7 disulfide bond is the most accessible to chemical reaction and has been demonstrated to be electroactive, since it is located directly on the surface of the insulin molecule (91). The A20-B19 disulfide is partially shielded from the molecular surface, but is still accessible and reacts slower. The A6-A11 bond is folded into the molecule in a hydrophobic pocket and should not be readily available for reaction.

One possible approach to electrochemical detection of insulin is a reduction at a mercury electrode. Indeed, electrochemical behavior of insulin was first studied at mercury electrodes based on reduction of its disulfides (90). It has been shown that disulfides, including insulin, are reduced at mercury electrodes in buffers that are similar to physiological buffer in pH and ionic strength. Cyclic voltammograms of insulin are characterized by a double peak on the cathodic scan with one peak due to the reduction of adsorbed insulin and the other peak presumably due to reduction of diffusing insulin. Unfortunately, this electrochemical method is unlikely to be useful for detection of insulin. This is because that the adsorption of insulin is a slow process and causes a slow response time at the electrode thus, in the interest of the temporal resolution it is desirable to avoid adsorption. In addition, strong adsorption of insulin at mercury electrode causes the electrochemistry of insulin to be complicated. Another potential problem with the use of reduction at a mercury electrode is interference from oxygen. Oxygen is irreversibly reduced in a two-step process to H_2O at mercury electrodes, and cathodic waves overlap with the expected reduction waves for insulin (90).

Another possibility of electrochemical detection of insulin is to oxidize insulin on gold (Au) electrodes. It has been shown that during an anodic scan or step at Au electrodes, an oxide layer is formed at the electrode surface. As the oxide layer is formed, the electrode can catalyze the oxidation of a number of sulfur compounds (92-95). The electrocatalytic effect apparently involves oxygen transfer (92). A problem with the use of this electrode is that once the oxide layer is fully developed, the electrode is passivated. The oxide layer can be dissolved to yield a fresh electrode surface by a

cathodic step or scan. A technique based on repetitively pulsing the potential of an Au electrode between the cathodic cleaning and oxidative detection potentials, known as pulsed amperometric detection (PAD) has been developed for detection of sulfur compounds after liquid chromatography (93). In this technique, the sulfur compounds adsorb at the electrode during the cathodic step and are oxidatively removed on the anodic step. During the latter part of the anodic step (typically 400 to 1000 ms long) the current is recorded as a measure of the amount of compound adsorbed at the electrode and thus in solution. Even though this technique has been used in a variety of electrolytes and at different pH and the reduction of oxygen does not interfere with the cathodic stripping step at Au electrodes, there are several disadvantages to eliminate the possibility to use this technique for this project. First, the concentration can only be measured once during each pulse waveform. Since the pulsing is usually carried out at 1-2 Hz, the time resolution of this method is significantly less than the continuous detection with fixed potential detection. Second, Au electrode cannot be used in the biological buffers containing large amount of chloride ion (Cl^-), because Cl^- promotes anodic dissolution of the Au electrode.

Recently, the application of chemically modified electrodes (CMEs) as chemical sensors has provided the possibility of analyzing compounds, which are not electroactive at common electrode surfaces (85, 86, 96). The reversible redox center immobilized on the chemically modified electrode acts as a fast electron-transfer mediator for the analytes.

Anodic detection of several disulfide compounds, including insulin, has been reported at electrodes modified with a thin film of a composite of a cyano-bridged ruthenium dimer, $(\text{CN})_3\text{Ru(II)CNRu(III)(CN)}_3$,⁶ and a cationic, polynuclear, mixed-valent oxide of ruthenium (Ru-O/CN-Ru) (97-99). Previous reports have indicated that the response of insulin at glassy carbon electrode chemically modified with mixed-valent RuO/RuCN composite, was diffusion limited, stable, reproducible, and linear over three orders of magnitude with a detection limit of 95 nM (97). Although the mechanism of catalysis has not been worked out in detail, it has been suggested that the oxidation of insulin may be catalyzed through electron mediation and/or oxygen transfer (98). This is significant because oxidation of disulfides usually results in the formation of thiol radicals which adsorb to the electrode surface and passivate the electrode (100). The transfer of oxygen to the oxidized disulfide alters this mechanism and yields a non-passivating product. Thus, the response of the electrode is stable (98).

Compared with mercury and gold electrodes discussed above, the electrode chemically modified with mixed-valent RuO/RuCN film has the most potential as a sensor for detecting insulin secretion from pancreatic individual β -cells.

However, mixed-valent RuO/RuCN -modified electrodes have been primarily used in acidic solutions ($\text{pH} < 4$) (97-99). Thus, the unknown factors regarding the mixed-valent RuO/RuCN -modified microelectrode are its ability to detect insulin, its stability and catalytic activity in physiological buffers at pH 7.4. In this chapter, the preparation and characterization of a microelectrode modified with the mix-valent RuO/RuCN film, which can detect insulin under physiological conditions, are described.

Experimental

Electrode preparation. Glass encased carbon fiber microelectrodes were prepared as follows (101). A single, carbon fiber of 9 μm diameter (P-55S from Amoco Performance Products) was inserted into a microfilament glass capillary (1.2 mm o.d., 0.68 mm i.d., 4'' long, AM systems). This can be done by using a small amount of suction on one end of the capillary to pull the fiber into the other end. The capillary with the carbon fiber was then placed in a micropipette puller (Narishige PE-2) and pulled to a fine tip with the magnetic setting at 5 and current at 15 A. The fiber was cut yielding two electrodes. The pulled ends of the capillary were trimmed with a scalpel under microscope so that there was small space between fiber and the glass tip of the electrode. If the space is too big, the electrode tip will be large and difficult to position in a single cell measurement. If the space is too small, the epoxy will not be able to enter the capillary for sealing the fiber. The fiber is then tapped out of the capillary a little bit (around 1 mm in length) to make sure the fiber not broken and also for better sealing. The carbon fibers were sealed at the tip of the glass by dipping them in epoxy. The epoxy was made by weighing 3 mg Shell EPON Resin 828 (Miller-Stephenson Chemical Company, Inc.) in a 5 mL glass vial, then slowly heated to approximately 80 °C on the Corning stirrer/hotplate at low heating level. When the resin became virtually not viscous like water, 0.5 g metaphenylenediamine (MPDA), the hardening reagent, was added. When MPDA was totally dissolved, the electrode was dipped into the epoxy for 10-20 s to allow the epoxy to enter the capillary tip. The electrodes were placed horizontally on Scotch tape fixed to cardboard. The epoxy was cured by letting the

electrode sit overnight, and the electrode was then baked in an oven at 100 °C for 2 h. and 150 °C for another 2 h. If the curing procedure is not properly performed, gaps between the carbon fiber and epoxy will occur, resulting in high residual currents. Proper electrode fabrication is essential to minimize residual currents. Once the epoxy was cured, the electrodes were ready to be polished. The electrodes were polished at a 30 to 45° angle on a micropipet beveler (Sutter Instruments). The smaller the polishing angle is, the bigger the electrode surface will be. Immediately after polishing, electrodes were dipped in isopropanol for 10-15 min. and then ultrasonicated in H₂O for 5 min. The electrical connection in the electrode was accomplished by injecting mercury into the glass capillary of the electrode and inserting a silver-coated stainless steel wire into it.

An electrochemical deposition procedure similar to that described for macroelectrodes was used to apply the Ru-O/CN-Ru film to the microelectrodes (102). The solution containing 2 mM RuCl₃·H₂O and 2 mM K₄Ru(CN)₆ for electrode modification was prepared by dissolving these two compounds directly in 10 mL N₂-purged (degassing for 10 min.) stock solution containing 0.5 M KCl at pH 2.0. (pH was adjusted with HCl.) Freshly prepared, deareated solutions are strongly recommended for the modification. A two electrode system was used for electrochemical deposition. For all experiments, the reference electrode is connected first, and then the working electrode. However, the working electrode is always disconnected first when the experiment is done. The electrode potential was cycled between +0.47 V and +1.07 V (all voltages are versus a sodium saturated calomel electrode (SSCE, home made)) at 50 mV/s for 25 min.

Slow decomposition and oxidation takes place in the $\text{RuCl}_3 + \text{K}_4\text{Ru}(\text{CN})_6$ mixture and the formation of dark green or gray-blue gels has been observed in solution.

Electrodes were removed from solution, rinsed with deionized water, and allowed to air dry for 30 min. at room temperature before use. In general, the electrode modification did not require special electrochemical pretreatment of the carbon fiber substrates, such as cycling electrode from 0.0V to 1.8 V.

Electrode Testing. Response times and calibration curves for the electrodes were obtained in a flow injection apparatus (shown schematically in Figure 2-1). This system consisted of a syringe pump (Harvard Apparatus 11) connected by Teflon tubing to a six port valve (5701 Rheodyne) equipped with a 500 μL sample loop. The Teflon tubing from outlet of the valve was mounted to the electrochemical cell. The working electrode was positioned in the outlet of the tubing using a micromanipulator, while the reference electrode (SSCE) was placed in the cell. A pneumatic actuator (Valco Instrument Co., Inc.) coupled with the valve was triggered by the computer to turn the loop injector in a rapid and consistent manner. The flow rate was 1.5 mL/min. The entire flow injection system was housed in a Faraday cage.

In order to calculate the amount of insulin oxidized on the modified electrode by Faraday's law, the number of electrons transferred per mole (n) for insulin oxidation on the modified electrode were determined using chronoamperometry at a modified microelectrode according to a previously described method (87). The theory about this method has been described in chapter 1 and this method has been further validated by

determining the number of electron transferred per mole of dopamine on bare carbon fiber disk electrode since that number is known for dopamine.

For this experiment, the background subtracted steady state current (Δi) was measured following a square potential pulse for 2s from +0.1 to +0.65V for dopamine, and from +0.40 to +0.85 V for insulin. The voltage pulse was generated by turning a battery-powered voltage supply on and off, which was used as the external source of with an EI-400 potentiostat (Ensman Instrumentation). Values for n were calculated according to the following equation: $n = \Delta i / 4rC\text{CDF}$ where r was the radius of the electrode (electrodes were polished at a 65° angle, so that $r = r_0 / \sin 65^\circ = 4.5 \mu\text{m} / 0.9063 = 4.96 \mu\text{m}$, where r_0 is the radius of the carbon fiber), C was the concentration of insulin (0.5 mM bovine insulin dissolved in 0.5 M KCl solution with pH 2.0), D was the diffusion coefficient, and F was the Faraday constant.

The diffusion coefficients for insulin used for these calculations was $1.98 \pm 0.02 \times 10^{-6} \text{ cm}^2/\text{s}$. The value was calculated using a method based on measuring the dispersion of an insulin concentration pulse as it flowed through a capillary tube. At sufficiently high flow rates, the Golay equation (108), which predicts dispersion in open tubular chromatography columns, simplifies to: $D = d^2 v / (96H)$ where d (cm) is the inner diameter of the capillary, v (cm/s) is the flow velocity in the capillary, and H (cm) is the height equivalent of a theoretical plate. Details of using this method are as follows (108). A piece of fused silica capillary (150 μm i.d., Polymicro Technology, Inc.) was used as diffusion capillary in this experiment. Flow through the capillary was generated by a SSI 222D pump (Fisher Scientific). The capillary was 360 cm long from the inlet to the

detection window. In order to generate the necessary linear velocity of solution in the diffusion capillary (about 3 cm/sec), another piece of capillary (50 μm i.d. and 15 cm in length) was used as a splitter between the pump and the diffusion capillary. The dopamine and insulin samples were the same as used for electron number per mole measurement. The gravity injection was performed by raising the inlet of diffusion capillary 10 cm higher than the outlet and dipping the inlet into sample vial for 10 s. The UV absorbance was measured at 210 nm wavelength. The data was collected by Gateway2000 4DX2-66 with an in-house program in Lab Window 2.3 version. The diffusion coefficient was measured by Mr. Hong Shen.

The number of electron transferred per mole for dopamine is 1.9 ± 0.1 (average of three experiments and standard deviation), which agrees with the known number, 2. The number of electron transferred per mole for insulin at this modified microelectrode is 1.1 ± 0.1 (average of three experiments and standard deviation).

Better detection of response time of insulin at the modified electrode was performed by applying the sample solution directly onto the electrode surface through a pressure ejection system. The Petri dishes were filled with 0.15 M phosphate buffer at pH 7.4 on the stage of an inverted microscope equipped with phase contrast optics (Zeiss axiovert 35). A working microelectrode was positioned facing up using a combined mechanical/piezoelectric micropositioner (Burleigh PC-1000). 20 μM bovine insulin sample was applied to the electrode surface by pressure ejecting solutions from the tip of micropipette which was positioned very close to the electrode. The micropipettes were prepared by pulling 1 mm outer diameter (o.d.) by 0.58 mm i.d. glass capillaries (AM

systems) on a Narishige PE-2 pipette puller with magnet setting of 5 and heater setting of 5 (15 Amps). The pipettes were broken off to a tip o.d. of about 10 μm . The pressure ejection system (General Valve Picospritzer) allowed pressure pulses of variable magnitude and duration to be applied. When pressure pulses of 10 p.s.i. were used, flow rates through the pipette tips were approximately 1 nL/s as evaluated by measuring the size of solution droplets formed after ejection under mineral oil. The duration for the pressure pulse was 1 sec.

Data Collection and Analysis. Data for the electrode testing obtained in the flow injection system were collected using an EI-400 potentiostat. The data were low pass filtered with a cut-off frequency of 20 Hz. The data points collected in flow system were 100 ms apart. The data were collected by an IBM-compatible personal computer (Gateway 2000 386-25 MHz) via a TecMar multifunction board (LabMaster DMA TM-40 PGH). Data were analyzed using locally written software called VA.

Data obtained in “puffer” system were collected by using home-made battery voltage supplier and Keithley 428 current amplifier. The data were low-pass filtered at 100 Hz and 1 kHz by Krohn-Hite model 3341 filter and collected at 500 and 6kHz, respectively, by an IBM-compatible personal computer (Gateway 2000 486-66 MHz) via a National Instruments multifunction board (AT-M1016-F5). The data collection program was locally written and using Lab Window.

The mean of measurements are presented with the standard deviation and number of samples (n).

Results and Discussion

Electrode Preparation. Voltammograms obtained during modification of one of the microelectrodes are shown in Figure 2-2. The voltammograms are characteristic of surface deposition of an electroactive species with increasing surface coverage with time. The waves began with a sigmoidal shape and eventually became dominated by peak shaped voltammograms. The peak anodic currents at +0.90 V averaged 10.1 ± 0.4 nA ($n = 4$) following 25 minutes of electrochemical deposition. The peak current is increasing during the modification process and the amplitude of peak current change between initial and final voltammogram is important for determining whether the electrode will have good catalytic ability or not. In general, the bigger the current increases, the better electrode sensitivity. Different thickness of the film could be obtained by varying the experimental parameters during the modification steps (97). Longer cycling times in the fresh modification mixture resulted in thicker films. The thicker film yielded increased baseline currents.

An interesting feature of the data in Figure 2-2 is that in the potential range from 0.47 to 1.07 V, the Ru-O/CN-Ru film underwent well-defined double reduction and the reduced film showed double oxidation, respectively. This can be correlated with the fact that two stable forms of ruthenium at oxidation states higher than +3, namely $\text{-Ru}^{\text{III}}\text{-O-Ru}^{\text{IV}}$ - and $\text{-Ru}^{\text{IV}}\text{-O-Ru}^{\text{IV}}$ - (99), are being formed during the electrode reaction. The approximate ratios of the atomic concentrations, O: Ru : CN, obtained, can be expressed as 3: 5: 12, which is consistent with the hypothesis that the deposit was formed during

electrostatic interaction of the $\text{Ru}_2(\text{CN})_{11}^{6-}$ dimer with the $\text{Ru}_3\text{O}_2^{6+}$ and/or $\text{Ru}_2\text{O}_5^{5+}$ species (103).

After the electrode was coated with mixed-valent RuO/RuCN composite, a scanning electron microscope was used to compare the surface morphology of modified and unmodified carbon fiber electrodes. The surface morphology of both electrodes were quite different. There were some uneven particles deposited on the modified electrode surface, while there was no such film observed on the bare electrode surface.

Electrode Testing. Microelectrodes prepared in this manner were highly active in acidic media, as reported in the literature for macroelectrodes (97, 99). Steady state surface waves on the microelectrodes in 0.15 M sodium phosphate buffer at pH 2.0, shown in Figure 2-3 (A), were similar to those reported previously for films deposited on macroelectrode e.g. glassy carbon with 3 mm in diameter (99, 102). The anodic peaks observed at +0.78 V and at +0.96 V have been attributed to the two-step oxidation of ruthenium in the ruthenium oxide portion of the film from the Ru(III) to the Ru(IV) state (99).

Measurements of insulin in the flow injection apparatus had detection limits of 0.1 μM and a linear range of 3 orders of magnitude in several acidic electrolytes including 0.1 M K_2SO_4 at pH 2.0, 0.15 M potassium phosphate buffer at pH 2.0, and 0.15 M sodium phosphate buffer at pH 2.0. The detection limit was defined as the concentration which gave a signal equal to the signal from a blank injection plus 3 times the standard deviation of the blank. These figures of merit are in agreement with those reported for macroelectrodes under similar conditions (97). The electrode response to insulin was

stable for over 1 hour when held at a fixed potential of +0.85 V. This potential was also used as the testing potential in pH 7.4 buffers. As shown in Figure 2-4, a hydrodynamic voltammogram revealed that this voltage gave the peak current response in phosphate buffer at pH 7.4. Here, each reported current was background subtracted response measured at the stated potential after injection of 20 μM insulin sample. The background current at this modified electrode increases with the potential which was the same as described in the previous report (99).

When the electrode was used in 0.15 M sodium phosphate buffer at pH 7.4, it was observed that the response to insulin deteriorated markedly. An example of the time profile of the response is shown by the hollow symbols in Figure 2-5. The peak current resulting from a 3 s wide concentration pulse of 10 μM insulin, applied in the flow stream, was used to obtain the points. The times indicate the time since the electrode was brought in contact with the buffer. While the decrease slows down after 30 min, the signal is low relative to the initial response.

A surface voltammogram obtained in pH 7.4 sodium phosphate buffer after the electrode response decreased is shown in Figure 2-3 (B). As can be seen, the voltammetric response was drastically altered relative to the voltammograms obtained in the pH 2.0 sodium phosphate buffer. The voltammograms indicate that an electroactive film of some type still existed on the electrode, however it was significantly different from the initial film and it did not effectively catalyze the oxidation of insulin. Similar results were obtained in pH 7.4 potassium phosphate buffer and pH 7.4 Kreb's Ringer

bicarbonate (KRB) buffer. It was concluded that the higher pH of the buffer had a significant role in degrading the response of the electrode.

The stability study was repeated, but with the electrode held at +0.4 V between injections of insulin to determine if the deleterious effect of electrolyte pH was dependent on electrode potential. The response is shown by the solid symbols ("rested" electrode) in Figure 2-5. The electrodes maintained catalytic activity for much longer times if the potential was not constantly at +0.85 V. It was possible to maintain stable responses for two hours as long as the electrode was held at +0.85 V for less than 60 s at a time and held at +0.4 V for at least 120 s at a time. The longer the electrode was held at 0.4 V, the better the stability. This suggested that the polymer film at low oxidation states of Ru is much more stable than that of the high oxidation states of Ru (at 0.85V) in pH 7.4 buffer.

A surface wave voltammogram obtained in the pH 7.4 sodium phosphate buffer after 30 minutes at +0.4 V is shown in Figure 2-3 (C). The irreversible voltammetry may indicate that at neutral pH oxidation of the film results in formation of an irreversible product. It may also indicate that the polymer film coated on the electrode was dissolving at neutral pH. This voltammetric wave under these conditions was not as stable as that obtained in pH 2.0 buffers. Voltammograms obtained every 10 min with the electrode held at +0.4 V between scans showed progressive decreases in current levels so that after 2 hours the background waves were approximately one half those obtained initially. In 0.15 M sodium phosphate buffer at pH 2.0 the surface waves (shown in Figure 2-3 (A)) showed no changes over a 2 hour period whether the resting potential was +0.40 V or +0.85 V.

In physiological buffer, with the electrode periodically held at +0.4 V, the detection limit, defined as described above, was approximately 0.5 μM . In Figure 2-6, a typical calibration curve obtained with insulin concentrations of 0, 5, 10, 20, and 40 μM had a slope of 0.441 pA/ μM , a y-intercept of 0.23 pA, and a linear correlation coefficient of 0.9992. The high y-intercept was due to signals obtained from blank injections which resulted from an artifact of the injector. An example of the response of the electrode to an injection of 20 μM insulin in the flow stream is shown in Figure 2-7. The data points are 100 ms apart. Therefore, the response time was less than 200 ms to 90% of the full height.

Characteristics of the modified electrode. Based on the results discussed above, the modified electrode is not very stable under physiological conditions. In order to improve the stability, several experiments have been tried to determine how to best handle the electrode after modification. In a previous report, mixed-valent RuO/RuCN modified macroelectrodes were placed into supporting electrolyte solution (0.5 M KCl solution at pH 2.0) and stored under this condition before use (98). Therefore, the modified microelectrode was stored in 0.5 M KCl for 1 hour or longer after modification and was tested in flow injection system. Unfortunately, the signal of 10 μM insulin decreased to 60 % of its original after 3 min, which was not similar to what have been described for macroelectrode. Sudden pH change seems to degrade the electrode greatly. Another modified electrode was tested right after its modification without placing it into the supporting electrolyte solution. The degradation of the electrode was similar to that of the modified electrode kept in KCl solution before testing. The third modified

electrode was dried in the air for half an hour and then tested. The signal decays 25 % in 10 min. Therefore, air-drying helps to improve the stability of the electrode to some extent in physiological buffer. The question raised here is how long the modified electrodes need to be dried for better stability. Electrodes dried for 30 min, 50 min, 100 min, 150 min, 250 min and overnight were tested in the flow injection system after injection of 10 μ M cystine. Cystine is the dimer of amino acid cysteine connected with one disulfide bond, which has been demonstrated electroactive on this modified electrode (98). Each sample injection was made after the modified electrode had been “resting” at 0.4 V for 2 min. In the period of 20 min, the signal decays with time at a similar speed and levels off after 20 to 30 min regardless of drying time. However, the baseline current is higher when the air-drying time is longer, which causes greater baseline drift at the beginning of electrode use.

Response time. A good microvoltammetric electrode needs to have fast response time. In flow injection system, the response time is limited by the flow dispersion. Therefore, the pressure ejection system was used to apply the sample directly to the electrode surface. The distance between the electrode and the pipet filled with sample solution was about 2 μ m. The fast data collection frequencies (500 Hz and 6 kHz) and high low-pass filter frequencies (100 Hz and 1 kHz) were used to investigate the response time of insulin on this modified electrode. As a control experiment, the response time of dopamine was detected on the modified electrode and bare electrode. The current responses of buffer, insulin and dopamine are illustrated in Figure 2-8. The background current caused by pressure ejection is much smaller than the signal due to insulin.

Compared with the response time of dopamine, the response time of insulin is also very fast. The results are summarized in Table 2-1. The response time of dopamine on both modified electrode and bare electrode are about the same, which indicates that coated film on modified electrode does not affect the response time. And the response time of insulin is around 25 ms, which will be fast enough for measuring insulin secretion from single β -cells.

Thus, these experiments indicated that the electrode could be used as an amperometric detector of insulin under physiological conditions as long as the electrode could be "rested" at +0.4 V in between periods of measurement at +0.85 V. Therefore, it is possible that this kind of microelectrode can be used to measure insulin secretion from individual pancreatic β -cells with high temporal resolution. The details will be discussed in next chapter.

Table 2-1. Response Time of Insulin and Dopamine.

Analytes	f (filter) = 100 Hz f (collection) = 500 Hz	f (filter) = 1 kHz f (collection) = 6 kHz
20 μ M Insulin (on modified electrode*)	25.2 \pm 6.9 (ms)	24.1 \pm 5.8 (ms)
10 μ M Dopamine (on modified electrode*)	10.1 \pm 0.9 (ms)	10.6 \pm 1.5 (ms)
10 μ M Dopamine (on bare electrode)	-	11.0 \pm 1.1 (ms) (n=3)**

* Four modified electrodes were tested.

** One bare electrode was used and repeated for three times.

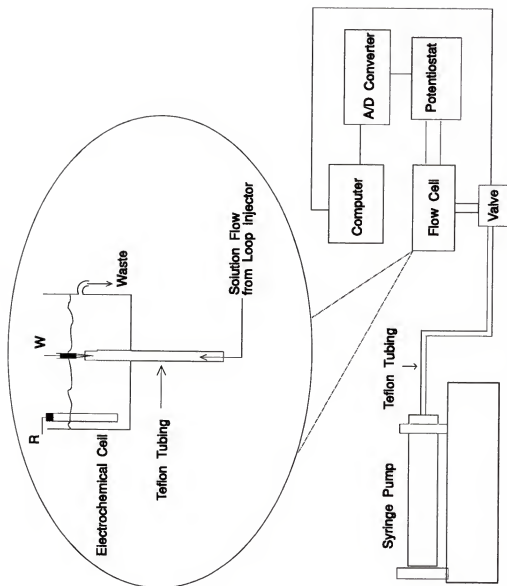


Figure 2-1. Schematic diagram of flow injection system. R indicates reference electrode (SSCE), W indicates working electrode.

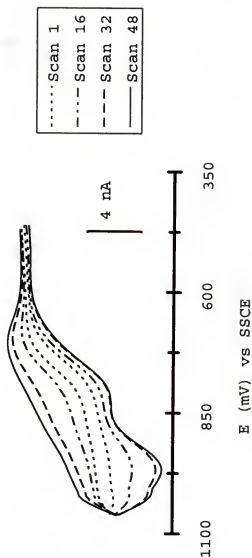


Figure 2-2. Voltammograms from electrochemical deposition of Ru-O/CN-Ru film onto carbon fiber microelectrode. Conditions for voltammetry are described in the experimental section. Only four scans are shown for clarity.

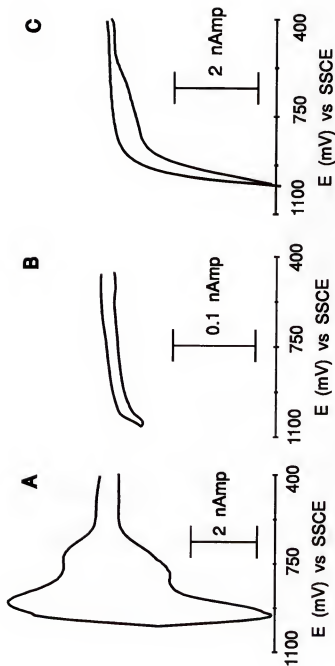


Figure 2-3. Surface voltammetric waves on Ru-O/CN-Ru-modified electrodes as a function of electrolyte and resting potential. All voltammograms were obtained at 50 mV/s in unstirred solutions of electrolyte. Conditions were as follows: (A) after 30 minutes in 0.15 M sodium phosphate buffer at pH 2.0 with a resting potential of +0.85 V, (B) after 30 minutes in 0.15 M sodium phosphate buffer at pH 7.4 with a resting potential of +0.85 V, and (C) after 30 minutes in 0.15 M sodium phosphate buffer at pH 7.4 with a resting potential of +0.40 V.

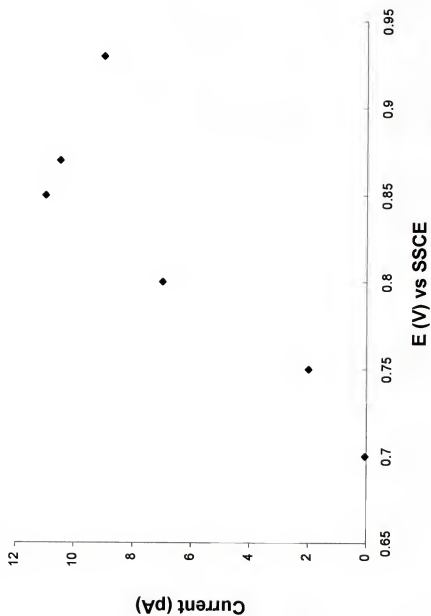


Figure 2-4. Hydrodynamic voltammogram for the oxidation of insulin at the modified electrode. The injected sample concentration was 20 μ M insulin in phosphate buffer at pH 7.4.

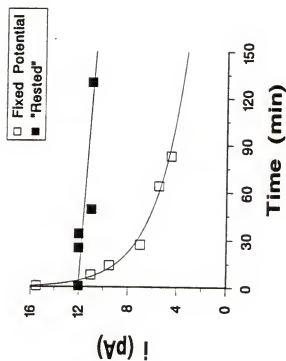


Figure 2-5. Stability of the peak current at Ru-O/CN-Ru-modified electrodes in physiological buffer resulting from injection of $10 \mu\text{M}$ insulin. The lines through the points are only intended to highlight the trends.

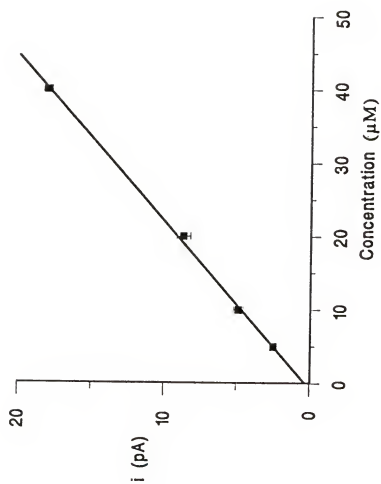


Figure 2-6. Calibration curve for insulin obtained at pH 7.4 physiological buffer in flow injection system.

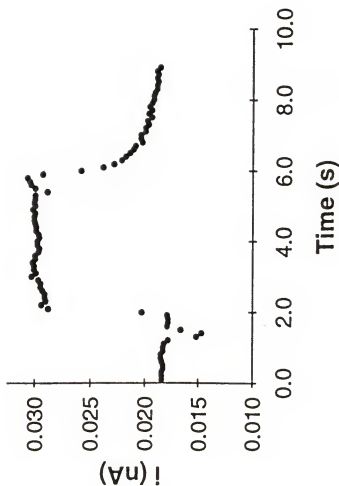


Figure 2-7. Response of Ru-O/CN-Ru-modified electrode to 20 μ M insulin injected in a flowing stream. The dips in current are artifacts resulting from the activation of a solenoid which turns the injection valve and are convenient markers of the injection time. The delays before initial increase in current after injection are due to the dead volume of the flow system.

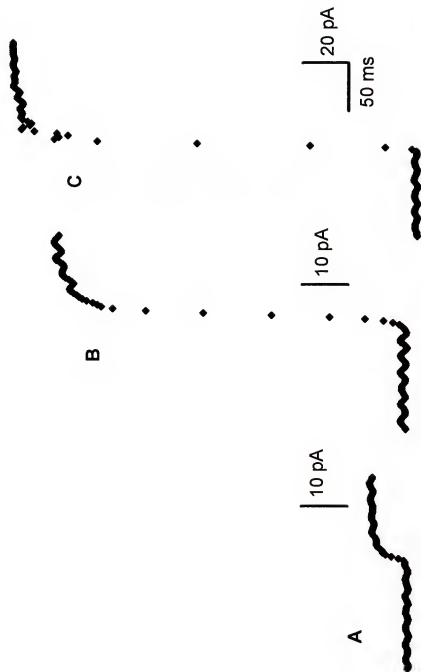


Figure 2-8. Current responses of Ru-O/CN-Ru-modified electrode to the analytes puffed to the electrode by pressure ejection system. A) buffer, B) 20 μ M insulin, C) 10 μ M dopamine. All the samples dissolved in 0.15 M phosphate buffer at pH 7.4. Data was low-pass filtered at 100 Hz and collected at 500 Hz.

CHAPTER 3

DETECTION OF INSULIN SECRETION AT SINGLE β -CELLS

Introduction

The process of exocytosis is common to many different types of cells and is central to our current understanding of the process of chemical intercellular communication. Substances that are involved in chemical communication between cells are frequently stored in vesicles. These vesicles fuse with the cell membrane in the presence of an appropriate stimulus, and their multimolecular contents are extruded (76, 104). Thus, the minimum amount of chemical secretion should be dependent on the volume of the vesicle and the concentration of its contents.

It is generally accepted that insulin is secreted from pancreatic β -cells by exocytosis. Numerous lines of evidence provide strong support for this conclusion. For example, insulin is localized in vesicles in the β -cells (36) and electron micrographs of stimulated β -cells show vesicles that have fused with the cell membrane in a way that would allow vesicular contents to be released (2). In addition, the capacitance of β -cells has been shown to increase, indicating an increase in cell surface area as expected for exocytosis, following application of depolarizing potentials to the cell (105, 106). In spite of the strong evidence however, insulin secreted from a β -cell has not been measured with sufficient sensitivity, temporal resolution, and spatial resolution to detect

the small concentration pulses that would be the consequence of insulin secretion by exocytosis. Thus, the time-resolved measurement of insulin secretion at the level of single cells would provide the first direct chemical evidence supporting the exocytotic theory of secretion. The ability to measure insulin at the level of single exocytosis events is also important because it could be useful in further unraveling the complexities of insulin secretion.

In the previous chapter, it has been demonstrated that insulin can be detected amperometrically in flow injection system under physiological conditions using a carbon fiber microelectrode modified with mix-valent RuO/RuCN polymer composite (107). Therefore, it appeared that this electrode might be useful for detection of insulin secretion from single β -cells. In this chapter, the modified microelectrode has been used to make amperometric recordings near single β -cells. It is demonstrated that the electrode can be used to detect insulin secretion at single cell level. The electrodes for detection of insulin released from single human, dog and rat pancreatic β -cells have been investigated. Current spikes were observed at the electrode placed next to a stimulated- β -cell with insulin secretagogues. All the experiment results and chromatographic evidence have supported the hypothesis that the current spikes observed are due to detection of packets of insulin concentration pulses released from the β -cell by exocytosis. The measurements have demonstrated to improve the temporal resolution of insulin secretion measurements by 3 orders of magnitude and allow unique insights into the secretion process. On a broader scale, the measurements represent the first practical use of a sensor in a biological

system for peptide hormone measurements. The data reported in this chapter are detection of insulin secretion at rat and human β -cells.

Experimental

Electrode preparation. Glass encased carbon fiber microelectrodes were prepared using previously described techniques in chapter 2.

Electrode testing. Response times and calibration curves for the electrodes were obtained in a flow injection apparatus which has been described in previous chapter. The number of electrons transferred during oxidation of insulin on the modified electrode has been obtained in chapter 2.

Cell culture solution preparation. All chemicals used for cell culture were from Life Technologies, Inc. (Gibco), unless stated otherwise. All the equipment were purchased from Fisher Scientific, unless stated otherwise.

100 mL of 1X Ca^{2+} , Mg^{2+} -free hanks were prepared by mixing 10 mL 10X Ca^{2+} , Mg^{2+} -free hanks with 1 mL penicillin-streptomycin (Pen/Strep) and 90 mL water, then adjusting pH to 7.4 by couple of drops of saturated sodium bicarbonate.

1 mg/mL trypsin solution was made by dissolving trypsin (1: 250) in 1X Ca^{2+} , Mg^{2+} -free hanks and filtering through a low protein binding non-pyrogenic sterile acrodisc filter (0.22 μm , Gelman Sciences, Product # 4192).

Modified CMRL 1066 solution (G-100) was made through following steps: 1) prepare 1X 1L CMRL 1066 (solution I) by mixing 100 mL 10X CMRL 1066 with 900 mL water, then adding 2.2 g sodium bicarbonate into the solution, adjusting pH to 7.2-7.4 by NaOH; 2) prepare 1X CMRL 1066 with additives (solution II) by adding 1.3 mL

10 M NaOH and 5.95 g HEPES to 100 mL 1X CMRL 1066 made in step 1; 3) make pre-G-100 by mixing solution I and solution II at 9 to 1 ratio; 4) make final G-100 media by supplementing pre-G-100 with 10% Fetal Bovine Serum (FBS), 1% Pen/Strep, and 1% L-glutamine. The final media then were refiltered to be sterile. This culture media can be kept in the refrigerator and used for a couple of months.

Two Hanks Balanced Salt Solution (HBSS) were prepared for rat islet isolation. One is Ca^{2+} -free HBSS, containing (in mM), 137 NaCl, 5.4 KCl, 4.2 NaH_2PO_4 , 4.1 KH_2PO_4 , 10 HEPES, 1 MgCl_2 and 5 glucose. The other one is HBSS with Ca^{2+} , which contains the same components as in Ca^{2+} -free HBSS, and plus 1 mM CaCl_2 .

All the solutions were sterilized by filtering the solution through sterile filter top and sterilized glass bottle.

Human β -cell culture. Fresh human islets of Langerhans were obtained from the medical schools at Washington University or the University of Miami. The islets were usually kept in culture for overnight before cell dispersion. Islets were dispersed into individual cells and maintained in culture media according to the following procedure. Approximate 3000 islets were transferred from culture dish to 15 mL conical centrifuge tube by transfer pipet, and washed twice with 1X Ca^{2+} , Mg^{2+} -free Hank's media. Following washing, the islets were centrifuged at 1,300 RPM at room temperature for 2 min by using IEC Centra MP4R (International equipment company). After removing the media, 7 mL of straight versene (1:5000) was added and the islets resuspended at the beginning and one more time by transferring pipet in the middle of 7 min incubation at room temperature. After incubation, the islets were centrifuged at 1,300 RPM for 2 min.

The supernatant was sucked off by vacuum and 7 mL of trypsin solution with the concentration of 1 mg/mL (prewarmed to 37° C) was added. The islets were gently mixed in the trypsin solution by pipetting, then shaken gently in water bath for 3 min at 37° C. The islets were pipetted again and returned to waterbath for another 30 to 40 s shaking. 8 mL of culture media (provided with islets or G-100 media) was added to the vial and centrifuged at 1,500 RPM for 5 min at 4° C. The supernatant was removed and 3 mL of culture media added.

The cells were resuspended and counted on a hemacytometer. The steps are as follows. First, 90 μ L trypan blue stain solution (1:10 phosphate balanced solution) and 10 μ L cell suspension solution were mixed in a 1 mL plastic vial and resuspended. Secondly, the stained cell solution was filled to hemocytometer chamber. Then, let the preparation stand for one or two minutes or until the cells are settled onto the bottom of the counting chamber to make certain that the cells were evenly distributed. Any irregularity of distribution will not give an accurate estimation of the number of cells. After that, the cells distributed in a one square millimeter counting area on the hemacytometer were counted under a microscope. Only bright cells were considered live for counting. The stained cells were considered dead cells. The number of the cells then was calculated by the following equation: The total number of cells dispersed = number of cells counted in one square millimeter \times 10 (depth correction factor) \times 10 (cell dilution factor) \times 1000 (number of cubic millimeters in one milliliter) \times total volume (the last volume of cells before diluted with trypan blue solution with the unit of milliliter).

Cells were then plated at a density of approximately 10^6 cells per 35 mm petri dish. The petri dishes were used either Corning polystyrene tissue culture dish or suspension dish. The tissue culture dish has been treated to enhance cell attachment, while the suspension dish is not treated. Sometimes cells were also plated onto the uncoated glass cover slip or poly-L- lysine coated cover slip for enhancing the cell attachment which was placed in the suspension dish. Among these cell plating techniques, Corning polystyrene tissue culture dish seems the best for β -cells adhering. Cells were incubated at 37° C, 100% humidity, and 5% CO₂. Cells were used on days 2-6 of culturing.

The cell counting was only performed the first time this procedure was used. The rest of the time, all estimations of the number of cells were based on that. All solutions used were sterile. All the pipets, culture dishes and centrifuge tubes used for this procedure were also sterile. And almost all of the experiments were performed under the sterilized hoods, except waterbathing, centrifugation and the cell counting. Sterile techniques were critical for experiment success.

Rat islet isolation and cell culture. Rat islets were isolated from 180-300 g male Sprague-Dawley rats, according to the digestion method of Gotoh (110) with modifications as follows. Two rats were usually used each time. The rats were sacrificed by exposure to an inhalant anesthetic (methoxyflurane) followed by cervical dislocation. The rat then was sprayed with 70% alcohol and a crude midline incision was made by three big cuts to expose the pancreas. During this step, more cuts would get rat's fur onto the organs under the skin. Therefore, caution was needed to avoid this because the fur

was not easy to be removed during the whole process and it also might cause some contamination. The pancreatic duct was ligated at the liver and the pancreas distended by injection through the duct (using #271/2 or #261/2 gauge needle) of 15 mL of 1.0 mg/mL collagenase (Sigma, type XI C-7657) in Ca^{2+} -free HBSS. During the injection, once the enzyme solution got into the duct, the pancreas started to dilate. The successful dilation of pancreas is most critical step for the success of pancreas digestion. This part was done under illuminated desk magnifier (1.77X, Fisher). The distended pancreas was dissected out starting from the spleen to the stomach and placed into a siliconized glass vial (details in appendix) with an additional 2 mL of the collagenase solution. The dilated pancreas were then incubated in a 37 °C water bath for 15 min. 2-3 mL cold Ca^{2+} -free HBSS was added to the vial with pancreas and the vial was shaken vigorously by hand for 15 s. After shaking, the pancreas should be disrupted to small parts of tissues. The digested pancreas was then transferred to 50 mL centrifuge tube, and the vial was washed with Ca^{2+} -free HBSS 2-3 times to make sure everything in the vial to be transferred. The digested pancreas was washed 8 to 10 times with 40 mL HBSS each time. This was accomplished by allowing the suspended digest to sediment out (~4 min), removing and discarding 35 mL supernatant, and resuspending the pellet in 35 mL fresh HBSS. This would remove a great deal of the acinar cells. The Ca^{2+} concentration of washing solution was gradually increased from 0 to 1 mM by mixing Ca^{2+} -free HBSS and HBSS with 1mM Ca^{2+} during the first three wash. After third wash, all the HBSS solution for washing contained 1 mM Ca^{2+} .

The islets were further isolated using a Ficol gradient (Sigma, F-9378). After the final wash, the islets were resuspended in 40 mL HBSS and centrifuged at 1100 RPM for 11 sec. The supernatant was then all sucked out, and the islets were resuspended in 12 mL of 23% Ficol solution made with HBSS w/w. Subsequent layers of 4 mL each at 21% (9.25g stock of 23%/10g HBSS) and 20% (8.7g stock 23%/10 HBSS) of Ficol solution with a final layer of HBSS were carefully applied to make four layers. Then, the gradient was centrifuged at 1100 rpm for 8 min at room temperature. The top two layers containing islets were removed to a new 50 mL centrifuge tube, and washed twice with 35 mL HBSS with Ca^{2+} . The supernatant was discarded. The islets were usually located at the top two layer. However, sometimes, the gradient layers were not clearly distinguishable, then the islets were also distributed in the bottom two layers. In that case, the bottom two layers will also be collected and treated the way for the top two layers.

All the experiments described above were performed in non-sterile but clean environment. All the dissection instruments used were clean but non-sterile. However, all the solutions used were sterile and kept on ice at all the times. 70% alcohol was used to clean the dissection instruments and wash the fur on the rat skin before dissection for killing bacteria.

The final pellet was resuspended in 5-10 mL RPMI 1640 culture media supplemented with 10% Fetal Bovine Serum and 1% pen/strep and 1% L-glutamine. The islets were then hand-picked and placed into a 60 mm suspension culture petri dish with RPMI 1640 culture media with supplements. This step was done under the sterile

hoods to keep from getting germs into culture media. When whole islets were used for experiments, the media was changed every 2 days.

In the rat islet isolation procedure, collagenase is the only enzyme used for pancreas digestion. The amount of the enzyme and the incubation time are critical for the whole process. The error in the process of evaluating collagenase is the subjective decision of dissociation endpoint, since this enzyme activity varies with different lot number. It is critical determination since under-dissociation leads to sub-optimal islet cleavage from exocrine tissue, and over-dissociation extends islet exposure to dissociating enzymes, resulting in islet fragmentation and cellular damage. However, there are no rules on which to base this decision other than the investigator's experience. Based on the experiment we tried, the amount of collagenase and incubation time are summarized in Table 3-1. When the enzymatic activity of collagenase decreases, the concentration of collagenase and incubation time used have to be increased to certain extent. When different lots of collagenase are used, several tests have to be performed based on the information in Table 3-1 to get optimal conditions for best yield of islets from each rat.

Table 3-1. Selections of Collagenase for Rat Islet Isolations.

Lot number	Enzymatic activity (collagen digestion) (units/mg solid)	concentration used for isolation (mg/mL)	incubation time for dilated pancreas (min)
52H-6829	2030	1.0	15
113H6844	1460	1.5	20

Isolated rat islets were allowed to recover overnight in an incubator at 37 °C and 5% CO₂. For dispersion, 100 islets were transferred to a 15 mL conical tube by a transfer

pipet and spun down at 1100 rpm for 11 sec. The supernatant was discarded and 0.8 mL 0.05% trypsin/EDTA warmed to 37 °C was added. Islets were triterated (like doing pipetting) gently with a glass, flamed, siliconized Pasteur pipette and placed into a 37°C water bath for 1 min. They were removed from the incubator and resuspended for 30 sec. The reason for doing triteration was to mechanically break up the cell clusters. During this triteration, the cell suspension solution became cloudier, which means the islets has been dispersed into single cells. 3 mL of warmed RPMI 1640 media was added to stop the trypsin activity. The cell suspension then was spun down at 900 RPM for 2 min. The supernatant was discarded and the bottom of centrifuge tube with the pellet was tapped by finger. The cells were then washed one more time with a warmed modified CMRL 1066 media, centrifuged and supernatant was discarded. The final pellet was resuspended in 1.5 mL modified CMRL 1066 media. The cells were placed in 35 mm tissue culture dish at about 10^5 cells per dish.

All the experiments for islets dispersion were done under the sterile hoods, and every solution used was sterilized. More details for this procedure are discussed in the appendix.

Single cell measurements. Single cell measurements were performed in the following manner (75, 76). Petri dishes containing the cells were removed from the incubator and rinsed 3 times with a Kreb's buffer. The Kreb's buffer (KRB) contained (in mM): 118 NaCl, 5.8 KCl, 2.4 CaCl₂, 1.2 MgSO₄, 1.2 KH₂PO₄, 25 NaHCO₃, and 3 d-glucose. The buffer was adjusted to pH 7.4 by bubbling 95% air/ 5% CO₂ through it. The dishes were filled with buffer and placed in a microincubator (Medical Systems, Inc.)

on the stage of an inverted microscope equipped with phase contrast optics (Zeiss axiovert 35). The microincubator maintained the temperature at 37 °C. The pH of the KRB buffer in petri dish was maintained by applying 95% air and 5% CO₂ gas continuously through a gas wash bottle to microincubator gas inlet, which provided a CO₂ level at 5% around the cell-containing petri dish. A SSCE was fixed in the dish. To perform measurements, a cell was located with the microscope and a working microelectrode brought near the cell using a combined mechanical/piezoelectric micropositioner (Burleigh PC-1000). Under the magnification (256x), the electrode tip was allowed to lightly touch the cell, denoted by the cell moving, and then retracted the distance desired. Experiments were performed with an approximately 1 µm gap between electrode and cell. The schematic diagram is shown in Figure 3-1. Substances were applied to individual cells by pressure ejecting solutions from the tips of micropipettes which were positioned approximately 30 µm from the cell. The micropipettes were prepared the same way as described in chapter 2. Pressure pulses of 10 p.s.i. were used. Flow rates through the pipette tips were approximately 1 nL/s as evaluated by measuring the size of solution droplets formed after ejection under mineral oil. Stimulants were dissolved in KRB. If glucose stimulation was performed, the solution in the pipettes consisted of KRB buffer with 16 mM glucose. In this case, the pressure pulses were 30 or 60 s long. If K⁺ stimulations were performed, the pipette solution contained KRB buffer with 60 mM KCl and NaCl reduced an appropriate amount to maintain salt balance. Pressure pulses of 2 s or 10s were used in this case. Unless stated otherwise, tolbutamide stimulations were 10 s duration. The concentration of tolbutamide used in

this case were from 100 μM to 500 μM . The pipette tips were positioned next to the cells using a mechanical micromanipulator (Narishige MM-333). For recordings, the working electrode was at +0.85 V unless noted otherwise. Between measurements, the sensing electrode was at +0.40 V to prevent rapid degradation of the electrode as described in chapter 2. The microscope was housed in a Faraday cage and signal collecting was isolated from other electrical interferences.

Data collection and analysis. Some data for the single cell measurements and electrode testing were collected using an EI-400 potentiostat with built-in voltage supplier, preamplifier and filter(Ensman Instrumentation). The data were low pass filtered with a cut-off frequency of 20 Hz and were collected at 60 Hz by an IBM-compatible personal computer (Gateway 2000 386-25 MHz) via a TecMar multifunction board (LabMaster DMA TM-40 PGH). The data collecting program were locally written.

The other data were collected by using home-made battery voltage supplier and Keithley 428 current amplifier and Krohn-Hite model 3341 filter. The second data collection system is better than the first one because the noise is eliminated by removing some alternative current (AC) interferences. The data were filtered at 30 Hz and collected at 80 to 220 Hz by an IBM-compatible personal computer (Gateway 2000 486-66 MHz) via a National Instruments multifunction board (AT-M1016-F5). The data collection program was run in version 2.3a lab window.

All data from single cells measurement were analyzed using locally written software. The mean of measurements are presented with the standard deviation and number of samples (n).

HPLC analysis of islet releasates. Releasates from islets were analyzed using HPLC. The HPLC system utilized SSI 222D pumps (Fisher Scientific) and a standard 6 port injection valve equipped with a 50 mL injection loop (Valco, Houston, TX). Flow rates were 1.00 mL/min. Separations were performed using a Keystone Scientific C-8 column packed with 5 mm porous particles. Unless stated otherwise, the mobile phase was 72% 50 mM K_2SO_4 and 10 mM KH_2PO_4 adjusted to pH 2 with H_2SO_4 and 28% acetonitrile (v/v). Some HPLC experiments were also done using a PerSeptive Biosystems hydrophobic interaction chromatography column. A thin layer electrochemical cell was used for detection and was built in-house using a design similar to that reported previously (111). The detector electrode was a glassy carbon disk (3 mm diameter) modified using the same conditions as used for the microelectrode. To analyze the releasates, 100 islets, which had been incubated in RPMI 1640 media for 1 to 5 days, were placed in 100 mL KRB with 3 mM glucose and incubated at 37 °C, 5 % CO_2 for 20 min. This media was then removed and directly injected onto the HPLC to obtain a pre-stimulation background. The media was replaced with 100 mL of KRB with 16 mM glucose and 200 mM tolbutamide and allowed to incubate for 20 min. This solution was then removed and directly injected onto the HPLC to obtain the stimulated islet chromatograms. HPLC data were collected using a system similar to that for the electrochemical recordings.

Ca^{2+} -free experiments. Everything is the same as described in single cell measurement except that the biological buffer used for the test without Ca^{2+} in it. And two glass pipettes were used, one was filled with stimulation solution containing 2.4 mM

Ca^{2+} , and the other was filled with stimulation solution only. The two pipettes were held on the micromanipulator and about 0.5 cm apart.

Results and Discussion

Single cell measurements. The modified electrode was held close to the single pancreatic β -cell and the sufficient voltage was applied to oxidize insulin. The typical amperometric current recordings taken with the electrode about 1 μm away from the human β -cell following tolbutamide, potassium and glucose stimulation are shown in Figure 3-2. As shown, the different stimulations all produce a series of current spikes which appear to occur at random times at the electrode. Spikes generally occurred only after a stimulation and rarely were observed before a cell was stimulated. In addition, application of buffer to a cell produced no spikes (Figure 3-2 (D)). This eliminates the possibility that spikes are introduced by the stimulation solution application or movement of the stimulated cell. The spikes appear to be the direct detection of substances secreted from β -cells. Similar results were observed from rat β -cells.

The variability between spikes. Although all secretagogues cause current spikes to be observed, the time course and frequency of the spikes vary with the stimulation conditions. The time between the end of the stimulation and the beginning of spiking (i.e. initiation of spike activity) and the time for spiking observed to occur (i.e. duration of spike activity) varied also with cells attempted. The differences and the ranges are summarized for both rat and human cells in Table 3-2.

The variability in time course of spike occurrences with different stimulation methods corresponds well with what is known about insulin secretion. The potassium

and tolbutamide stimulations cause secretion to occur almost immediately after their application to the cell. Furthermore, spikes are observed to cease soon after the stimulation is ended (Figure 3-2 (A) and (B)). These results are consistent with the ideas that: 1) tolbutamide and K^+ act by directly depolarizing the cell, since tolbutamide can bind to sulfonylurea receptor to close potassium channel and high concentration of K^+ also close potassium channel, and 2) the steps leading to exocytosis following depolarization are rapid. In contrast, the current was stable immediately following application of glucose stimulation (Figure 3-2 (C)). After a few seconds, however, the current began to fluctuate in a series of rapid spikes. In general, glucose stimulation is relatively slow to initiate secretion, but secretion is longer lasting. The slow step in stimulus-secretion coupling is apparently associated with the formation of internal messengers responsible for initiating depolarization. Glucose itself can not directly lead to depolarize the cell, since glucose has to be transported into the cell and metabolized and one of its metabolites, ATP, is suggested to be responsible for causing cell depolarization (112). Therefore, the time to initiate cell depolarization should be longer than that associated with tolbutamide and K^+ stimulations. As a result, the spiking occurrence is delayed. However, once the internal messenger responsible for cell depolarization is present, it can persist even after glucose is lowered back to non-stimulus levels. For glucose stimulation, spiking was generally observed to occur for over 2 min at both human and rat cells and for as long as 10 min for one occasion at human β -cells. Because of the need to "rest" the electrode, it was difficult to determine exactly the time between stimulation and beginning of spiking and how long the spiking continued. The

end of a series of current spikes was characterized by a decrease in the frequency of the spikes but not a change in their shape or height.

The frequency of spikes, determined by counting the number of peak maxim that occurred during a 5 s period, varied between 5 and 10 Hz for glucose stimulation, and between 1 and 4 Hz for tolbutamide and K^+ stimulations. The frequency of spiking, which refers to the frequency of vesicular fusion events on the portion of the cell surface sampled by the electrode, varies with the stimulation methods. This may be also due to different stimulus-secretion coupling mechanism involved.

Signal confirmation. The current spikes observed with different stimulation methods at different β -cells occur randomly at the electrode, which is expected if exocytosis is detected. However, the randomly occurring current spikes could also be some “noise”. Therefore, the hypothesis was that the current spikes represent rapid changes in insulin concentration at the electrode surface resulting from secretion of insulin by exocytosis. In testing the hypothesis, the other following sources of “noise” were considered: 1) sampling artifacts or electrical noise from external sources, 2) background currents generated by ion fluxes or potential fluctuations at the cell, and 3) anodic detection of other compounds released from the cell. In addition, an analysis of the spike frequency and areas was performed to determine if they were consistent with the hypothesis.

The possibility of external noise or sampling artifacts was eliminated by moving the electrode away from the cell following a glucose stimulation. If the external noise or sampling artifacts existed, they would be observed even when the electrode was far away

from the cell. An example of the data obtained from human β -cells is shown in Figure 3-3. The height and number of spikes decreased as the electrode was moved away from the electrode for all attempts of this experiment ($n=4$). Spikes were still observed if the electrode was moved closer to the cell again. The current spikes were dependent on the distance between the electrode and the cell. Similar results were also obtained with tolbutamide stimulation at rat β -cells. It was concluded that the spikes were due to the cell and not an external artifact.

The average width of the spikes, calculated as the full width at half-height from a random sampling, was 52 ± 11 ms ($n=33$) with a $15 \mu\text{m}$ cell-electrode spacing and 38 ± 13 ms ($n=38$) with a $1 \mu\text{m}$ spacing. These differences are statistically significant to a greater than 99% confidence level. (The peak widths are given only for comparison to each other and should not be taken as absolutely accurate since the spikes have been overfiltered, the detector time constant was 50 ms, and undersampled, the data collection rate only allowed a few points to be collected across the narrower peaks.) The trends observed in peak width and height are consistent with the notion that spikes are the detection of a packet of molecules diffusing to the electrode from the cell. If the spikes observed are indeed from the extrusion of vesicle contents following fusion of the vesicle with the cell surface, this is expected behavior. The mean vesicle diameter is around 350 nm, and thus, the origin of the concentration pulse can be considered as an instantaneous small source. As this packet of molecules diffuse toward the electrode, the concentration pulse spatially broadens by diffusion. The greater the diffusion distance, the more dilute and drawn out a concentration pulse will appear (113). The lack of spikes at a $30 \mu\text{m}$

distance is also consistent with the idea of detection of a diffusing packet of molecules. When the electrode is close to the cell, it effectively traps molecules which originate at the cell in a thin layer. As the electrode is pulled away, secreted molecules are more likely to diffuse away from the electrode without being detected.

Two experiments were performed to test the possibility of background currents being generated at the electrode by the cell. If background currents observed, the signal should not be as strongly dependent on the voltage applied at the electrode as faradaic current, and it may be observed on different types of electrode, in this case, modified electrode and bare electrode. In the first, measurements were taken from a glucose-stimulated cell with the electrode at +0.85 V and then at +0.4 V. An example of the two measurements is depicted in Figure 3-4. Decreasing the voltage to below the oxidation potential of insulin resulted in a quiet baseline compared to the signal at +0.85 V. This result was observed for every time spiking was observed. The current spikes are strongly dependent on the applied voltage at the modified electrode. Thus, these results are consistent with the idea that the current spikes are most likely due to faradaic current caused by oxidation of the secreted substances from the cell.

It has been demonstrated that spikes resulting from glucose stimulations at human β -cells were only observed when the electrode potential was sufficient to oxidize insulin (107). The voltage dependence of the signal also should be observed when other stimuli are applied to the cell. Figure 3-5 demonstrates that K^+ and tolbutamide stimulations produce current spikes with similar voltage dependencies. These results further imply

that the spikes are due to the anodic detection of a substance with an oxidation potential similar to insulin.

In a second experiment, measurements at glucose-stimulated cells using both an unmodified carbon-fiber electrode and a modified electrode were performed. A modified and a bare electrode were both held at +0.85 V and mounted in a dual electrode holder which held the electrode tips approximately 0.5 cm apart. The cell was stimulated with a modified electrode in place. If spiking was observed, the bare electrode was quickly positioned near the cell. A typical comparison of traces from the two electrodes is depicted in Figure 3-6. Current spikes were never observed for a bare electrode ($n=4$). Similar experiment results were also obtained at rat β -cells following tolbutamide application. It was expected that if the current spikes were due to a background current source, then similar noise would be observed at both electrode types. Furthermore, the current change would not vary with different insulin secretagogues and the current signal would not occur as spikes. Thus, this experiment also discounts the possibility of background currents being generated by the cell.

These results, taken with those in Figure 3-2 and Table 3-2, demonstrate that the spikes detected following application of tolbutamide, K^+ , and glucose to rat and human cells correspond to detection of chemicals secreted from the cell. In other words, the current spikes are not electrical artifacts or background current changes.

A final possibility that was considered was that another chemical species was secreted by the cell resulting in the observed currents. Fast scan cyclic voltammetry is often used to identify substances detected electrochemically in biological systems (69,

75). In this case, voltammetry is difficult to use and would not provide definitive evidence. The large background currents due to the electroactive film on the surface prevent the use of scan rates high enough to measure rapid concentration fluctuations. In addition, since the film works at least partially by electron mediation (99, 102), all substances oxidized yield voltammograms similar to the surface waves. Therefore, voltammetric identification was not pursued.

The first approach was to determine if substances known to be secreted by the cells would be oxidized by the electrode. The other primary constituents of the vesicles that are released with insulin are C-peptide, proinsulin and ATP(114). Proinsulin is present in low levels in the vesicles and is not likely to be detected (2). ATP and C-peptide, although present in high levels in β -cell vesicles, were not detectable by the electrode in flow injection experiments at 1 mM and 1 μ M, respectively.

Catecholamines such as norepinephrine (NE) are also suspected to be present in the vesicles and released simultaneously with insulin (114). NE is detectable at the Ru-O/CN-Ru-modified electrode, therefore the observed spiking could be due to detection of NE. However, NE is also detectable at a bare electrode and no significant signals have been observed at bare electrodes (see Figure 3-6). The detection limit for NE by modified electrodes was 50 nM compared to about 80 nM for bare electrodes. (Detection limits were calculated as for insulin in the flow stream. The slightly better detection limits were due to larger signals obtained using the modified electrodes.) Given the similar sensitivities of the two electrode types, it is reasonable to conclude that the absence of spikes observed using bare electrodes indicates that NE does not significantly

contribute to the spikes observed using modified electrodes. This may be due to a low level of NE present in the vesicles.

5-hydroxytryptamine (5-HT) is also thought to be contained in β -cells and cosecreted with β -cells (46). However, 5-HT can be easily oxidized on bare carbon fiber electrode. If 5-HT concentration is high enough to be detected, the current spikes should be observed at bare electrode after application of insulin secretagogues. It should be noted that there may be unknown constituents of the vesicles which were not tested for here and which may have contributed to the spikes.

Chromatographic Analysis of Islet Releasates. Although it is clear that the electrodes used in these experiments detect insulin (97, 107), it is not clear that the secreted molecules which are detected as current spikes are only due to insulin.

In order to further identify the secreted substance(s) detected at the electrode, HPLC analysis of releasates from islets of Langerhans was performed. The electrode used for detection was identical to that used for single cell measurements except it was larger to accommodate the HPLC system. Figure 3-7 illustrates results from this experiment. The pre-stimulation background chromatogram, obtained by injecting incubation media (KRB) from islets prior to stimulation, shows a few small peaks. The large peak occurring early in the chromatogram is due to the injection of KRB onto the column. Clearly the dominant change in the chromatogram after incubation of islets with tolbutamide is the appearance of peaks due to rat insulin I and II. No other peaks are observed to change significantly. Equivalent results were obtained when using mobile phases with different organic content (5% and 50% acetonitrile were used), different

chromatography columns (hydrophobic interaction stationary phase), and human islets. These results performed by Mr. Hong Shen demonstrate that insulin was the only substance that was secreted at a high enough level to be detected at the electrode.

The Ru-O/CN-Ru electrode is not especially selective for insulin; however, it is not surprising that it can be successfully used for monitoring insulin in these experiments when one considers the unique environment around a β -cell. The most obvious chemical change outside a β -cell following stimulation is the release of vesicular contents. Although many substances are present in vesicles, the dominant compounds are insulin and C-peptide. It has been demonstrated that 80% of the protein in a vesicle is an equimolar mixture insulin and C-peptide (115). Since C-peptide is not detected at the electrode as discussed above (107), insulin is the main protein that could be detected. Although many other proteins are known to be present in the vesicle, and some may be detected, they are at such low levels relative to the insulin that they do not contribute significantly to the spikes observed. The most likely proteinaceous interferent is amylin. Amylin has been shown to be present at up to 10% of the level of insulin in a vesicle (116). As a disulfide containing peptide, it is detectable at the electrode with a similar sensitivity to insulin. However, amylin, which has a retention time of 12.2 min on the HPLC column used for these experiments, was not secreted at a high enough level to be detected for the cells used here.

Ca²⁺ Dependence of Signals. In order to support the hypothesis that the signal measured by the electrode is due to insulin secreted from the β -cells by exocytosis, it is necessary to establish the dependence of the signal on extracellular Ca²⁺, since it is well

known that external Ca^{2+} is required to support exocytosis when β -cells are stimulated with depolarizing secretagogues such as sulfonylureas and high concentrations of K^+ (117). After the depolarization of the cell membrane, Ca^{2+} enters the cell through voltage-dependent channels. The increased concentration of intercellular Ca^{2+} triggers exocytosis where vesicle membranes fuse with the cell wall and vesicle contents are subsequently expelled to the cell exterior. Thus, only the last step in the secretion process is dependent on Ca^{2+} . Removal of Ca^{2+} from the media allows most of the ion influx into the cells and potential fluctuations around the cell to occur while preventing insulin secretion. Thus, if insulin is the source of the signal at the cells, the stimulation in Ca^{2+} -free media should result in no observed signal. An electrical artifact would most likely still occur in Ca^{2+} -free media however.

In order to ascertain the Ca^{2+} dependence of the signals observed, two experiments were performed when the cells were stimulated in Ca^{2+} -free media. In the first experiment, stimulations were performed by applying 200 μM tolbutamide with 2.4 mM Ca^{2+} and 200 μM tolbutamide without 2.4 mM Ca^{2+} to the same cell. Figure 3-8 shows the results obtained from this type of experiment. Clearly a high frequency series of spikes can be observed when tolbutamide and Ca^{2+} are applied to the cell in Ca^{2+} -free media. In contrast, only a background shift was observed when tolbutamide by itself is applied to the cells. Similar experiments performed with K^+ stimulations produced similar results.

The second experiment was also performed to further support the hypothesis that current spikes are due to detection of exocytosis, and signal obtained are due to both

effects of stimulus and extracellular Ca^{2+} . This was accomplished by comparing the signal obtained at the same cell after the application of stimulus solution containing 2.4 mM Ca^{2+} with 200 μM tolbutamide and solution containing only 2.4 mM Ca^{2+} but no tolbutamide. The results are illustrated in Figure 3-9. Based on the signal observed from the experiment, the current spikes were only observed when both tolbutamide and Ca^{2+} were applied to the cell. Spikes were barely observed in the absence of a secretagogue. Table 3-3 summarizes the Ca^{2+} dependence data for different types of stimulations. In general, current spikes occurred only when Ca^{2+} was present in the stimulation media. Therefore, it is concluded that the spikes observed are strongly dependent on extracellular Ca^{2+} . Furthermore, this supports the idea that the spikes are due to detection of stimulus-coupling insulin secretion from single pancreatic β -cells by exocytosis.

Current spike shapes. Analysis of spike shapes can help to support the hypothesis that current spikes are due to detection of insulin secretion by exocytosis. It has been suggested that the shape of current spikes due to detection of exocytosis is diffusion controlled (82). In many cases, the spikes occur at a rate that causes them to overlap and form a broad envelope as in Figure 3-6(A) and Figure 3-8. In these cases, it is difficult to evaluate the shapes and area of individual spikes. At other times however, such as in Figure 3-6(C), the rate of spike generation was low enough that apparently resolved spikes could be seen. Figure 3-10 shows examples of spikes that were resolved from neighboring spikes. The spikes rise rapidly with typical rise times of 25 to 40 ms. Given that the filter setting was 20 Hz, it is likely that the spikes were changing faster than could be detected using this system. Qualitatively, the fast rise and drawn out decrease of

the spikes is consistent with idea of a rapidly opening vesicle followed by diffusion from the point of exocytosis to the electrode (82). Quantitative analysis of the peak shapes will require an improved detection system that does not distort the peaks. Attempts to use wider bandwidths for the measurement have been made and will be discussed in next chapter.

Spike areas. Analysis of the area of current spikes is also useful in testing the exocytosis hypothesis. As mentioned before, the vesicle size is much smaller than the size of the electrode used in this work, therefore, sites of exocytosis on the cell surface would be expected to be spatially localized with respect to the sampling electrode. Thus, the current spikes appear to be a consequence of fusion of the storage vesicles, release of the vesicle contents and subsequent diffusion of insulin molecules to the electrode. A packet of insulin molecules secreted by exocytosis diffuse to the electrode and are oxidized immediately, which results in the signal on the electrode in the form of current spikes.

Therefore, single spikes could be considered detection of entire contents (all substances which could be oxidized on the electrode) from a single exocytotic event, and multiple spikes would represent detection of multiple exocytotic events occurring at the same time which cannot be resolved temporally (spikes temporarily separated by < 2 msec would appear emerged as one) (76). Thus, if a spike represents the detection of insulin secreted by exocytosis of a single vesicle, then the area under the spikes would depend on the number of moles contained in the vesicle and the number of moles captured by the electrode.

Although the patterns of spikes that are observed vary with different stimulations, the area under isolated spikes does not vary significantly with stimulation as shown in Table 3-4. This is because the area of the spike measured in amperometric mode, which has units of coulombs, represents the charge passed to oxidize the compound(s) detected. The charge passed is directly proportional to the number of moles oxidized according to Faraday's law, which is $Q = nNF$, as described in chapter 1. If a spike represents the detection of the contents of a vesicle, the mean value observed should be independent of the stimulation method since acute stimulations should not affect the vesicular content. Different stimulations may, however, affect the overall frequency and number of exocytosis events that occur as described before.

Some limitations of the measurements need to be considered for quantitative interpretations (76). For example, some spike areas may be underestimated because not all of the vesicle contents passed to the electrode surface. Errors could arise in the estimation of the area of spikes that are superimposed on the secretion envelop in some cases (Figure 3-8). Some small spikes could also be lost in the noise. The observed spike frequency only reflects the number of events adjacent to the electrode, not the total that occur, because the electrode only samples from a portion of the cell surface.

It is clear that the current spikes that have been measured are clearly due to detection of a chemical that is secreted from the cell. Chromatographic results show that the primary substance secreted by the cells which can be detected by the electrode is insulin. These facts combined lead us to the conclusion that current spikes are due to detection of packets of insulin. The strong Ca^{2+} dependence, stimulation by known

secretagogues of insulin, constant area of spikes with stimulation, and apparently random occurrence of the spikes during a stimulation combine to provide a powerful argument that the current spikes are detection of exocytosis events occurring at the cell.

Distribution of spike areas. To further tie the current spikes to the vesicular contents of β -cells, it is useful to examine spike areas in more detail. A distribution of spike areas for human and rat β -cells is shown in Figure 3-11 and Figure 3-12, respectively. In constructing this distribution, only spikes that appeared well-resolved from neighboring spikes and had a smooth shape, suggestive of single events, were used. In addition, only spikes with a signal to noise ratio greater than 5 were used. The spike area, which has units of charge, can be converted to a number of moles oxidized by Faraday's law as described in chapter 1. Using isolated spikes and the value of 1.1 ± 0.1 electron per mole (measured as described in experimental section of chapter 2) the average spike area for human cells was 1.7 attomoles or 1.0×10^6 molecules of insulin. For rat cells, the average spike area corresponds to 1.6 attomoles or 9.6×10^5 molecules of insulin. A previous estimate for the maximum amount of insulin per vesicle in rats was 8 to 9.6×10^5 molecules (118). Thus, the values show good agreement with these upper limits. The average value may be skewed to higher values since smaller vesicle contents could give signal to noise ratio less than 5.

With a knowledge of vesicle sizes and their distribution, and the assumption that the concentration of insulin is constant in vesicles and electron microscopy has shown they are spherical, it is possible to write a probability density function that predicts the frequency of spike area occurrences of a given charge (76). For the case of a Gaussian

distribution of vesicle sizes, the probability density function $f_Q(Q)$ is expressed by the following equation:

$$f_Q(Q) = \frac{1}{3\sigma \left[\left(\frac{\pi}{2} \right)^{1/2} + \left(\frac{\pi}{2} \left[1 - \exp\left(-\frac{\mu^2}{2\sigma^2} \right) \right] \right)^{1/2} \right]} \left(\frac{4}{3} \pi n F C Q^2 \right)^{1/3} \exp \left(-\frac{\left[\left(\frac{Q}{\frac{4}{3} \pi n F C} \right)^{1/3} - \mu \right]^2}{2\sigma^2} \right)$$

where μ (cm) is the mean vesicle radius, σ (cm) is the standard deviation of the vesicle diameters, Q (C) is the charge of the spike, and C (mole/cm³) is the concentration in the vesicle.

Vesicle sizes in human β -cells have been measured by electron microscopy and found to have an average diameter of 300 ± 61 nm (119). Using this data, the equation predicting the frequency of areas was fit to the actual data and a good correlation obtained ($R = 0.9732$) as shown in Figure 3-11. Similarly, the spike area distribution from rat β -cells could be fit with good correlation ($R = 0.9779$) using a diameter of 342 ± 43 nm as shown in Figure 3-12 (118). Thus, the distribution of spike areas that is observed can be attributed to the distribution of vesicle sizes that are expected to be encountered.

The equation used for making the correlations has a single adjustable parameter, that is the concentration of insulin in the vesicle. The concentration calculated to give the best fit in human cells was 118 mM insulin and for rat cells it was 74 mM. Previous studies had estimated an insulin concentration of 41.6 mM inside vesicles of rat insulinomas (115). As stated above, there may be some preference for measuring larger spikes, thus skewing the average to higher values in our case. In addition, semi-quantitative immunohistochemical studies indicate that insulinomas have lower concentrations of insulin per vesicle than primary β -cells (120). Given these differences,

the estimates of insulin concentration in the vesicle are in remarkable agreement. Thus, the concentration and amount of insulin detected in the current spikes correlates well with the amounts of insulin expected to be found in the vesicles.

Stimulation success rate. It is intriguing that current spikes were recorded at only 37% of the glucose-stimulated cells, 33% of the K^+ -stimulated cells and 32% for tolbutamide-stimulated cells. These numbers are in reasonable agreement with those obtained using the reverse hemolytic plaque assay which have shown that only 31.5% of isolated pancreatic β -cells secrete detectable amounts of insulin in response to 30 min incubations with 16.7 mM glucose (58). The reason for the low response rate of the cells is unknown, however it underscores the value of chemical evaluation at the single cell level.

Conclusions. The combined evidence shows that the current spikes that are observed at the electrodes following stimulation are due to anodic detection of insulin near the cell. The frequency and area of the spikes are consistent with the hypothesis that the detected substance is secreted by exocytosis. Thus the electrode has the sensitivity and time resolution to detect exocytosis events from individual β -cells based on anodic detection of secreted insulin molecules. This is the first time that secretion has been observed with this resolution at β -cells; thus many new opportunities for studying secretion should be afforded by the technique.

Table 3-2. Summary of Current Spike Observations for Three Different Stimulation Conditions.

Stimulus	Stimulus duration	Cell type	Cells tried	Cells responded	Initiation of spike activity*	Duration of spike activity**	Frequency***
16 mM glucose	30 s	human	30	10	60-240 s	180-300 s	6-10 Hz
60 mM K ⁺	10 s	human	35	13	0-2 s	5-9 s	1-3 Hz
500 μ M tolbutamide	10 s	human	37	12	0-2 s	4-9 s	2-4 Hz
16 mM glucose	30 s	rat	24	4	40-60 s	120-200 s	5-10 Hz
200 μ M tolbutamide	10 s	rat	74	18	0-2 s	3-9 s	1-3 Hz

*Initiation of spike activity refers to the time between the end of the stimulation and the beginning of spiking after application of stimulation solution.

**Duration of spike activity refers to the time for spiking observed to occur during and after stimulation.

***Frequency refers to the number of peaks observed during the spike activity divided by the duration of spike activity. Only peaks with heights 5x the peak to peak noise level were used. Note that the number of exocytosis events could be higher than this since overlapping spikes may yield a number of peaks lower than the actual number of spikes that occur.

Table 3-3. Analysis of Isolated Spike Areas for Different Stimulation Conditions.

Stimulation conditions	Cell type	# of spikes*	Spike area (pC)
16 mM glucose	human	61	0.23 ± 0.087
60 mM K ⁺	human	58	0.29 ± 0.16
100 μ M Tolbutamide	human	107	0.26 ± 0.097
500 μ M Tolbutamide	human	216	0.29 ± 0.17
200 μ M Tolbutamide	rat	528	0.23 ± 0.088
16 mM glucose	rat	63	0.20 ± 0.094

* Spikes with an amplitude at least 5x the peak to peak noise level were used. No effort was made to reject spikes that were not well-resolved from neighbors. Mean \pm SEM is given.

Table 3-4. Summary of Ca^{2+} Dependence for Tolbutamide and K^+ stimulations.

Stimulation conditions*	Species	# of cells	# of current spikes/stimulation**
200 μM tolbutamide/ 2.4 mM Ca^{2+}	human	16	33 ± 10
200 μM tolbutamide/ no Ca^{2+}	human	6	0.2 ± 0.2
2.4 mM Ca^{2+}	human	6	1.5 ± 0.9
60 mM K^+ / 2.4 mM Ca^{2+}	human	8	14 ± 2
60 mM K^+ / no Ca^{2+}	human	8	0.9 ± 0.7
200 μM tolbutamide/ 2.4 mM Ca^{2+}	rat	6	9.6 ± 1.9
200 μM tolbutamide/ no Ca^{2+}	rat	6	0.2 ± 0.2

*Stimulation buffer consisted of Ca^{2+} free KRB with 3 mM glucose plus the agents indicated. Ca^{2+} and K^+ were added as the chloride salts. Stimulants were applied from a pipette for 10 s as described in the experimental section.

**The number of peaks greater than 5x the peak-to-peak noise level were counted. Mean \pm SEM is given.

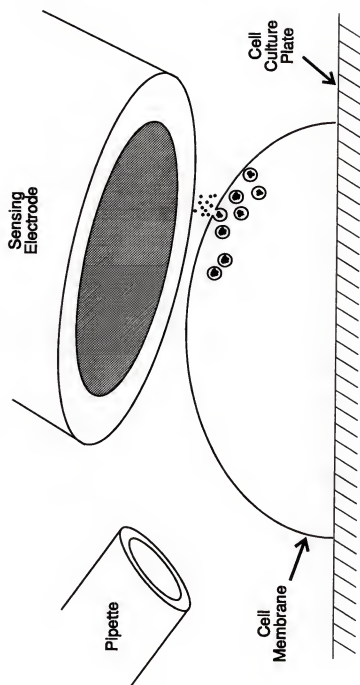


Figure 3-1. The schematic diagram of electrode and pipette placement for monitoring insulin secretion from single β -cell. The pipet is filled with stimulation solution.

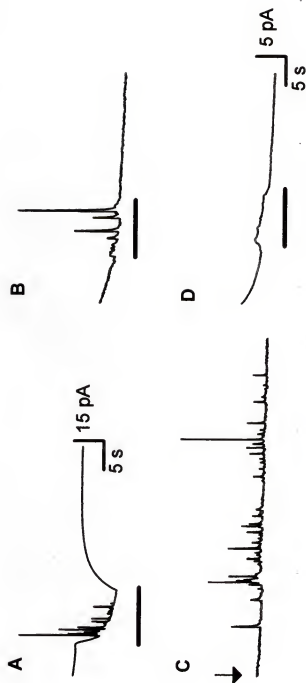


Figure 3-2. Current recordings from stimulation of human β -cells with: A) 200 μ M tolbutamide, B) 64 mM K^+ , C) 16 mM glucose, and D) KRB. A), B), and C) were obtained at different cells. D) was obtained from the same cell as B). Bars indicate stimulation except for the glucose case, where the arrow indicates the end of a 30 s stimulation. Scale bars on section (D) also apply to sections (B) and (C). All data were obtained by EI-400.

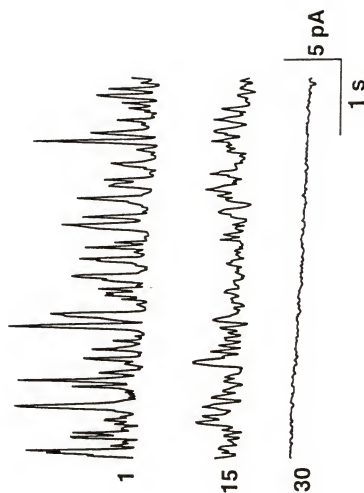


Figure 3-3. The effect of distance between electrode and cell on signal measured at a glucose-stimulated human β -cell. The numbers beside the recording indicate the distance in μm . The data were collected by EI-400.

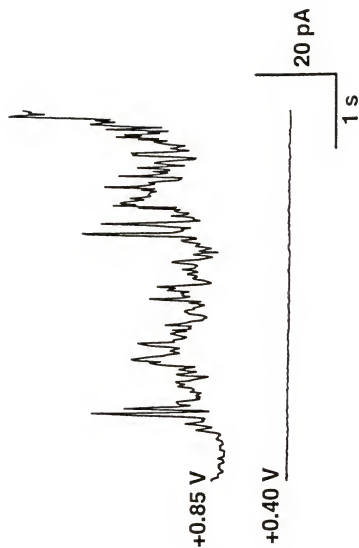


Figure 3-4. The effect of electrode voltage on amperometric recording at a glucose-stimulated human β -cell. Data were collected by EI-400.



Figure 3-5. Voltage dependence of K^+ and Tolbutamide induced current spikes. A) Current recordings from stimulation of rat β -cell with 200 μ M tolbutamide and electrode at +0.85 V. B) Repeat of (A) with electrode at +0.40 V. C) Current recordings from stimulation of human β -cell with 64 mM K^+ and electrode at +0.85 V. D) Repeat of (C) with electrode at +0.40 V. Data were collected by EI-400.

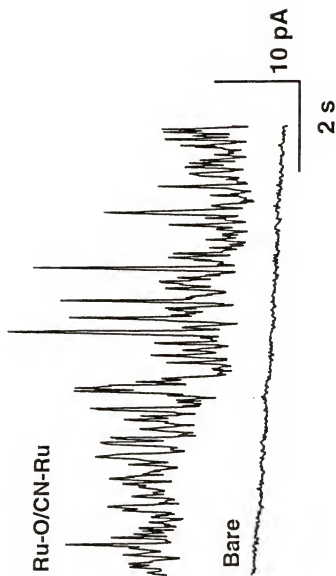


Figure 3-6. Comparison of amperometric recording from a single, glucose-stimulated human β -cell using a bare (unmodified) carbon-fiber microelectrode and a Ru-O/CN-Ru-modified electrode. Data were collected by EI-400.

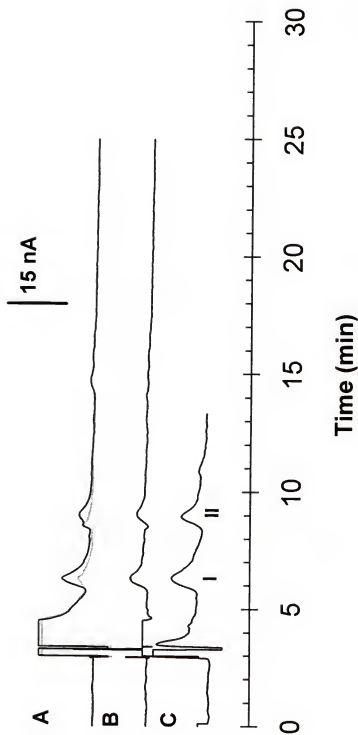


Figure 3-7. Chromatograms from releasates of islets of Langerhans. (A) Samples injected were supernatant following 15 min incubation over 100 islets in KRB (light line, pre-stimulation chromatogram) and supernatant from same islets incubated with 200 μ M tolbutamide for 15 min (dark line, stimulated islet chromatogram). (B) Subtraction of pre-stimulation chromatogram from stimulated islet chromatogram in (A). (C) Sample injected was rat I and II insulin as indicated on the chromatogram. Total concentration of insulin was 3 μ M in KRB. Data were collected by Hong Shen.



Figure 3-8. Ca^{2+} dependence of tolbutamide induced current spikes. The same cell was used for all recordings. The cell was in Ca^{2+} free KRB. The bar indicates the stimulation. In all cases the stimulating solution contained $200 \mu\text{M}$ tolbutamide. The tolbutamide dissolved in (from left to right): Ca^{2+} -free KRB, KRB (includes $2.4 \text{ mM } \text{Ca}^{2+}$), KRB (includes $2.4 \text{ mM } \text{Ca}^{2+}$), and Ca^{2+} -free KRB. 5 min were allowed between each stimulation.



Figure 3-9. Comparison of signal observed on application of tolbutamide with Ca^{2+} and Ca^{2+} -free KRB. A) 10 s puff of KRB buffer with 2.4 mM Ca^{2+} containing no tolbutamide. B) 10 s puff of stimulation solution with 2.4 mM Ca^{2+} and 200 μM tolbutamide. the bar indicates the stimulation. The experiments were performed in Ca^{2+} -free KRB solution.

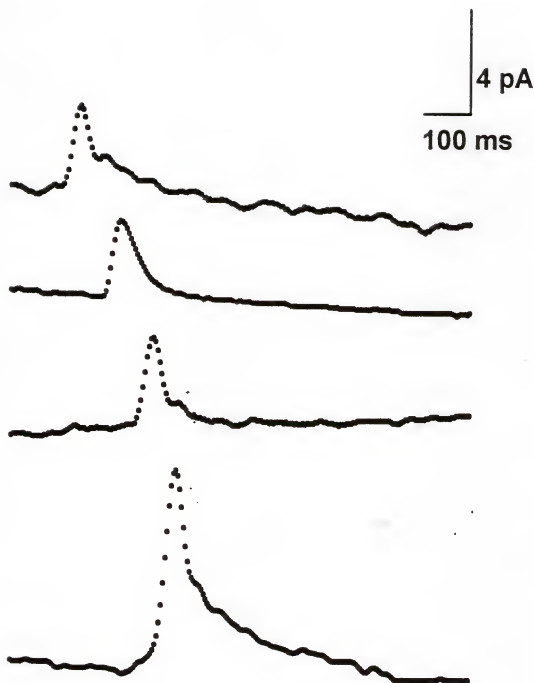


Figure 3-10. Examples of isolated spikes recorded at single β -cells. In all cases, the data were collected at 220 Hz (data points 4.5 ms apart). From top to bottom, the current spikes are from: a human β -cell after glucose stimulation, a rat β -cell after glucose, a human β -cell after tolbutamide stimulation, and a rat β -cell after tolbutamide stimulation.

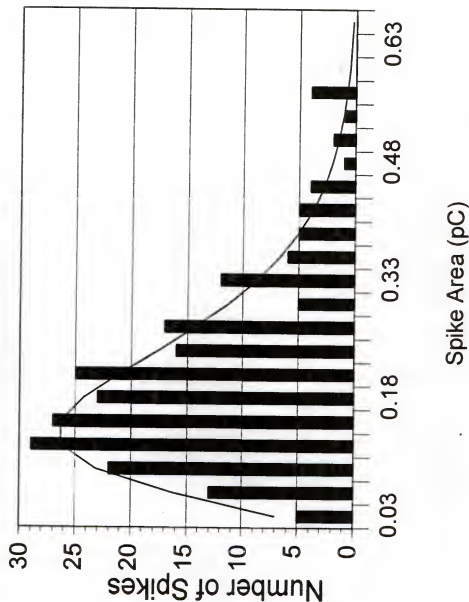


Figure 3-11. Distribution of spike areas measured by amperometry at single human β -cells. Data is combined from tolbutamide and glucose stimulations (222 spikes). Only isolated spikes defined as those which showed a smooth shape similar to that in Figure 3-11, were used. Solid line is the best fit from the probability density function with 118 mM as the insulin concentration per vesicle.

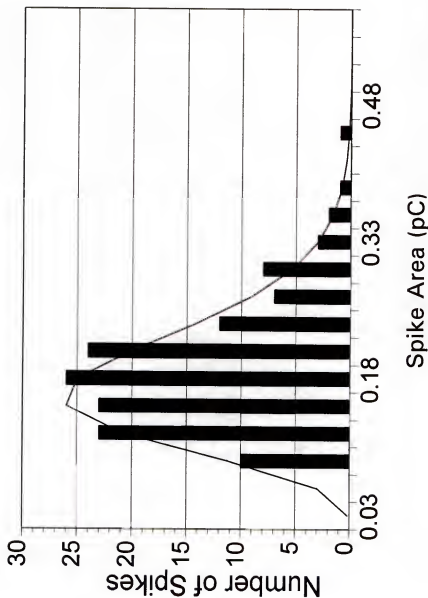


Figure 3-12. Distribution of spike areas measured by amperometry at single rat β -cells. Data is combined from tolbutamide and glucose stimulations (140 spikes). Only isolated spikes, defined as those which showed a smooth shape similar to that in Figure 3-11, were used. Solid line is the best fit from the probability density function with 74 mM per vesicle.

CHAPTER 4

COMPARISON OF 5-HYDROXYTRYPTAMINE AND INSULIN SECRETION

Introduction

The amperometric method has been successfully applied to detection of insulin secretion from single pancreatic β -cells (107, 121), as described in chapter 3. In this case, a chemically modified carbon fiber microelectrode is used to catalyze oxidation of insulin. Although this method is able to detect single exocytosis events, there are some limitations to its use. The modified electrode is more difficult to prepare than simple carbon fiber electrodes. In addition, the modified electrode is not very stable at physiological pH as described in chapter 2. The electrode has to be “rested” at low potential during each measurement. Thus, measurements can only be made for brief periods.

Because of the limitations of using the modified electrode, it may be useful to consider other approaches for studying insulin release. An alternative to directly measuring insulin released from β -cells is to measure secretion of a marker (a substance that is co-secreted with insulin). If the marker is easily oxidized, then it would be possible to use a simple carbon fiber electrode to detect secretory activity at single β -cells. It has been suggested that 5-hydroxytryptamine (5-HT), which is easily oxidized at carbon fiber electrodes, may be a good marker for insulin secretion (122-124).

Pancreatic β -cells, in common with many endocrine cells that secrete polypeptide hormones, will accumulate or “load” biogenic amines from extracellular medium (125, 126). Studies involving ultrastructural histochemistry, fluorescence microscopy, autoradiography and electron microscopy have provided evidence that amines are stored in insulin-containing secretory vesicles of the β -cells (127-129). Thus exocytosis should cause release of 5-HT in addition to insulin as shown in Figure 4-1. Indeed, measurements from whole mouse islets have shown that insulin and accumulated 5-HT are released simultaneously following glucose stimulation (122). Although this data supports the notion that 5-HT release is a good marker for exocytotic insulin secretion, the data are not unequivocal. For example, time-resolved data show that the ratio of insulin to 5-HT released changes during a stimulation (122). This is not expected if 5-HT and insulin are co-released from the same secretory granules by exocytosis. More recently, amperometry has been used to measure accumulated 5-HT release from β -cells (123, 124). In this case, 5-HT secretion is detected as a series of current spikes which have many of the characteristics expected of exocytosis. Furthermore, the spikes occur under conditions which are expected to cause insulin secretion. These findings suggest that 5-HT is released by exocytosis and may be used as a marker for insulin secretion.

In this chapter, the secretion of accumulated 5-HT and insulin from single rat and dog β -cells as recorded by amperometry are discussed. The goal is to determine the benefits and limitations of using 5-HT as a marker of insulin secretion as compared to direct measurement of insulin. It is found that exocytosis events for 5-HT and insulin occur with similar patterns; however, the shape of individual current spikes are different

suggesting differences in the mechanism of clearance from the vesicles for the two analytes.

Experimental

Electrode preparation and testing. For detection of 5-HT, glass encased carbon fiber microelectrodes were prepared using previously described techniques in chapter 2. For detection of insulin, the electrodes were further treated by electrochemical deposition of Ru-O/CN-Ru (107) as also described in chapter 2.

Electrodes were tested in a flow injection system similar to that described in chapter 2. The number of electrons transferred per oxidation (n) for 5-HT was determined using chronoamperometry at a microelectrode according to a previously described method in chapter 2. For this experiment, the background subtracted steady state current (Δi) was measured following a potential step from +0.10 V to +0.65 V. (All voltages are versus SSCE.) The pulse was 3 s each time. Values for n were calculated according to the following equation: $n = \Delta i / 4rCDF$ where r was the radius of the electrode (disk carbon electrodes were used for these experiments), C was the concentration of 5-HT, D was the diffusion coefficient, and F was the Faraday constant. 1 mM 5-HT was dissolved in KRB buffer with 20 mM HEPES instead of sodium bicarbonate, at pH 7.4. The disk electrode was made by polishing the electrode at 65° angle. The number of electron transferred per oxidation for 5-hydroxytryptamine is 2.0 ± 0.1 (average of 3 experiments and standard deviation).

Data collection and analysis. Data for single cell measurements and electrode testing were collected using a Keithley 427 current amplifier and voltages were applied to

the reference electrode using a battery and voltage divider circuit. In most cases, data were collected at 60 to 100 Hz by an IBM-compatible personal computer (Gateway 2000 486-66 MHz) via a National Instruments (Austin, TX) multifunction board (AT-MIO16-F5) and low pass filtered at 30 Hz. For high resolution recordings, data were collected at 3 to 6 kHz and low pass filtered at 333 Hz. Areas of currents spikes were measured using locally written software from University of North Carolina, called Tim-Stat. In data analysis, spikes were used only if their peak height was three times the peak to peak noise. All mean values are reported \pm 1 standard deviation. Statistical differences between means were evaluated using a two-tailed Student's t test.

Islet isolation and cell culture. All the procedures for rat islets isolation and cell dispersion are the same as described in chapter 3. The dog islets were supplied by University of Miami, Medical Center. The dispersion of dog islets were similar to the procedures used for human islets as described in chapter 3.

Single cell measurements. Single cell measurements were performed in a manner similar to that described in chapter 3. For accumulation of 5-HT, loading buffer which consisted of 1 mM 5-HT dissolved in modified Kreb's Ringer buffer (KRB, 118 mM NaCl, 5.8 mM KCl, 2.4 mM CaCl_2 , 1.2 mM MgSO_4 , 1.2 mM KH_2PO_4 , 20 mM 2-(N-hydroxyethyl)piperazin-N'-yl)ethanesulphonic acid (HEPES), and 3 mM d-glucose) was used. The loading buffer does not necessarily need to be sterilized. However, if the loading buffer is sterile, it is necessary to perform the loading steps in the sterile hoods. The culture media was completely removed by sterile glass pipet and about 2 mL loading buffer was added to the petri dish containing cells. Then the cells were incubated for 2

hours at 37 °C, 5% CO₂ in the incubator. In some cases, loading was performed overnight in sterile modified CMRL 1066 culture media containing 1 mM 5-HT at 37 °C, 5% CO₂. To make this loading culture media, 5-HT was simply dissolved in modified CMRL 1066 media and were filtered to be sterile. After loading, the cells were rinsed 3 times with room temperature modified KRB. The Petri dish filled with modified KRB was placed in a microincubator maintained at 37 °C (Medical Systems, Inc.) on the stage of an inverted microscope (Zeiss axiovert 35) without bubbling 5 % CO₂, 95% air for controlling pH. Single cell measurement was done in the same way as described in chapter 3. To perform 5-HT measurements, the sensing tip of a carbon fiber microelectrode was brought to within 1 µm of a cell using a micropositioner (Burleigh PC-1000). For measurement of insulin secretion, the cells were not allowed to accumulate 5-HT and a Ru-O/CN-Ru electrode was used for detection. The cells were bathed in KRB for the insulin measurements since HEPES interferes with the insulin measurement. For 5-HT measurements, the sensing electrode was at +0.65 V unless noted otherwise.

Stimulants were dissolved in the media used for bathing the cells. For glucose stimulation, the total glucose concentration was 16.7 mM. Tolbutamide stimulations (200 µM) were 10 s duration and glucose stimulations were 30 s duration.

Ca²⁺-free experiment. Same as described in chapter 3.

Results and Discussion

Glucose stimulations. Figure 4-2 illustrates amperometric recordings taken with a bare carbon electrode at a 5-HT loaded β-cell (16 and 2 hour incubation) and with a Ru-

O/CN-Ru electrode at an untreated β -cell following glucose stimulation. The current spikes detected by the modified electrode have previously been shown to be detection of insulin secretion by exocytosis (121). (The downward drift in the current recording for the Ru-O/CN-Ru electrode is characteristic of this electrode and occurs in the absence of cells (Figure 4-2 (C)). The down drift of the bare electrode used for detection secretion of 2 hour incubation (Figure 4-2 (B)) is probably due to the bad sealing at the electrode tip, since most of this batch of bare electrodes had this problem, not other batches, as shown in Figure 4-2 (A).) The current spikes detected at bare electrodes were only observed if the cells had been loaded with 5-HT. As summarized in Table 4-1, the spikes due to 5-HT and insulin following glucose stimulation were similar in numbers of spikes that were detected, the delay between stimulation and the first spikes (about 20 to 30 s), and the duration of spike activity (about 200 s). No statistical difference was found for any of these parameters between detection of 5-HT (2 or 16 hour incubation) and insulin. The most notable differences were for the 16 hour incubations which showed higher numbers of spikes and larger variability in the time to first spike than the other two conditions. This may be due to fact that these experiments were performed on different batches of cells. It may also be because after 16 hour incubations, the spikes were larger, which means their peak areas bigger than those obtained after 2 hours incubation (see Table 4-2). Therefore, the large spikes were easier to detect.

The pattern of occurrence of spikes was evaluated in more detail by comparing the time interval (Δt) between spikes for both insulin and 5-HT detection. Histograms of time intervals for insulin and 5-HT following glucose stimulation are shown in Figure 4-

3. As shown, the patterns for 5-HT and insulin spike occurrence are similar for both stimulation conditions. The time intervals apparently have an exponential distribution which is characteristic of random, unrelated events (130). The histogram data were fit to the following probability density function to determine the time constant (τ) for occurrence of spikes:

$$F(t) = (1/\tau)\exp(-t/\tau)$$

where $F(t)$ is the frequency of occurrence of time intervals with value t . The time constants were similar. For 5-HT detection, the time constant was 0.51 s (correlation coefficient of 0.996) and for insulin the time constant was 0.45 s (correlation coefficient of 0.970). This time constant can be used to compute the probability of detecting two events within the time of an average spike (131). The time of an average spike is about 37 ms and 7 ms for insulin and 5-HT, respectively, which was determined by the half-height peak width obtained at high time resolution (details in chapter 5). The probability distribution function $P(t) = F(t) * \tau$, which gives the probability of finding events separated by a time equal to or longer than t . Then the probability of finding two events separated by a time smaller than or equal to t , is simply given by: $1 - P(t) = (1 - \exp(-t/\tau))$. Therefore, the probability of temporally overlapping spikes is 0.07 and 0.015 due to insulin and 5-HT secretion, respectively, which are very small. Thus, it is reasonable to consider a single spike is detection of a single exocytotic event.

In addition to a similar pattern of occurrence, the spikes observed at the bare electrode and the Ru-O/Ru-CN electrode have the characteristics of diffusion-controlled spike shape as shown in the insets of Figure 4-2. The spikes observed with the modified

electrode have previously been demonstrated to be detection of concentration pulses of insulin secreted by exocytosis (107, 121). This shape is qualitatively what would be expected for diffusion of analyte from a point source, such as exocytosis event, to the electrode (82). The main difference between the spikes measured by the two different techniques is their area as shown in Table 4-2. However, at this point, these spikes were filtered at low frequency (30 Hz), the rising part of the spike shapes could be distorted. In order to investigate the details of exocytosis process, the spike shapes obtained at high filtering frequency are discussed later in this chapter.

Tolbutamide stimulations. Another insulin secretagogue, tolbutamide was also used to study the similarity of secretion patterns of insulin and 5-HT. Figure 4-4 illustrates amperometric recordings taken with a bare carbon fiber microelectrode at a 5-HT loaded β -cell (2 hour incubation) and with a Ru-O/CN-Ru electrode at an untreated β -cell following tolbutamide stimulation. The current spikes at the modified electrode have previously been shown to be detection of insulin secretion by exocytosis (107). As with glucose stimulation, the current spikes detected at bare electrodes were only observed if the cells had been loaded with 5-HT. Furthermore, the current spikes were only observed if the electrode potential was sufficient to oxidize 5-HT as shown in Figure 4-5. No spikes were observed when +0.24 V was applied to the electrode. As summarized in Table 4-1, tolbutamide stimulation resulted in a small number of spikes that began within about 1 s of stimulation and continued for several seconds whether detecting 5-HT or insulin. No statistical difference was found for latency, duration, or numbers of spikes between detection of 5-HT and insulin. However, for both 5-HT and insulin, the latency,

duration, and numbers of spikes were significantly less for tolbutamide stimulation than for glucose stimulation.

The area of spikes due to insulin was independent of stimulation method as illustrated in Table 4-2. This is expected since spike area is a direct measure of the amount detected per exocytosis event (76), and should not vary with acute stimulations. Similarly, the area for 5-HT detection after 2 hour loading was independent of stimulation method (Table 4-2). However, as shown for glucose stimulation data in Table 4-2, a longer incubation time significantly increased the spike area for 5-HT. When β -cells are incubated in 5-HT loading solution, 5-HT is taken up by cells through passive flux (132). Therefore, longer incubation time would accumulate more 5-HT and stored in β -cells.

Ca^{2+} dependence of signal. Since the pattern of 5-HT secretion is similar to that of insulin secretion after application of glucose and tolbutamide to the cell, it is suggested that 5-HT is also secreted by exocytosis. In exocytosis process, it is well known that external Ca^{2+} is required to trigger exocytosis when β -cells are stimulated with depolarizing secretagogues such as tolbutamide (117). In order to ascertain the Ca^{2+} dependence of the signals observed from 5-HT loaded cells, the cells were stimulated in Ca^{2+} -free media. Stimulations were performed by applying 200 μM tolbutamide with 2.4 mM Ca^{2+} and 200 μM tolbutamide without Ca^{2+} to the same cell. An example of the amperometric recordings from such an experiment is shown in Figure 4-6. When Ca^{2+} -free tolbutamide solution was applied to the loaded β -cell, no spikes were observed. (The hump which occurred in Figure 4-6 (B) during stimulation is an artifact from the application of stimulant solution). When the stimulus with Ca^{2+} was used, a series of

current spikes was obtained. On average, 12.6 ± 12.9 spikes were observed with Ca^{2+} ($n = 5$) and no spikes were observed without Ca^{2+} . These results clearly demonstrate that the spikes observed at 5-HT loaded cells using carbon fiber microelectrodes are due to a Ca^{2+} -dependent process in the cells. A similar dependence on Ca^{2+} has been observed for the spikes at the Ru-O/CN-Ru electrode for insulin secretion as described in chapter 3 (121).

The average area of spikes measured in Ca^{2+} -free media from 5-HT loaded cells was 70.3 ± 74.0 fC ($n = 132$). This value is significantly higher ($p < 0.005$) than that obtained for tolbutamide elicited spikes from cells continually bathed in media containing Ca^{2+} (Table 4-2). In contrast, the area for insulin spikes were not affected by incubating the cells in Ca^{2+} -free media prior to the stimulation (see Table 4-2).

A time interval analysis was also performed on current spikes obtained following tolbutamide/ Ca^{2+} stimulations in Ca^{2+} -free buffer. The histogram and curve fit is shown in Figure 4-7. The time constant for the tolbutamide stimulations was similar for both analytes, but were about twice those found for glucose stimulations. For insulin the time constant was 0.92 s (correlation coefficient was 0.994) and for 5-HT release, τ was 1.1 s (correlation coefficient was 0.983). The good fit to an exponential equation again suggests random events.

Detection of 5-HT Secretion. Quantitative evaluation of the natural occurrence of indoleamine and catecholamine in rat islets has given conflicting results (126, 133, 134). In all cases however, the total amount of amine found in islets is low. For example, a study using HPLC with electrochemical detection (134) reported that rat islets contain

undetectable quantities of 5-HT and a total of 22 $\mu\text{mole/kg}$ of catecholamine (norepinephrine, epinephrine, and dopamine). While it is possible that biogenic amines are released simultaneously with insulin under normal conditions, catecholamine or 5-HT release have been unable to be detected in untreated β -cells using carbon fiber microelectrodes as described in chapter 3. This is expected considering the likely amine content of individual vesicles as illustrated with the following calculation. A single β -cell has a volume of 900 fL assuming it is a sphere with a 12 μm diameter. At a density of 1 g/mL, this volume corresponds to 900 pg of tissue. At 22 $\mu\text{mole/kg}$, a single β -cell would contain 20 amol of catecholamine. Assuming that all of the amine is in insulin secretory vesicles, and using a value of 13,000 vesicles/ β -cell (135) it can be calculated that a single vesicle should contain 1.5×10^{-21} moles of catecholamine. This level is below the detection limit of our system.

Because of the low natural levels of amine, it is necessary to use uptake by the β -cell to increase the concentration of 5-HT so that a detectable amount is secreted. With 5-HT loaded cells, current spikes were observed following treatment of β -cells with insulin secretagogues at carbon electrodes. The requirement for 5-HT loading, the dependence of the signals on electrode potential, and the known uptake of 5-HT by β -cells (136) provide substantial evidence that the current spikes seen are due to 5-HT released from the β -cells.

Comparison with Insulin Secretion. The pattern of spikes due to 5-HT matches well the patterns of insulin spikes that were observed following tolbutamide and glucose stimulation at Ru-O/CN-Ru electrodes. The time constant, time to start, duration and

number of spikes are nearly identical for both 5-HT and insulin for both stimulation methods. Furthermore, the patterns of spikes in both cases correspond well with what is known about stimulus-secretion coupling in β -cells. For example, tolbutamide should cause a rapid onset of secretion since it acts by closing a K^+ channel to depolarize the cell which should rapidly lead to exocytosis. In addition, once the tolbutamide is removed, it would be expected that the secretion would end soon afterwards. As in Figure 4-4, the spikes end soon after end of tolbutamide stimulation. With glucose stimulation, a delay in onset of secretion may be expected since secretion requires the build-up of internal messengers by metabolism. Secretion may be expected to persist after the glucose is removed as the internal messengers are cleared from the cell. In Figure 4-2, the spikes for both 5-HT and insulin continue for some time after the glucose stimulation.

Since 5-HT and insulin were not simultaneously measured at the same cell, the conclusion that 5-HT and insulin come from the same vesicles cannot be unequivocally made. However, the strong similarities between the secretion patterns provide evidence that 5-HT and insulin release are similarly regulated and are released from the same vesicles. This conclusion is supported by previous studies that found 5-HT in insulin-containing vesicles of β -cells (127-129,136). This does not rule out the possibility however, that 5-HT is also contained in another vesicle type that could be released independently of insulin.

Spike area and shape. Current spike areas have units of Coulombs and can be directly related to the number of moles detected by Faraday's Law ($Q = nFN$ where Q is the charge, n is the number of electrons transferred per oxidation, F is Faraday's constant,

and N is the number of moles detected). As discussed elsewhere (76), the close spacing of electrode and cell results in high collection efficiency so that the amount detected in isolated current spikes corresponds to the amount released by single exocytosis events. Assuming that all of the vesicle contents are released during exocytosis, the amount detected corresponds to the amount contained in a vesicle.

Using a value of 2.0 for n (measured as described in Materials and Methods), we calculate that the average spike corresponds to 0.29 amol of 5-HT from the spike areas after 16 h of incubation in 5-HT. The average vesicle diameter in rat β -cells is 342 nm (118). Assuming a membrane thickness of 10 nm, this diameter corresponds to an interior volume of 1.75×10^{-17} L. Therefore, for 0.29 amol/vesicle, the concentration of 5-HT in the vesicle after 16 hours of 5-HT loading is 17 mM. For cells incubated for 2 hours in 5-HT, a similar calculation gives 8.6 mM in the vesicle. The dependence of spike area on incubation time is indicative of lack of equilibrium of 5-HT into the cell at shorter (2 hour) incubation times. The practical conclusion is that 16 h incubations will significantly improve the signal to noise ratio for detection of secretion, therefore, improve the success rate of secretion detection.

The higher concentration is in approximate agreement with what is expected from previous work. For example, in rat insulinomas 5-HT enters the cytosol by simple diffusion. Isolated granules of the insulinomas, using an uptake process driven by the proton gradient across the vesicular membrane, accumulate 5-HT up to 38 times the extragranular concentration (136). Therefore, for cells incubated in 1 mM 5-HT the expected vesicular concentration is 38 mM. Thus, the 17 mM 5-HT calculated following

16 hour loading times is reasonable, but lower than what might be expected. The lower level may be due a lack of equilibrium with the extracellular 5-HT. The decrease may also be due to basal efflux of 5-HT from the cells. It is known that there is constant efflux of 5-HT from loaded rat β -cells once the cells are removed from the 5-HT-containing media (122). The mechanism of this efflux is unknown; however, it has been suggested that it is a non-exocytotic form of release (122). Thus, leaking of 5-HT may decrease its concentration in the vesicles resulting in the smaller peaks. Unfortunately, the existence of non-exocytotic release can not be confirmed by amperometry. A non-exocytotic form of release would not be expected to give the current spikes as observed. A constant rate of efflux would result in a steady background current which would be hard to detect on top of normal background current at the electrode.

The vesicular 5-HT content was also affected by the presence of Ca^{2+} in extracellular media after the loading step. This is reflected by the larger area of spikes for tolbutamide stimulation when the cell was bathed in Ca^{2+} -free media (the stimulation media contained Ca^{2+}) compared with that obtained when the cell was constantly bathed in buffer containing Ca^{2+} (see Table 4-2). A possible explanation for the larger spike area is that the basal efflux of 5-HT is Ca^{2+} -dependence. In contrast to the results with 5-HT, the spike areas observed for insulin did not vary with stimulation or incubation conditions. This is expected since the insulin vesicular content should not be affected by the acute stimulation or incubations used here. The difference in spike areas and their dependency on incubation conditions for 5-HT and insulin detection highlights the fact that spike area is of limited use when using a marker, like 5-HT, for detecting secretion.

Another difference between the 5-HT and insulin spikes were their shapes. Comparisons of high resolution recordings of current spikes due to 5-HT and insulin are illustrated in Figure 4-8. In many cases, 5-HT spikes had a small current increase, or “foot”, prior to the abrupt increase to the apex of the spike as shown in Figure 4-8 (A) and (B). Such features were observed on 14% of the spikes due to 5-HT detection. In contrast, such features were not found on any insulin spikes as shown in Figure 4-8 (D)-(F). The shape of spikes is affected by exocytosis dynamics, clearance of detected material from vesicles, and diffusion to the electrode. Spikes with a “foot”, similar to that observed on 5-HT spikes, have also been observed in detection of catecholamine release from adrenal chromaffin cells (75, 78) and 5-HT release from mast cells (79). This shape has been attributed to leakage of material from a fusion pore prior to complete opening of the vesicle (75, 78, 79). The lack of a foot for detection of insulin suggests that insulin does not leak from the fusion pore. This may be due to a difference in the storage of insulin and 5-HT. 5-HT is likely to be in a soluble form and readily escapes from the vesicle. In contrast, insulin is stored as a solid granule (36) and therefore must dissolve to escape the vesicle and be detected. Slow dissolution would prevent significant leakage during fusion. This difference in dynamics of exocytosis affects the peak shape and reflects an important difference in detecting 5-HT and insulin release. These differences have been further investigated and the details will be given in the next chapter. The point here is that 5-HT and insulin peak shapes are different and suggests a limit on using 5-HT as a substitute for detecting insulin.

Spike differences in different species. All the data discussed above were obtained from rat β -cells. Besides rat β -cells, dog β -cells were also tested for 5-HT secretion from loaded cells. Figure 4-9 and Figure 4-10 have illustrated the current recordings of 5-HT and insulin secretion from rat and dog β -cells, respectively. (the humps in current recordings for Figure 4-9 (A) and Figure 4-10 (A) are due to the multiple spikes. The dip for Figure 4-9 (B) are due to the artifacts caused by pressure injection of stimulant solution.) The spikes were obtained during Ca^{2+} -free experiment when the 2.4 mM Ca^{2+} and 200 μM tolbutamide were applied to the cells. Both of these β -cells have shown Ca^{2+} -dependence signal for either insulin or 5-HT secretion. And the patterns of current spikes are similar for both species due to either insulin or 5-HT secretions. Furthermore, the patterns of 5-HT and insulin secretion are very similar for both species, respectively. Furthermore, current spikes due to 5-HT secretion obtained with high time resolution from loaded dog cells also show pre-spike feature, or "foot" as illustrated in the insets of Figure 4-11. This further supports the idea that 5-HT is stored in a loosely bound form in insulin-containing vesicle and leaks out upon the fusion of vesicle and cell membranes. Based on the experiment results, there is no significant difference in current spikes observed between these two species. However, compared with current spikes obtained from rat β -cells due to insulin and 5-HT secretion, the number of spikes per stimulation and the amplitude of current spikes from dog β -cells are usually larger. In general, the success rate with dog β -cells is higher. The reason behind this is not very clear. It may be due to different concentrations of insulin in the vesicles of these two different species

or due to the different quality of the β -cells, since they have been handled differently during islet isolation and cell dispersion procedure.

Practically, it is more difficult to get dog β -cells than rat β -cells, since there is no constant supply of dog β -cells and rat β -cells are easier to obtain by sacrificing the rats in the lab. However, the basic principles involved in insulin secretion are the same for different species, which have been also observed between human and rat cells as described in chapter 3. Thus, the characteristics of insulin secretion detected at single rat β -cells can provide useful information for understanding insulin secretion mechanism from other types of single β -cells.

5-HT as a marker for insulin secretion. The data presented here provide solid evidence that 5-HT is released by exocytosis in addition to any non-exocytotic release that occurs. The similarity in the pattern of exocytosis events for 5-HT and insulin observed provide strong evidence that 5-HT is released with the same regulation as insulin and presumably from the same vesicles as insulin. Thus, 5-HT may be a useful marker of insulin secretion. Spike area and shape for 5-HT vary from that seen with insulin and therefore cannot be used as a substitute for insulin detection. There may be some other limitations to detecting 5-HT instead of insulin. For example, 5-HT may affect insulin secretion (137-139), which may need to be taken into account in such studies. Related to this, the incubation of β -cells in 5-HT may affect cell behavior. No significant effects were observed in these tests however.

Table 4-1. Summary of Spike Occurrences for 5-HT Detection and Insulin under Different Stimulation Conditions.

Conditions	# of cells	# of spikes observed per stimulation*	Delay to first spike [†] (s)	Duration of spikes [‡] (s)
2 hour 5-HT loading, glucose stimulation	5	25 ± 23	47 ± 21	201 ± 80
16 hour 5-HT loading, glucose stimulation	6	37 ± 17	34 ± 45	245 ± 86
insulin detection, glucose stimulation	4	22 ± 16	50 ± 11	199 ± 103
2 hour 5-HT loading, tolbutamide stimulation	5	7.3 ± 4.9	0.9 ± 1.4	11.9 ± 11.0
insulin detection, tolbutamide stimulation	13	9.4 ± 6.1	1.3 ± 0.8	6.0 ± 3.5

* Detailed stimulation conditions given in the experimental section

[†] The time from the beginning of the stimulation to the first spikes was measured

[‡] The time from the first spike detected to the last spike detected was measured

Table 4-2. Summary of Isolated Spike Areas for Different Stimulation Conditions.

Stimulation conditions	Analyte	# of spikes	5-HT loading time (hours)	[Ca ²⁺] in extracellular media during stimulation experiments	Spike area (fC)
16 mM glucose	5-HT	107	2	2.4 mM	26.4 ± 15.6
16 mM glucose	5-HT	190	16	2.4 mM	57.5 ± 41.8*
200 µM Tolbutamide	5-HT	142	2	2.4 mM	30.5 ± 14.7
200 µM Tolbutamide	5-HT	132	2	0.0 mM	70.3 ± 74.0**
16 mM glucose	insulin	63	--	2.4 mM	200 ± 94
200 µM Tolbutamide	insulin	528	--	2.4 mM	230 ± 88
200 µM Tolbutamide	insulin	65	--	0.0 mM	230 ± 108

*Statistically significant difference from area for 5-HT following 2 hour incubation and glucose stimulation ($P < 0.005$).

**Statistically significant difference from area for 5-HT following 2 hour incubation and tolbutamide stimulation ($P < 0.005$).

Uptake and Release of 5-hydroxytryptamine (5-HT)

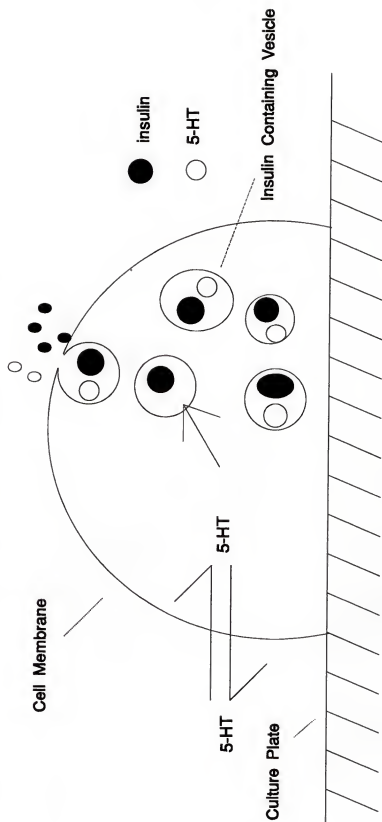


Figure 4-1. Schematic diagram of 5-HT uptake and localization in β -cells.

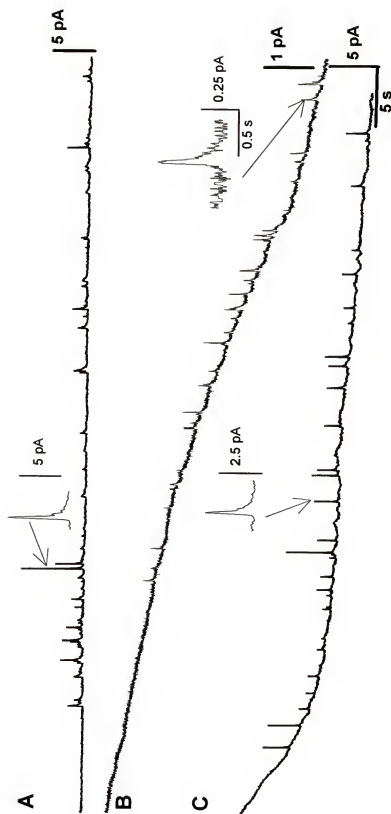


Figure 4-2. Current recordings from stimulation of rat β -cells with 16.7 mM glucose. A) detection using bare carbon fiber microelectrode at a β -cell incubated for 16 hours with 5-HT loading culture media; B) detection using bare carbon fiber microelectrode at a β -cells incubated for 2 hours with 5-HT loading buffer; C) detection of insulin secretion from untreated β -cells using Ru-O/CN-Ru microelectrode. Recordings begin at the end of glucose stimulation. Recordings are from different cells. Insets show isolated spikes. All the current recordings have same time scale and the insets have the time scale.

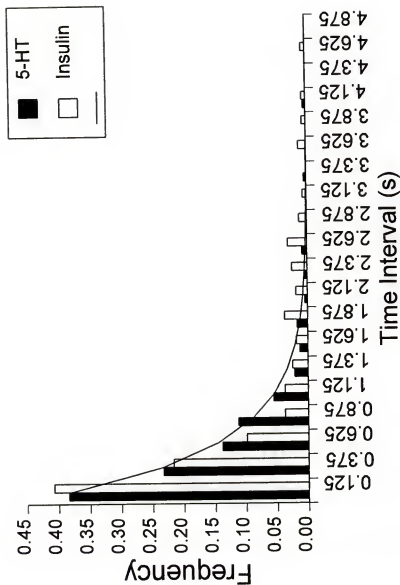


Figure 4-3. Histograms of time intervals between spikes for detection of 5-HT and insulin following glucose stimulations. Frequency (y-axis) is calculated as the number of events with a given time interval divided by the total number of events. Total number of events was 234 for 5-HT (taken from 5 cells) and 204 for insulin (from 4 cells). The x-axis is labeled with the mid-point of the bin used for counting intervals. The solid line is the best fit of equation 1 to the 5-HT data. Overlapping spikes were not used in the histogram. To obtain the fits, equation 1 was normalized for bin size of the histogram as described elsewhere (130).

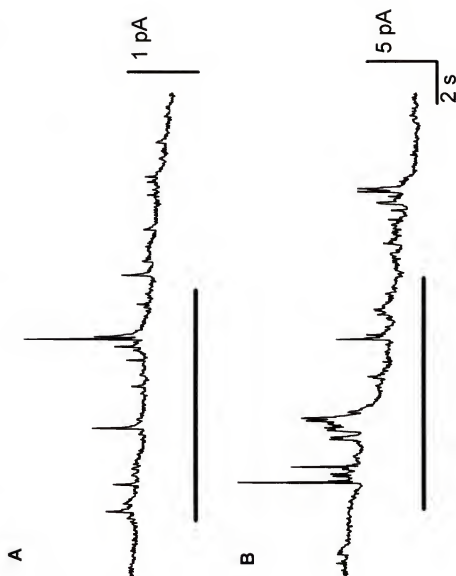


Figure 4-4. Current recordings following stimulation with 200 μ M tolbutamide. A) Detection from 5-HT loaded β -cells at bare carbon fiber microelectrode. B) Detection of insulin secretion from untreated β -cells at Ru-O/CN-Ru modified electrode. Lines indicate stimulation. Current bar is 1 pA for (A) and 5 pA for (B). Recordings are from different cells.

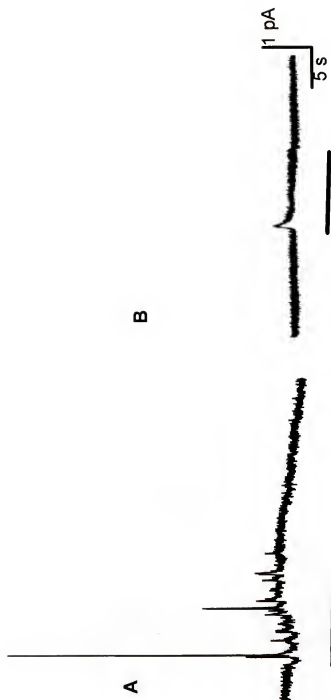


Figure 4-5. Detection of 5-HT secretion from 200 mM tolbutamide stimulation of rat β -cells incubated for 2 hours with 1 mM 5-HT loading buffer. The applied voltage was A) 0.65 V, B) 0.24 V. Bars indicate stimulation.

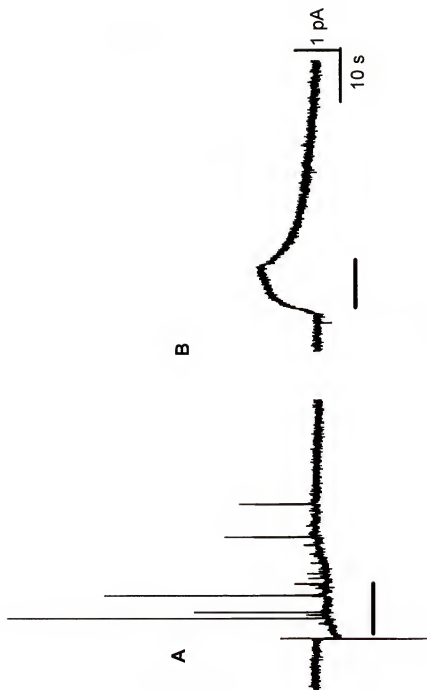


Figure 4-6. Ca^{2+} dependence of tolbutamide-induced current spikes at rat β -cells. The cell used in this experiment was bathed in Ca^{2+} -free modified KRB and had been loaded with 5-HT (2 hour incubation with 1.0 mM). Stimulation solutions were (A) and (C) 200 μM tolbutamide with modified KRB (includes 2.4 mM Ca^{2+}), and (B) and (D) 200 μM tolbutamide in Ca^{2+} -free modified KRB. Bars indicate the stimulation. 5 min was allowed between stimulations.

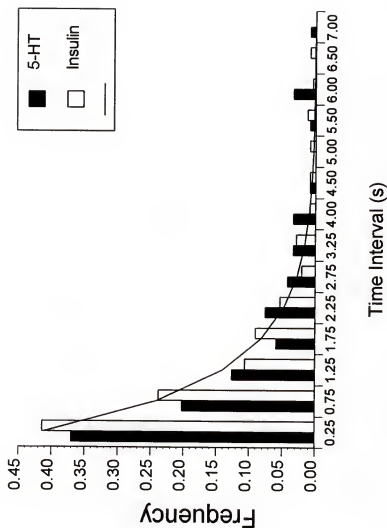


Figure 4-7. Histograms of time intervals between spikes for detection of 5-HT and insulin following tolbutamide stimulations. Data treatment was the same as that described in Figure 4-3. Total number of events was 119 for 5-HT (taken from 25 cells) and 244 for insulin (from 29 cells). The x-axis is labeled with the mid-point of the bin used for counting intervals. The solid line is the best fit of probability density equation to the insulin data.

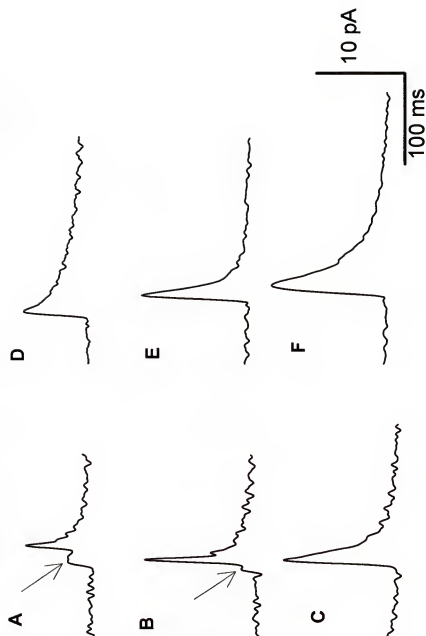


Figure 4-8. Comparison of spike shapes for insulin and 5-HT at pH 7.4. (A-C) Spikes due to detection of 5-HT. Arrows indicate a "foot" in (A) and (B). (D-F) Spikes due to detection of insulin. All measurements were made following stimulation for 10 s with 200 μ M tolbutamide. Data were collected at 6000 Hz and filtered at 333 Hz.

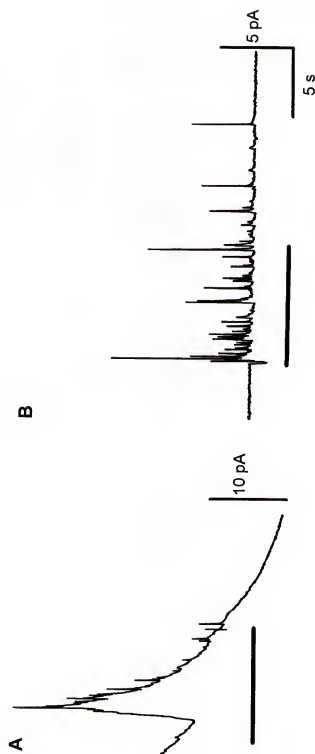


Figure 4-9. Current recordings of tolbutamide-induced secretion at rat β -cells. Stimulation solutions were 200 μ M tolbutamide with 2.4 mM Ca^{2+} . A) detection of insulin secretion on RuO/RuCN electrode. B) detection of 5-HT secretion from the cells bathed in loaded with 5-HT (2 hour incubation with 1.0 mM 5-HT). Bars indicate the stimulation.

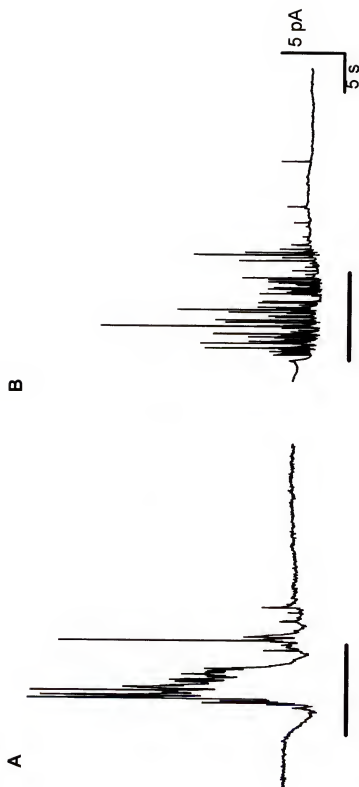


Figure 4-10. Current recordings of tolbutamide-induced secretion at dog β -cells. Stimulation solutions were 200 μ M tolbutamide with 2.4 mM Ca^{2+} . A. detection of insulin secretion on RuO/RuCN electrode. B) detection of 5-HT secretion from the cells bathed in loaded with 5-HT (2 hour incubation with 1.0 mM 5-HT). Bars indicate the stimulation.

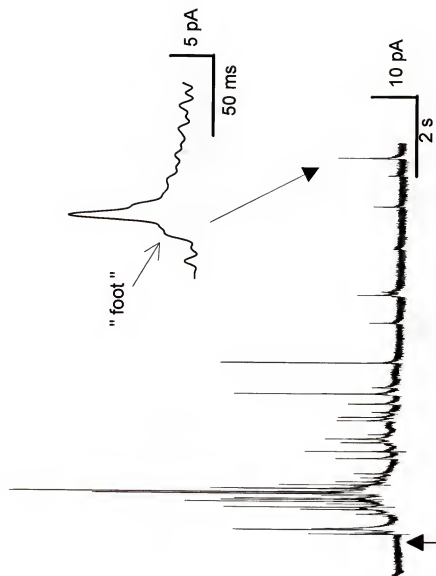


Figure 4-11. Current spikes of 5-HT secretion following 10 s application of 200 μ M tolbutamide from dog β -cells collected with high time resolution. The inset shows a blowup of a current spike with "foot". Data were collected at 3000 Hz and low pass filtered at 150 Hz. Arrow at the beginning of current spikes indicates the start of stimulation solution.

CHAPTER 5

EFFECTS OF EXTRACELLULAR pH ON INSULIN SECRETION

Introduction

Pancreatic β -cells secrete insulin in response to glucose, tolbutamide and potassium. Many details of the secretion process are not well understood. One of the most enigmatic aspects of secretion is exocytosis, which is the last step in secretion. This process is often referred to as quantal secretion (140), which can be viewed as four consecutive events, adhesion of the vesicle to the interior of the plasma membrane, fusion of the vesicle with the membrane, expansion of the initial fusion point and discharge of the vesicular contents (36, 140, 142). The vesicle membrane is eventually reclaimed by the cell by endocytosis. While much evidence supports this view, the regulatory mechanisms of each event and their interrelationships are not understood at molecular basis. The study of relationships between each steps involved in exocytosis will help to understand more about the secretion mechanism.

Single exocytotic events involving the release of insulin can be quantitated by oxidation with a modified carbon fiber microelectrode placed adjacent to a β -cell, which has been described in chapter 3 and 4 in detail. Exocytotic secretion is seen as a series of randomly occurring current spikes due to the detection of packets of insulin molecules secreted from individual vesicles. Because the concentration packets measured

electrochemically are the last step of the exocytotic process, their temporal characteristics will reflect the prior, rate-limiting steps. Events associated with the discharge of the vesicle contents, such as dissociation of the vesicular matrix, expulsion of its contents and transport away from the cell, could affect the temporal characteristics of the spike.

The final step of exocytosis in insulin secretion is clearance of stored insulin from the vesicle interior. Electron micrographs of insulin secretory vesicles show a dark, crystalline core surrounded by a clear halo (33, 36). The halo presumably contains soluble components such as proinsulin, C-peptide, ATP and some proteins, while the dark core contains crystalline Zn-insulin (36). The insulin is likely stored as a hexamer unit associated with two Zn atoms (91,143). Release of insulin requires dissolution of the granule and dissociation of the Zn-insulin complexes. The time scale of this process is unknown, although previous measurements of the efflux from perfused islets utilizing C-18 chromatography have found that insulin is free of Zn in no more than 60 s after release (143). Furthermore, the important factors that control release of insulin from the Zn-insulin precipitates are not clear. The hypothesis that sudden exposure of the vesicle interior to extracellular pH during exocytosis causes rapid release of insulin from the solid Zn-insulin was tested. This hypothesis was developed based on the facts that the intravesicle pH is around 5.5 to 6.0 (144) and Zn-insulin hexamers prepared in vitro are insoluble below pH 7.0 (91, 143, 145, 146).

In order to test this hypothesis, insulin secretion from single β -cells measured with high time resolution at different extracellular pH's is described in this chapter. Insulin was measured by amperometry at a carbon fiber microelectrode modified with a

composite of ruthenium oxide and cyanoruthenate (Ru-O/CN-Ru) as described in chapter 3 (107, 121). And as a control experiment, measurement of 5-HT secretion with high time resolution at different extracellular pH's is also described in this chapter. 5-HT was measured by amperometry at a bare carbon fiber microelectrode as described in chapter 4. Normally, 5-HT is not present in β -cells at levels that are high enough to be detected by amperometry (107), however β -cells will accumulate 5-HT into secretory vesicles (127-129). The accumulated 5-HT is released by exocytosis which is detectable as current spikes at unmodified carbon fiber microelectrodes (123, 124). Thus, detection of 5-HT can serve as an indicator of vesicle fusion and opening at β -cells. The peak area and shape of individual current spikes are examined to support the hypothesis.

Permeabilized β -cells were also used in order to further test the hypothesis. The use of permeabilized cells provides a way to introduce reagents directly into biological cells while bypassing events associated with the cellular membrane. It may help to study the dynamics of chemical secretion from single cells. Digitonin, a steroid glycoside which interacts specifically with 3 β -hydroxysterols (a cholesterol in plasma membranes), increases the membrane permeability of cells to Ca^{2+} and proteins (147). As discussed before, the influx of extracellular Ca^{2+} is necessary for triggering exocytosis in stimulus-secretion coupling. It has been demonstrated that digitonin-treated bovine adrenal medullary cells release catecholamines upon addition of micromolar Ca^{2+} to the medium in the absence of secretagogue in a manner consistent with exocytosis (147, 148). The shape and peak area of current spikes obtained by amperometry due to oxidation of catecholamine induced by Ca^{2+} on permeabilized cells were similar to that induced by

secretagogues on non-permeabilized cells. In common with chromaffin cells, pancreatic β -cells are also permeabilized by digitonin and insulin secretion is induced by the micromolar range of extracellular Ca^{2+} after permeabilization (149, 150). Therefore, the dissociation of Zn-insulin hexamer could be monitored by detection the exocytotic event of insulin secretion from permeabilized cells. The details will be described next.

Experimental

Electrode preparation and testing. The modified electrode for insulin detection and bare carbon fiber electrode were prepared and tested in the flow injection system as described in chapter 2.

Zn(II)-insulin hexamer was formed by mixing ZnCl_2 and insulin in 2 to 1 ratio in 5 mM phosphate buffer containing 100 mM NaCl at pH 7.4 (151, 152). The flowing buffer used in the flow injection system for testing electroactivity of Zn(II)-insulin hexamer on mix-valent RuO/RuCN modified electrode was 5 mM phosphate buffer containing 100 mM NaCl. The insulin sample used was 50 μM bovine insulin dissolved in flow injection buffer. Two background samples were prepared, one was flowing buffer, the other one was flowing buffer with same amount Zn(II) as that in Zn(II)-insulin hexamer sample.

Islet isolation and cell culture. All the procedures for rat islets isolation and cell dispersion are the same as described in chapter 3. The dog islets were supplied by University of Miami, Medical Center. The dispersion of dog islets were similar to the procedures used for human islets as described in chapter 3.

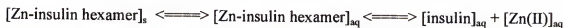
Single cell measurement. The steps for insulin secretion detection from unloaded β -cells were the same as performed in chapter 3, and that for 5-HT secretion detection from loaded β -cells in chapter 4. For detection of insulin secretion, Kreb's buffer at pH 7.4 and modified Kreb's buffer at pH 6.4 were used. 3 mM sodium bicarbonate was used instead of 25 mM in order to make modified pH 6.4 Kreb's buffer. The ion strength was balanced by adding more NaCl into the buffer. For detection of 5-HT secretion, Kreb's/HEPES buffer was used, pH was adjusted by NaOH to pH 6.4 and 7.4 respectively. The β -cells were loaded in 1 mM 5-HT containing media for 3 hours or overnight as described in chapter 4.

The cells were permeablized with pressure ejection of 20 μ M digitonin from a micropipette for 15 to 20 s, which was prepared in a Ca^{2+} -free Kreb's buffer. The cells were maintained in an identical buffer but containing 100 μ M Ca^{2+} .

Data collection and analysis. The procedures are similar to those described in chapter 4.

Results and Discussion

Electrochemistry of Zn(II)-insulin complex. When insulin molecules dissociate from the Zn-insulin hexamer precipitates stored in the vesicle, the following chemical equilibrium is proposed:



where s indicates solid state, aq indicates aqueous state. When the electrode is placed next to the cell to detect the secreted molecules from individual vesicles, a series of current spikes are observed after application of insulin secretagogues. The hypothesis is

that the current spikes are due to oxidation of insulin molecules. However, which form of insulin responsible for the current spikes is not known at this point. Insulin has been previously demonstrated to be electroactive on mix-valent RuO/RuCN polymer modified microelectrode in chapter 2. Here, Zn-insulin hexamer was tested as a sample in flow injection system. The results are shown in Figure 5-1. Only free insulin can be oxidized on the modified electrode and give a positive current response in phosphate buffer at pH 7.4 (Figure 5-1 (A)). The Zn-insulin hexamer did not give a positive current response, instead, a negative current was observed which was the same as that observed on the injection of Zn-containing buffer (Figure 5-1(B) and (D)). There is no response on the injection of buffer without Zn (Figure 5-1 (C)). Thus, the negative current change is caused by Zn present in the solution. Therefore, Zn-insulin hexamer is not electroactive on the modified electrode. Furthermore, it is suggested that insulin monomer is responsible for current spikes occurring on the electrode after the cell is stimulated.

Effects of extracellular pH on secretion. Since Zn-insulin hexamer precipitate stored in the vesicle is sensitive to pH, extracellular pH change may affect the dissolution and/or dissociation of Zn-insulin hexamer to insulin molecules, which will change the temporal characteristics of current spikes due to the detection of exocytosis. The insulin detected at the modified electrode is likely dissociated from Zn since addition of ZnCl_2 to a solution of insulin at pH 7.4 abolishes the amperometric signal for insulin in flow injection experiments (Figure 5-1). The hypothesis here is that sudden exposure of the vesicle interior to extracellular pH during exocytosis causes rapid release of insulin from the solid Zn-insulin. In order to test the hypothesis, current spikes due to insulin and 5-

HT secretion, respectively, from single pancreatic β -cells at different extracellular pH's following stimulation for 10 s with tolbutamide were observed as illustrated in Figure 5-2 and 5-3. (The slow drift in Figure 5-2 (A) and (B) are characteristic of the modified electrode. The dip in current for Figure 5-3 (A) and in (B) were artifacts of the stimulation.) When a rat β -cell is stimulated with 200 μ M tolbutamide in pH 7.4 media, a series of current spikes is observed at the electrode as shown in Figure 5-2 (A). Measurements made with a bandwidth of 333 Hz show that the spikes have an average half-width of 37.1 ± 26.8 ms ($n = 78$). (The width of the insulin spikes is not limited by the response time of the modified electrode since it has been measured to be < 25 ms). The average area under the spikes corresponds to 1.6 amol of insulin (121). This amount is in agreement with previous estimates of insulin vesicular content (121, 115). The narrow spikes and the amounts detected suggest that a large portion of the Zn-insulin complex dissolved and dissociated rapidly after vesicle opening.

When a similar experiment is performed with cells bathed in pH 6.4 media, no current spikes are detected as illustrated in Figure 5-2 (B). To determine if vesicle opening still occurred at the lower pH, secretion of 5-HT from β -cells at pH 6.4 and 7.4 were compared as illustrated in Figure 5-3 (A) and (B). No statistically significant differences in the number or area of spikes were observed for 5-HT at different pH's (Table 5-1); although there was a slightly longer duration of spike activity at pH 7.4 (illustrated in Table 5-1). These results demonstrate that lower pH did not inhibit vesicle fusion and pore opening, but rather hindered release of detectable insulin from the

granule. In other words, the lower pH inhibited dissolution and/or dissociation of the Zn-insulin complex.

The data show that a crucial step to releasing free insulin from Zn-insulin precipitates following vesicle opening is exposure of the granule to extracellular pH. An interesting question that is not easily answered from these results is the fate of insulin following stimulation at pH 6.4. It is possible that the granule did not dissolve and the vesicle closed up around the granule during endocytosis. This seems unlikely since studies of insulin secretion at low pH's have not reported complete elimination of insulin secretion (153) and endocytosis is considerably slower than exocytosis in β -cells (154). Lowering the extracellular pH removes the pH gradient between the vesicular matrix and the extracellular space that is generated upon vesicular fusion, which would lengthen the time for Zn-insulin complex to dissociate during the time the vesicle is open. It is possible that the granule dissolves slowly so that the insulin is released over relatively long periods of time. Insulin released slowly would be too dilute to be detected by the electrode. A final possibility is that the solid insulin granule dissolved as a Zn complex which was undetectable at the electrode. Because of this uncertainty, the precise role of the pH change in releasing insulin needs to be established by further experiments.

Differences in spike shapes. In order to find out more details about the secretion process (115), current spikes with high time resolution were obtained at pH 7.4. Analyzing the spike shapes of insulin and 5-HT secretion will help to study the dynamics process of exocytosis. In contrast to insulin, 5-HT is stored in a form (presumably in solution) that readily escapes from the vesicle at either pH. This point has been

illustrated by comparing the peak shapes for insulin and 5-HT measured at pH 7.4 as shown in chapter 4. Spikes due to 5-HT have average width at half-height of 6.99 ± 7.11 ms ($n = 102$) which is significantly less than the 37.1 ± 26.8 ms for insulin ($p < 0.005$). (The width of spikes due to 5-HT was apparently limited by the bandwidth of the measurement.) The larger width of the insulin spikes compared to the 5-HT spikes suggests that the dissolution/ dissociation process determines the spike width and is the rate limiting step to releasing free insulin during exocytosis. Furthermore, as described in chapter 4, 14% of the 5-HT current spikes have a “foot” prior to the rapid upstroke, which has been attributed to detection of material that “leaks” from a fusion pore prior to complete opening of the vesicle. In contrast to the foot observed on current spikes due to 5-HT, a foot was never observed on current spikes due to insulin detection. Thus a detectable quantity of insulin, which is stored in a solid form, does not leak out of the vesicle core during the brief time the fusion pore is open.

Extracellular pH effects on secretion from permeabilized cells. In order to further explore the effect of extracellular pH on dissolution/dissociation of Zn-insulin complex, insulin secretion from digitonin-permeabilized cells was investigated. Amperometric current recordings due to insulin secretion were observed after pressure ejection of 20 μM digitonin to β -cells incubated in 100 μM Ca^{2+} containing buffer at pH 7.4 and pH 6.4 as shown in Figure 5-4 (A) and (B). Insulin secretion is induced without insulin secretagogues present in the solution, and the extracellular Ca^{2+} concentration (micromolar range) is used for triggering exocytosis, which is different from that used for stimulus induced secretion (millimolar range) in this work. This approach avoids the

necessity for functional ion channels and receptors, and the use of a high Ca^{2+} concentration prolongs the duration of release (142).

Even though current spikes were observed from digitonin-permeabilized cells, the type of response obtained varies with different cells. As shown in Figure 5-5, three different types of signals observed from digitonin-treated cells incubating in pH 6.4 buffer containing $100\ \mu\text{M}\ \text{Ca}^{2+}$. 75% of the cells tried ($n=12$) showed the type of response as illustrated in Figure 5-5 (A) after application of digitonin solution for 20-30 s. In this case, no current spikes were observed, which is similar to tolbutamide-stimulated insulin secretion at pH 6.4. 8.3% of the cells tried gave the type of response as shown in Figure 5-5 (B), which are small broad spikes. And 16.7% of the cells tried had the type of response in Figure 5-5 (C) as a broad bump. The last two types of responses were not observed from tolbutamide-stimulated cells at pH 6.4, which may be due to insulin crystal start dissolving after cell permeabilization before exocytosis process.

For the responses observed at pH 7.4, two typical types of current spikes were observed as illustrated in Figure 5-6. There are 45.5% of the cells tried ($n=11$) giving the current spikes as shown in Figure 5-6 (A), which is similar to the spikes observed from tolbutamide-induced insulin secretion at pH 7.4. About 36.4% of the cells tried had the response as shown in Figure 5-6 (B). In this case, both spikes and large broad humps were observed, which are not observed from stimulus-induced insulin secretion.

Even though the current spikes were observed at pH 6.4 from small percentage of digitonin-treated cells, the spike width at half height is statistically significant different from that obtained at pH 7.4 ($P < 0.001$). The results are summarized in Table 5-2. (The

spike width in table 5-2 was measured from spikes obtained using low pass cutoff frequency at 30 Hz.) The spike width and spike area detected from permeabilized β -cells at pH 7.4 is similar to that obtained from stimulus-induced insulin secretion, which suggests that Ca^{2+} -induced insulin secretion from digitonin-treated cells is by exocytosis. The similar results were also obtained from the investigation of Ca^{2+} -dependent quantal release from permeabilized chromaffin cells (147, 148). Compared with the spikes obtained at pH 7.4, the current spikes at pH 6.4 either are observed with decreasing amplitude and increasing spike width or not observed at all. This is expected if low extracellular pH inhibits or slows down the dissolution and/ or dissociation of Zn-insulin complex, which will cause the current spikes temporally broadened and decreasing amplitude. The failure to observe spikes at pH 6.4 in most cases is due to the spikes of small amplitude easy to become buried in the background noise. It has been suggested that expulsion and dissociation of the condensed packet of material from the fused vesicle requires a finite time and a chemical driving force (142). The driving forces at pH 7.4 are pH gradient and insulin concentration gradient caused by amperometry. In amperometric mode, insulin is oxidized immediately after it arrives at the electrode, which gives insulin concentration zero at the electrode surface. Lack of pH gradient by lowering extracellular pH seems strong enough to slow down vesicular matrix dissociation. And the slow process cause the spikes be too broad and too dilute to detect at the electrode. This is consistent with the results observed in stimulus-induced secretion at these two pH's as described before. Furthermore, as summarized in table 5-2, the area of broad spikes observed at pH 6.4 is statistically significant different from that at pH 7.4 ($P < 0.001$).

The smaller area at pH 6.4 further supports the idea that extracellular pH change affects the dynamics of insulin secretion.

In comparison with insulin secretion from permeabilized β -cell, 5-HT secretion from permeabilized loaded β -cells was used again as a control experiment to check if the secretion is due to exocytosis from Ca^{2+} -induced secretion and how extracellular pH affects secretion. The current spikes due to 5-HT secretion from permeabilized loaded cells were observed at both pH's and the results are shown in Figure 5-7 and 5-8. Even though the spikes were observed at both pH's, the spike occurrence varies with cells. At pH 6.4, the responses from 40% of the cell tried ($n=15$) were observed as current spikes with a large broad hump as shown in Figure 5-7(A). And the responses from 26.7% of the cells tried was observed as spikes along with small broad humps as shown in Figure 5-7 (B). In comparison, at pH 7.4, about 43% of the total cells tried ($n=46$) gave the response as shown in Figure 5-8 (A), a large broad hump and very few spikes. The responses from 13% of the cells tried were observed as a few spikes as shown in Figure 5-8 (B). And 8.7% of the cells tried gave the response observed as current spikes (Figure 5-8 (C)), and the spiking lasted for a longer time compared with Figure 5-8 (B).

In order to compare the differences of spikes observed due to 5-HT secretion at these two pH's, the area and width of narrow spikes from Figure 5-7, 5-8 (B) and (C) are calculated and also summarized in Table 5-2. (In spike area calculation, overlapping spikes were not excluded). The spike area and spike width do not change much with the change of extracellular pH. The areas at both pH's are similar to that obtained from stimulus-induced 5-HT secretion. This further supports that the secretion induced by

Ca^{2+} observed as current spikes from digitonin-treated cells is caused by exocytosis.

Similar to stimulus-induced secretion, spike width of 5-HT secretion did not vary with extracellular pH much, which further supports the idea that 5-HT may be stored in the vesicle in a soluble form and it diffuses out immediately upon fusion of vesicle membrane and cell membrane. Therefore, the spikes are not broadened due to the fast expulsion of 5-HT molecules at low pH, which is different from the slow expulsion of insulin molecules from the individual vesicles.

The experiment with digitonin-treated cells demonstrate the feasibility of increasing the plasma membrane permeability and at the same time maintaining essential Ca^{2+} -dependent reactions of exocytosis. This technique may allow the direct intracellular introduction of drugs and other agents that may interfere with or alter exocytosis.

However, cautions are needed when the permeabilized cells are used. This is because broad humps were also observed from digitonin-treated cells in some cases, which may be caused by non-exocytotic secretion due to membrane lysis after digitonin treatment of the cell. Ca^{2+} -independent non-exocytotic secretion were observed from permeabilized chromaffin cells due to prolonged perfusion with digitonin-containing solutions (148). Since the granule membrane also contains a lot of cholesterol, it is possible that prolonged perfusion with the digitonin-containing solution could cause rupture of intracellular granules. Therefore, the chemicals stored in the granules may leak out through the holes caused by digitonin on the cell membrane(155). For 5-HT release from loaded cells, the humps were observed more often than insulin secretion, which may be due to the 5-HT soluble storage form in the cell and also due to some 5-HT stored in

intracellular spaces after loading the cell. However, at this point, the reasons cause broad humps to be observed are not clear. More details involving digitonin-treated cells need to be investigated in order to understand more about the process.

Dynamics of insulin secretion. From the combination of these results with previous observations, the following picture emerges concerning insulin storage and release. β -cells store about 1.6 amol of insulin in a vesicle with a diameter of about 342 nm (118). The ability to pack and store this amount of insulin is facilitated by the inclusion of Zn and the maintenance of a vesicular pH that is below that required to dissolve the Zn-insulin precipitate, by a proton pump (44). After vesicle fusion, dissolution and dissociation of the solid Zn-insulin granule occurs on the time scale of 37 ms in a process that is dependent upon exposure of the granule to extracellular pH. The possible change in intravesicle pH during fusion pore formation is not sufficient to cause substantial release of stored insulin. Although there are other differences between the ionic composition of the interior of the vesicles and the extracellular environment besides pH, these other ions must play a secondary role in freeing insulin from the granule since the lowered pH so radically altered the release of insulin.

These results are reminiscent of those from mast cells and adrenal chromaffin cells. Mast cells have vesicles that are large enough to be observed by light microscopy. At low extracellular pH, it was observed that the granule in the vesicle remained intact (156). Electrochemical measurements of catecholamine release at low pH also showed a retardation of the clearance of secretory products (157). In both of these cases however, the secreted products are stored in a condensed matrix of ionic polymer which undergoes

conformational changes with increases in pH. For example, in adrenal cells, catecholamine was stored in a matrix of chromogranin A which expands, dissociates, and loses affinity for catecholamine with a pH change from 5.5 (intravesicle pH) to extracellular pH. Thus, the use of pH gradients to drive release of vesicular contents following fusion is common in exocytosis, however the chemical changes that follow the pH changes vary with cell type and secretory product.

Table 5-1. Effect of Extracellular pH on Current Spikes Due to 5-HT⁺

Extracellular pH	Number of cells	Number of spikes per stimulation	Time to first spike (s) *	Duration of spike activity (s) **	Area of spikes (fC)
7.4	11	13.6 ± 8.3	2.9 ± 2.5	17.8 ± 11.3	53.1 ± 31.0 (n = 113)
6.4	4	12.8 ± 10.6	2.0 ± 1.1	8.5 ± 2.8	59.2 ± 34.1 (n = 45)

⁺ For all data, only spikes with peak heights five times the peak to peak noise were counted. All data were collected at 150 Hz with low pass filtering at 33 Hz. All data are reported as the mean ± 1 standard deviation.

* Time from the beginning of the stimulation to the first spike.

** Time from the first spike to the last spike for a given stimulation.

Table 5-2. Effect of Extracellular pH on Current Spikes at Permeabilized β -Cells[†].

Extracellular pH	Area of insulin spikes (fC)	Width at insulin spike half height (ms)	Area of 5-HT spikes (fC)*	Width at 5-HT spike half height (ms)*
7.4	208 \pm 13.4 (n=45)	29.8 \pm 9.4 (n=30)	41.4 \pm 2.5 (n=54)	21.8 \pm 2.2 (n=20)
6.4	173 \pm 3.8** (n=33)	116.1 \pm 49.8*** (n=26)	39.7 \pm 2.2 (n=37)	23.2 \pm 5.0 (n=19)

[†] For all data, only spikes with peak heights five times the peak to peak noise were counted. All data were collected at 180 Hz with low pass filtering at 33 Hz. All data are reported as the mean \pm 1 standard deviation.

* The loaded β -cells were incubated in 1 mM 5-HT containing buffer for 4 hours.

** Statistically significant difference from area for insulin obtained at pH 7.4 from digitonin-permeabilized cells ($P < 0.001$).

*** Statistically significant difference from spike width for insulin at pH 7.4 from digitonin-permeabilized cells ($P < 0.001$).

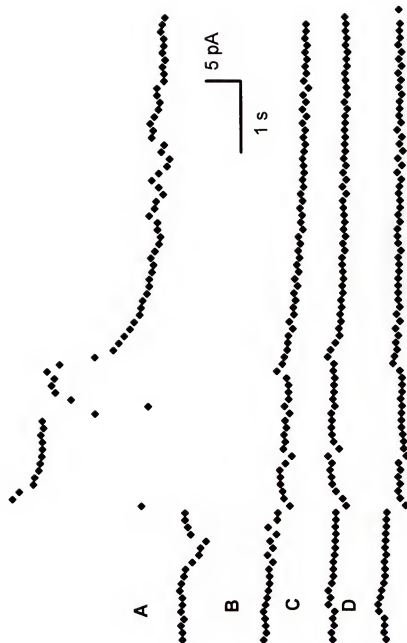


Figure 5-1. Current responses in flow injection system. (A) 50 μ M insulin, (B) Zn-insulin hexamer, (C) flowing buffer, (D) sample with the same components as in (B) except no insulin. The flowing buffer is 5 mM sodium phosphate and 100 mM NaCl. All the samples were dissolved in this buffer. E (applied) was 0.85 V vs. SSCE. Data were collected 100 ms apart.



Figure 5-2. Current spikes observed due to insulin secretion from single rat pancreatic β -cells at different extracellular pH's following stimulation for 10 s with tolbutamide. (A) insulin measurement at pH 7.4, (B) insulin measurement at pH 6.4. Lines below traces indicate application of stimulus. Data were low pass filtered at 33 Hz.

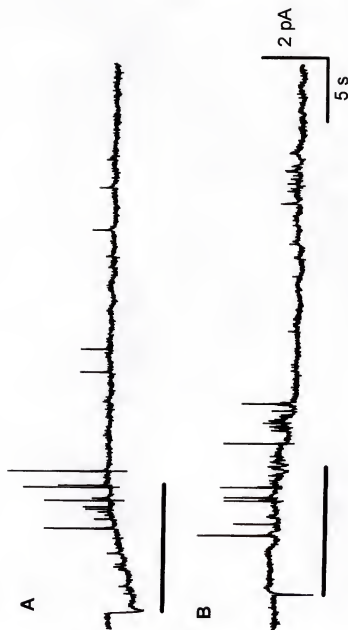


Figure 5-3. Current spikes observed due to 5-HT secretion from loaded single rat pancreatic β -cells at different extracellular pH's following stimulation for 10 s with tolbutamide. (A) 5-HT measurement at pH 7.4, and (B) 5-HT measurement at pH 6.4. All measurements of 5-HT were made at cells that had been allowed to accumulate 5-HT 3 hours. Lines below traces indicate application of stimulus. Data were low pass filtered at 33 Hz.

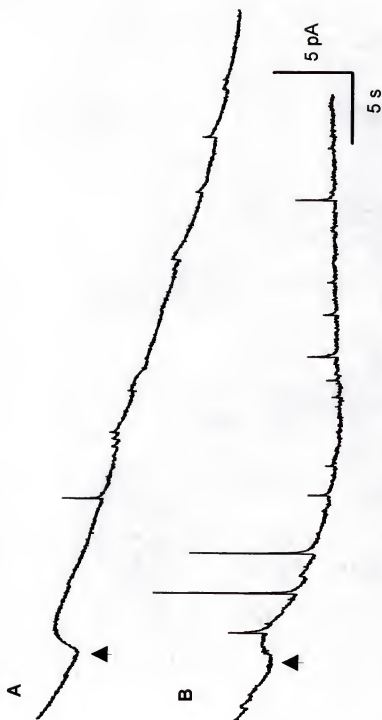


Figure 5-4. Current spikes observed due to insulin secretion from single rat pancreatic β -cells after application of 20 μ M digitonin solution for 20 s at different extracellular pH's. Cells were in Kreb's buffer with 100 μ M Ca^{2+} . (A) measurement at pH 6.4, (B) measurement at pH 7.4. Arrows indicate the beginning of application of digitonin solution. Data were filtered at low pass filter frequency 33 Hz.



Figure 5-5. Current spikes observed due to insulin secretion from digitonin-permeabilized single rat pancreatic β -cells. Cells were maintained in Kreb's buffer at pH 6.4 with $100 \mu\text{M Ca}^{2+}$. Arrows in (A) and (C) indicate the beginning of application of digitonin solution for 20 s. Current response in (B) was continuously recorded after 30 s digitonin treatment. Data were filtered at low pass filter frequency 33 Hz. Current bar is 2.5 pA for (A) and (B), and is 10 pA for (C).



Figure 5-6. Current spikes observed due to insulin secretion from digitonin-permeabilized single rat pancreatic β -cells. Cells were maintained in Kreb's buffer at pH 7.4 with $100 \mu\text{M Ca}^{2+}$. Arrows indicate the beginning of application of digitonin solution for 30 s. Data were filtered at low pass filter frequency 33 Hz.



Figure 5-7. Current spikes observed due to 5-HT secretion from digitonin-permeabilized single rat pancreatic loaded β -cells. Cells were maintained in Krebs's/HEPES buffer at pH 6.4 with $100 \mu\text{M Ca}^{2+}$. Arrows indicate the beginning of application of digitonin solution for 20 s. Data were filtered at low pass filter frequency 33 Hz. Cells were incubated in 1 mM 5-HT containing buffer for 4 h.

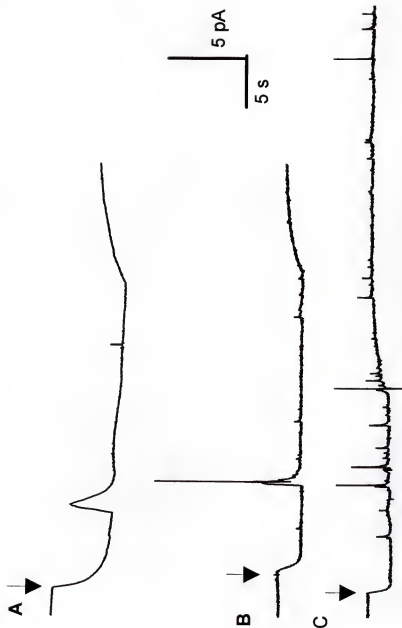


Figure 5-8. Current spikes observed due to 5-HT secretion from digitonin-permeabilized single rat pancreatic loaded β -cells. Cells were maintained in Krebs's/HEPES buffer at pH 7.4 with $100 \mu\text{M Ca}^{2+}$. Arrows indicate the beginning of application of digitonin solution for 20 s. Data were filtered at low pass filter frequency 33 Hz. Cells were incubated in 1 mM 5-HT containing buffer for 4 h.

CHAPTER 6

CONCLUSIONS AND FUTURE WORK

Amperometry has proven to be a powerful tool for studying chemical secretions from single cells. In this research, the electrode used was a carbon-fiber microelectrode modified with a polynuclear ruthenium oxide/cyanoruthenate film. The chemically modified electrode allowed anodic detection of insulin under physiological conditions with a detection limit of 0.5 μM using flow injection system. A series of randomly occurring current spikes were observed at the modified electrode by amperometry when the electrode was placed next to the cell that had been stimulated with insulin secretagogues glucose, K^+ or tolbutamide. The spikes decreased in height and increased in width as the electrode was pulled away from the cell. Spikes were only observed if a modified electrode was used and its potential was sufficient to oxidize insulin. Chromatographic and flow injection analysis showed that the primary secreted substance detected by the electrode was insulin. The current spikes were strongly dependent on external Ca^{2+} . Spike area were independent of stimulation method although spike frequency and duration change with stimulation conditions. Spike area with the unit of Coulomb, when converted to moles using Faraday's law, corresponded to the amount of insulin expected in a vesicle. Spikes had an area distribution which corresponded to the distribution of vesicle sizes in β -cells. It was concluded that the spikes were due to the

detection of concentration pulses of insulin secreted by exocytosis. This method has been successfully applied to measure insulin secretion from human, rat and dog β -cells (121), and the method allows insulin secreted by single exocytosis events to be detected with millisecond time resolution.

Amperometry at carbon fiber microelectrodes was used to monitor chemical secretions of single rat and dog pancreatic β -cells that had been allowed to accumulate 5-hydroxytryptamine (5-HT). It has been suggested that 5-HT is taken up and stored in insulin-containing vesicles when β -cells are incubated in 5-HT containing media. When insulin secretagogues glucose or tolbutamide were applied to 5-HT loaded β -cells, a series of randomly occurring current spikes were observed. The current spikes were strongly dependent on external Ca^{2+} and had an average area that was independent of the stimulation method. These results suggest that 5-HT is released by exocytosis from the β -cells. The pattern of 5-HT released from loaded cells was similar to that of insulin secretion from unloaded cells measured using a modified microelectrode. The shapes of current spikes were different for the different analytes suggesting a different mechanism of clearance from the vesicles. It was concluded that accumulated 5-HT may be a useful marker for secretory activity of β -cells, but is not a useful substitute for studying the dynamics of insulin clearance from vesicles.

In order to study the mechanism of insulin extrusion, the effect of extracellular pH on insulin secretion by exocytosis was investigated. Insulin is stored in a solid granule as a complex with Zn in secretory vesicles of pancreatic β -cells. In order for insulin to be released, the Zn-insulin complex must dissolve and dissociate. The modified electrodes

do not detect insulin in the presence of excess Zn^{2+} suggesting that they only detect free insulin uncomplexed with Zn^{2+} . With extracellular pH 7.4, insulin secretion was detected as a series of current spikes with width at half-height of 37.1 ± 26.8 ms. At extracellular pH 6.4, no current spikes for insulin were detected. As a control experiment, accumulated 5-HT release from β -cells was measured using a carbon fiber microelectrode. 5-HT release was detected as a series of current spikes (width at half-height 6.99 ± 7.11 ms) regardless of pH. The 5-HT detection results show that vesicle fusion and opening occurs regardless of extracellular pH. It is suggested that 5-HT is stored in loosely-bound form in the vesicles. The effect of pH on insulin detection indicates that exposure of the secretory granule to extracellular pH is required to free insulin from the solid Zn-insulin complex. At a pH 7.4, the dissolution and dissociation of insulin from the granule is rapid, occurring on the time scale of 37 ms. It was concluded that extracellular pH greatly affects the dynamics of insulin secretion. It is suggested that the effect is caused by inhibiting the dissolution and/or dissociation of Zn-insulin complex stored in the secretory vesicles.

Pancreatic β -cells can be permeabilized by digitonin and secretions of insulin and 5-HT were induced by micromolar extracellular Ca^{2+} . The characteristics of current spikes observed are similar to that of spikes caused by stimulus-induced secretion, which suggests that Ca^{2+} -induced secretion from permeabilized cells is also by exocytosis. The extracellular pH change has similar effect on both permeabilized cell and regular cell, even though stimulation mechanisms are different. This further supports the idea that extracellular pH plays a significant role in determining the kinetics of

dissolution/dissociation of insulin storage matrix, i.e. Zn-insulin hexamer precipitate in the vesicle.

This is the first time that insulin secretion has been measured with such high time resolution by directly monitoring chemical release during exocytosis process, which provides a great opportunity for the study of insulin secretion mechanism in detail at single cell level.

It has been successfully established that insulin is the primary substance detected, and the spikes are due to exocytosis. However there are some improvements of the current method needed to allow new aspects of insulin secretion to be studied.

A major limitation to the use of the modified electrode is its lack of stability under physiological conditions. Although the “resting” procedure allows measurements to be made, it is inconvenient and makes long term recordings of secretion impossible. New amperometric electrode needs to be developed for insulin secretion monitoring at longer time. Fast scan voltammetry might be used on a new insulin electrode, which would aid in the identification of the detected compounds by obtaining meaningful voltammograms.

An interesting aspect of the microtechnique for measuring insulin secretion is that it may allow multiple chemical measurements to be made at one cell. Higher spatial resolution could be achieved by using smaller electrodes for the measurements. Multiple ultramicroelectrodes could be used to monitor insulin secretion at different spot on the cell surface in order to examine heterogeneity of release from single cells. In addition, internal Ca^{2+} could be measured with insulin secretion by fluorescence microscopy. The

ability to simultaneously monitor other compounds which are intimately involved in secretion would be valuable in determining their role in secretion.

Another interesting future work is to study insulin secretion from single islets. Compared with single cell detection, the detection of insulin secretion from the single islet will be different in many ways, such as insulin secretion mechanism, the number of insulin molecules can be caught at the electrode surface, and the time for secreted insulin molecules to diffuse to the electrode surface. The study of insulin secretion at single islets is important and interesting because islets are the smallest unit for transplantation.

APPENDIX

SPECIAL PRECAUTIONS IN RAT ISLET ISOLATION AND CELL DISPERSION

Before planing to do islet isolation, four stock solutions are required to be made in advance and kept in refrigerator: 1) 10X Hanks Balanced Salt Solution (HBSS) containing (in mM), 1370 NaCl, 54 KCl, 42 NaH_2PO_4 , 41 KH_2PO_4 , 100 HEPES, adjusting pH to 7.4 by NaOH; 2) 1 M CaCl_2 ; 3) 1 M MgCl_2 (filtered); 4) 100 mM glucose. These solutions are not sterile and can be used for about 2 months.

All the glass bottle and pipets (5 3/4'') have to be autoclaved before the day for dissection. 20 mL siliconized scintillation vial was made by following steps: first, rinse the inside wall of the vial thoroughly with Sigma cote (Sigma, SL-2); then pour off the extra Sigma cote solution for reuse, drain the coated vial on paper towel overnight; finally, autoclave the siliconized vial before use.

For making glass, flamed and siliconized pasteur pipet, the steps are as follows: 1) siliconize the unplugged glass short pipet (5 3/4'' long) by placing 2 pipets into big test tube, pouring Sigma cote solution into the test tube, and totally immersing the pipets, then taking the pipet out, and letting them drain in a big dish with the tip down on the paper towel overnight; 2) flame the tip on bunsen burner in order to smooth the tip opening, not to tear the tissue apart; 3) autoclave pipets before use.

On the day for islet isolation, the first thing to do is to make two 1X HBSS. The first one is 1 L of 1X HBSS with Ca^{2+} containing (in mM), 137 NaCl, 5.4 KCl, 4.2

NaH_2PO_4 , 4.1 KH_2PO_4 , 10 HEPES, 5 glucose, 1 MgCl_2 and 1 CaCl_2 . and the second one is 500 mL 1X HBSS containing no Ca^{2+} , but the other chemical compositions are the same as the first 1X HBSS. Then these two solution are sterilized by filtering through sterile filter unit pack under the sterile hoods. After that, they are kept on ice all the time and bubbled with O_2 through autoclaved gas diffusing stone for 25 min. It seems that rich O_2 in HBSS works better for islet isolation procedure.

After 1X HBSS is made, the collagenase is taken out of the freezer and warmed up to room temperature before weighing. For two rats, usually 50-60 mL collagenase solution are made in a clean beaker by dissolving it in 1X HBSS without Ca^{2+} , and then kept on ice. After that, 23 % Ficol stock solution is made by dissolving 11.5 g Ficol (Sigma, F-9378) in 38.5 g 1X HBSS with Ca^{2+} . Since it usually takes at least an hour for Ficol to dissolve, this solution is needed before sacrificing the rats. During the last three wash steps of islets, the pH of Ficol solution is adjusted to 7.4 by 1-3 drops 0.1 M NaOH. Cautions are needed here for adjusting the pH in order to avoid adding acid to the Ficol solution because Ficol will dissociate in acidic environment. If that happens, the Ficol gradient might not work well for the islet isolation. Each 10g of 21% and 20% Ficol solution is then made by diluting 23% in 1X HBSS with Ca^{2+} .

REFERENCES

- 1) Weir, G. C.; Halban, P. A.; Meda, P.; Wollheim, C. B.; Orci, L.; Renold, A. E. *Metabolism* **1984**, *33*, 447.
- 2) Orci, L.; Vassalli, J. D.; Perrelet, A. *Scientific American* **1988**, *260*, 85.
- 3) Kahn, S. E.; Porte, D. In *Ellenberg and Rifkin's Diabetes Mellitus: Theory and Practice*, 4th ed., Rifkin, H.; Porte, D. Jr. eds., Chpt 26, p463, Elsevier Science Publishing Co., Inc., New York, 1990
- 4) Unger, R. H. *Science* **1991**, *251*, 1200.
- 5) Rajan, A. S.; Aguilar-Bryan, L.; Nelson, D. A.; Yaney, G. C.; Hsu, W. H.; Kunze, D.L.; Boyd A. E. *Diabetes Care* **1990**, *13*, 340.
- 6) MacDonald, M. J. *Diabetes* **1990**, *39*, 1461.
- 7) Robertson, R. P.; Seaquist, E.R.; Walseth, T.F. *Diabetes* **1991**, *40*, 1.
- 8) Volk, B. W.; Wellman, K. F. In *The Diabetic Pancreas*, Volk, B. W.; and Arquilla, E.R. eds., p 117. Plenum, New York and London, 1985.
- 9) Henderson, J. R. *Lancet*, **1969**, *2*, 469.
- 10) Bonner-Weir, S. In *Molecular and Cellular Biology of Diabetes Mellitus*, Drazin, B.; Melmed, S.; LeRoith, D. eds., Volume I, p1, Alan, R. Liss, Inc., New York, 1989.
- 11) Wollheim, C. B.; Meda, P.; Halban, P. A. *Meth. Enzy.* **1990**, *192*, 223.
- 12) Larsson, L.-I.; Sundler, F.; Hakanson, R. *Diabetologia* **1976**, *12*, 211.
- 13) Orci, L.; Unger, H. *Lancet*, **1975**, *2*, 1243.
- 14) Orci, L. In *Insulin and Metabolism*, Bajaj, J. S. eds., Experta Medica, Elsevier Publ., New York, 1977.
- 15) Gold, G. In *Molecular and Cellular Biology of Diabetes Mellitus*, Drazin, B.; Melmed, S.; LeRoith, D. eds., Volume I, p29, Alan, R. Liss, Inc., New York, 1989.

- 16) Orci, L.; Baetens, D.; Ravazzola, M.; Stefan, Y.; Malaisse-Lagae, F. *Life, Sci.* **1976**, *19*, 1811.
- 17) Hollenberg, M. D. ed, *Insulin, Its Receptor and Diabetes*, Marcel Dekker, Inc., New York, 1985.
- 18) Smith, L. *Am. J. Med.* **1966**, *40*, 662.
- 19) Pekar, A. H.; Frank, B. H. *Biochemistry*, **1972**, *11*, 4013.
- 20) Brange, J.; Langkjoer, L. *Pharm. Biotechnol.* **1993**, *5*, 315.
- 21) Blundell, T.; Dodson, G.; Hodgkin, D.; Mercola, D. *Adv. Protein Chem.* **1972**, *26*, 279.
- 22) Fredericq, E. *Arch. Biochem. Biophys.* **1956**, *65*, 218. Bonner-Weir, S.; Orci, L. *Diabetes*, **1982**, *31*, 883.
- 23) Fredericq, E. *Nature*, **1953**, *171*, 570. Gold, G.; Landahl, H. D.; Gishizy, M. L.; Grodsky, G. M. *J. Clin. Invest.* **1982**, *69*, 554.
- 24) Stranzza, S.; Hunter, H.; Walker, E.; Darnall, D. W. *Arch. Biochem. Biophys.* **1985**, *238*, 30.
- 25) Fredericq, E. *J. Am. Chem. Soc.* **1957**, *79*, 599.
- 26) Paker, Y.; Biswas, S. B. *Biochemistry* **1981**, *20*, 4354.
- 27) Jeffery, P. D. *Biochemistry* **1974**, *13*, 4441.
- 28) Carpenter, F.H.; Goldman, J. *Biochemistry* **1974**, *13*, 4566.
- 29) Roy, M.; Lee, R. W. K.; Brange, J.; Dunn, M. F. *J. Biol. Chem.* **1990**, *265*, 5448.
- 30) Gao, J.; Mrksich, M.; Gomez, F. A.; Whitesides, G. M. *Anal. Chem.* **1995**, *67*, 3093.
- 31) Dodson, E. J.; Dodson, G. G.; Hodgkin, D.; Mercola, D. *Can. J. Biochem.* **1979**, *57*, 469.
- 32) Sato, T.; Herman, L.; Fitzgerald, P. J. *Gen. Comp. Endocrinol.* **1966**, *7*, 132.
- 33) Greider, M. H.; Howell, S. L.; Lacy, P.E. *J. Cell Biol.* **1969**, *41*, 162.
- 34) Howell, S. L.; Young, D. A.; Lacy, P.E. *J. Cell Biol.* **1969**, *41*, 167.

- 35) Hazelwood, R. L. In *The Endocrine Pancreas*, Lynch E. eds., p39, Prentice-Hall, Inc., Englewood Cliffs, New Jersey, 1989.
- 36) Orci, L. *Diabetes* **1982**, *31*, 538.
- 37) Orci, L. *Diabetologia* **1985**, *28*, 528.
- 38) Abrahamsson, H.; Gylfe, E. *Acta Physiol. Scand.* **1980**, *109*, 113.
- 39) Hutton, J. C. *Biochem. J.* **1982**, *204*, 171.
- 40) Steiner, D. F.; Kemmler, W.; Clark, J. L.; Oyer, P. E.; Rubenstein, A. H. In *The Biosynthesis of Insulin: Handbook of Physiology*, Section 7, Endocrinology, Vol. 1, p 175, Steiner, D. F.; Freinkel, N. eds., Williams and Wilkins, Baltimore, 1972.
- 41) Oyer, P. E.; Cho, S.; Peterson, J. D.; Steiner, D. F. *J. Biol. Chem.* **1971**, *246*, 1375.
- 42) Leitner, J. W.; Sussman, K. E.; Vatter, A. E.; Schneider, F. H. *Endocrinology* **1975**, *95*, 662.
- 43) Tsumura, Y.; Kobayashi, K.; Yashida, K.; Kagawa, S.; Matsuoka, A. *Endocrinology, Japan*, **1979**, *26*, 245.
- 44) Hutton, J. C. *Diabetologia* **1989**, *32*, 271.
- 45) Howell, S.L. *Diabetologia* **1984**, *26*, 319.
- 46) Bird, J. L.; Wright, E.E.; Feldman, J.M. *Diabetes* **1980**, *29*, 304.
- 47) Sopwith, A. M.; Hansen, F.; Hutton, J. C. *Biochim. Biophys. Acta* **1984**, *803*, 342.
- 48) Hutton, J. C.; Hansen, F.; Peshavaria, M. *FEBS Lett* **1985**, *188*, 336.
- 49) Efendic, S.; Kindmark, H.; Berggren, P.-O. *J. Internal Med.* **1991**, *229*, 9.
- 50) Dean P. M. ; Matthews, C. K. *J. Physiol. (Lond)* **1970**, *210*, 225.
- 51) Atwater, I.; Carroll, P.; Li, M. X. In *Molecular and Cellular Biology of Diabetes Mellitus*, Drazin, B.; Melmed, S.; LeRoith, D. eds., Volume I, p49, Alan, R. Liss, Inc., New York, 1989.
- 52) Boyd III, A. E. *Diabetes* **1988**, *37*, 847.

- 53) Boyd III, A. E.; Rajan, A. S.; Gaines, K. L. In *Molecular and Cellular Biology of Diabetes Mellitus*, Drazin, B.; Melmed, S.; LeRoith, D. eds., Volume I, p93, Alan, R. Liss, Inc., New York, 1989.
- 54) Montague, W. eds. In *Diabetes and the Endocrine Pancreas*, p55, Oxford University Press, New York, 1983.
- 55) Malaisse, W. J.; Malaisse-Lagae, F. *Experientia* **1984**, *40*, 1068.
- 56) Barnett, D. M.; Presel, D. M.; Chern, H. T.; Scharp, D. W.; Misler, S. *J. Membrane Biol.* **1994**, *138*, 113.
- 57) Salomon, D.; Meda, P. *Exp. Cell Res.* **1986**, *162*, 507.
- 58) Bosco D.; Orci, L.; Meda, P. *Exp. Cell Res.* **1989**, *184*, 72.
- 59) Longo, E.A.; Tornheim, K.; Deeney, J. T.; Varnum, B.A.; Tillotson, D.; Prentki, M.; Corkey, B.E. *J. Biol. Chem.* **1991**, *266*, 9314.
- 60) Pralong, W. F.; Bartley, C.; Wollheim, C. B. *EMBO Journal* **1990**, *9*, 53.
- 61) Gillis, K. D.; Pun, R. Y. K.; Misler, S. *Pflugers Arch* **1991**, *418*, 611.
- 62) Gillis, K. D.; Misler, S. *Pflugers Arch* **1992**, *420*, 121.
- 63) Kennedy, R. T.; Oates, M.D.; Cooper, B. R.; Nickerson, B.; Jorgenson, J. W. *Science* **1989**, *246*, 57.
- 64) Kennedy, R. T.; Jorgenson, J. W. *Anal. Chem.* **1989**, *61*, 436.
- 65) Oates, M. D.; Cooper, B. R.; Jorgenson, J. W. *Anal. Chem.* **1990**, *62*, 1573.
- 66) Olefirowicz, T. M.; Ewing, A. G. *Anal. Chem.* **1990**, *62*, 1872.
- 67) Ewing, A. G. *J. Neuroscence Methods* **1993**, *48*, 215.
- 68) Tan, W.; Parpura, V.; Haydon, P.G.; Yeung, E.S. Submitted.
- 69) Millar, J.; Stamford, J.A.; Kruk, Z.L.; Wightman, R. M. *Eur. J. Pharm.* **1985**, *109*, 341.
- 70) Suaud-Chagny, M. F.; Mermet, C.; Gonon, F. J. *Neuroscience* **1990**, *34*, 411.

- 71) Marsden, C.A.; Joseph, M. H.; Kruk, Z. L.; Maidment, N. T.; O'Neill, R.D.; Schenk, J. O.; Stamford, J. A. *Neuroscience* **1988**, *25*, 389.
- 72) Chien, J. B.; Wallingford, R. A.; Ewing, A. G. *J. Neurochem.* **1990**, *54*, 633.
- 73) Lau, Y. Y.; Abe, T.; Ewing, A. G. *Anal. Chem.* **1992**, *64*, 1702.
- 74) Abe, T.; Lau, Y. Y.; Ewing, A. G. *Anal. Chem.* **1992**, *64*, 2160.
- 75) Leszczyszyn, D. J.; Jankowski, J. A.; Viveros, O. H.; Diliberto, E. J.; Near, J. A.; Wightman, R. M. *J. Biol. Chem.* **1990**, *265*, 14736.
- 76) Wightman, R. M.; Jankowski, J. A.; Kennedy, R. T.; Kawagoe, K. T.; Schroeder, T. J.; Leszczyszyn, D. J.; Near, J. A.; Diliberto, E. J.; Viveros, O.H. *Proc. Natl. Acad. Sci. USA* **1991**, *88*, 10754.
- 77) Meulemans, A.; Poulain, B.; Baux, G.; Tauc, L.; Henze, D. *Anal. Chem.* **1986**, *58*, 2088.
- 78) Chow, R.; von Ruden, L.; Neher, E. *Nature* **1992**, *356*, 60.
- 79) Alvarez de Toledo, G.; Fernandez-Chacon, R.; Fernandez, J. M. *Nature* **1993**, *363*, 554.
- 80) Chen, T. K.; Luo, G.; Ewing, A. G. *Anal. Chem.* **1994**, *66*, 3031.
- 81) Leszczyszyn, D. J.; Jankowski, J. A.; Viveros, O.H.; Diliberto, E. J.; Near, J. A.; Wightman, R. M. *J. Neurochem.* **1990**, *56*, 1855.
- 82) Schroeder, T. J.; Jankowski, J. A.; Kawagoe, K. T.; Wightman, R. M. *Anal. Chem.* **1992**, *64*, 3077.
- 83) Zhou, Z.; Misler, S. *Proc. Natl. Acad. Sci. USA* **1995**, *92*, 6938.
- 84) Paras, C.; Kennedy, R. T. *Anal. Chem.* **1995**, in press.
- 85) Faulkner, L. R. *Chem. Eng. News* **1984**, Feb. 27, 28.
- 86) Murray, R. W. *Acc. Chem. Res* **1980**, *13*, 135.
- 87) Heinze, J. *Angew. Chem. Int. Ed. Engl.* **1993**, *32*, 1268.
- 88) Wightman, R. M. *Anal. Chem.* **1981**, *53*, 1125A.

- 89) O'Neill, R. D. *Analyst* **1994**, *119*, 767.
- 90) Stankovich, M. T.; Bard, A. J. *J. Electroanal. Chem.* **1977**, *85*, 173.
- 91) Blundell, T.; Dodson, G.; Hodgkin, D.; Mercola, D.; Anfinsen, C. B.; Edshall, J. T.; Richards, F. M. "Advances in Protein Chemistry", Vol 26, p279, Academic Press, New York, 1972.
- 92) Johnson, D. C.; LaCourse, W. R. *Anal. Chem.* **1990**, *62*, 589A.
- 93) Ngoviwatchai, A.; Johnson, D. C. *Anal. Chim. Acta* **1988**, *215*, 1.
- 94) Polta, T. Z.; Johnson, D. C. *J. Electroanal. Chem.* **1986**, *209*, 159.
- 95) Polta, T. Z.; Johnson, D. C. *J. Electroanal. Chem.* **1986**, *209*, 171.
- 96) Imisides, M. D.; Wallace, G. G.; Wilke Wollongong, E. A.; Australia, N. S. W. *Trends Anal. Chem.* **1988**, *7*, 143.
- 97) Cox, J. A.; Gray, T. J. *Anal. Chem.* **1989**, *61*, 2462.
- 98) Cox, J. A.; Gray, T. J. *Anal. Chem.* **1990**, *62*, 2742.
- 99) Kulesza, P. J. *J. Electroanal. Chem.* **1987**, *220*, 295.
- 100) Pradac, J.; Koryta, J. *J. Electroanal. Chem.* **1968**, *17*, 167.
- 101) Kelly, R. S.; Wightman, R. M. *Anal. Chim. Acta* **1986**, *187*, 79.
- 102) Cox, J. A.; Kulesza, P. J. *Anal. Chem.* **1984**, *56*, 1021.
- 103) Anderson, D. F.; Warren, L. F. *J. Electrochem. Soc.* **1984**, *131*, 347.
- 104) Valtarta, F.; Fesce, R.; Grohovaz, F.; Haimann, C.; Hurlbut, W. P.; Lezzi, N.; Tarelli, F.; Villa, A.; Ceccarelli, B. *Neuroscience* **1990**, *35*, 477.
- 105) Gillis, K. D.; Misler, S. *Pflugers Archiv.* **1992**, *391*, 121.
- 106) Ammala, C.; Eliasson, L.; Bokvist, K.; Larsson, O.; Ashcroft, F. M.; Rorsman, P. *J. Physiol.* **1993**, *472*, 665.
- 107) Kennedy, R. T., Huang, L., Atkinson, M. A., & Dush, P. *Anal. Chem.* **1993**, *65*, 1882.

- 108) Golay, M. In *Gas Chromatography 1958*. Desty, D. H. eds., p.36, Butterworths, London, 1959.
- 109) . St. Claire III, R. L. (1986) Ph.D. Dissertation, University of North Carolina at Chapel Hill.
- 110) Gotoh, M.; Maki, T.; Kiyozumi, T. *Transplantation* **1985**, *40*, 437.
- 111) Kissenger, P. T. *Anal. Chem.* **1977**, *49*, 448A.
- 112) Misler, S., Barnett, D. W., Gillis, K. D., & Pressel, D. M. (1992) *Diabetes* **41**, 1221.
- 113) Engstrom, R. C.; Wightman, R. M.; Kristensen, E. W. *Anal. Chem.* **1988**, *60*, 652.
- 114) Fujita, T.; Kobayashi, S.; Serizawa, Y. In *Proinsulin, Insulin, C-peptide*. Baba, S.; Kaneko, T.; Yanaihara, N., Eds., p327, Excerpta medica, Oxford, 1978.
- 115) Hutton, J. C.; Penn, E. J.; Peshavaria, M. *Biochem. J.* **1983**, *210*, 297.
- 116) Fehman, H. C.; Weber, V.; Goke, R.; Arnold, R. *FEBS Lett.* **1990**, *262*, 279.
- 117) Hellman, B.; Gylfe, E. In *Calcium and Cell Function*, Cheung, W.Y. eds. vol. VI, p253, Academic Press, Orlando, FL, 1986.
- 118) Matthews, E. K.; McKay, D. B.; O'Connor, M. D. L.; Borowitz, J. L. *Biochim. Biophys. Acta* **1982**, *715*, 80.
- 119) Larsson, L.-I.; Sundler, F.; Hakanson, R. *Diabetologia* **1976**, *12*, 211.
- 120) Kalina, M.; Grimelius, L.; Cedermark, B.; Hammel, I. *Virchows Archiv A Pathol Anat* **1989**, *416*, 19.
- 121) Huang, L.; Shen, H.; Atkinson, M. A.; Kennedy, R. T. *Proc. Natl. Acad. Sci. USA*, **1995**, in press.
- 122) Gylfe, E. *J. Endocr.* **1978**, *78*, 239.
- 123) Smith, P.; Duchon, M.; Ashcroft, F. M. *J. Physiol. (London)* **1994**, *475P*, 157P.
- 124) Zhou, Z.; Misler, S. *Soc. Neurosci. Abstracts* **1995**, *4*, 334.
- 125) Falk, B.; Hellman, B. *Experientia* **1963**, *19*, 139.
- 126) Owmen, C.; Hankanson, R.; Sundler, F. *Fed. Proc.* **1973**, *32*, 1785.


- 127) Jaim-Echeverry, G.; Zieher, L. M. *Endocrinology* **1968**, *96*, 662.
- 128) Ekholm, R.; Ericson L. E.; Lundquist, I. *Diabetologia* **1971**, *7*, 339.
- 129) Hellman, B.; Lernmark, A.; Sehlin, J.; Taljedal, I-B *Biochem. Pharmac.* **1972**, *21*, 695.
- 130) Colquhoun, D.; Hawkes, D. In *Single-Channel Recordings*. Sakmann, B.; Neher, E. Eds., p135, Plenum Press, New York. 1983.
- 131) Alvarez de Toledo, G.; Fernandez, J. J. *Gen. Physiol.* **1990**, *95*, 397.
- 132) Lindstrom, P.; Sehlin, J.; Taljedal, I-B. *Br. J. Pharmac.* **1980**, *68*, 773.
- 133) Bird, J. L.; Wright, E. E.; Feldman, J. M. *Diabetes* **1980**, *29*, 304.
- 134) Lundquist, I.; Ahren, B.; Hansson, C.; Hakanson, R. *Pancreas* **1989**, *4*, 662.
- 135) Dean, P. M. *Diabetologia* **1973**, *9*, 115.
- 136) Hutton, J. C.; Peshavaria, M.; Tooke, N. E. *Biochem. J.* **1983**, *210*, 803.
- 137) Telib, M.; Raptis, S.; Schroder, K. E.; Pfeiffer, E. F. *Diabetologia* **1968**, *4*, 253.
- 138) Gagliardino, J. J.; Nierle, C.; Pfeiffer, E. F. *Diabetologia* **1974**, *10*, 411.
- 139) Feldman, J. M.; Lebovitz, H. E. *Diabetes* **1970**, *19*, 475.
- 140) Bekkers, J. M.; Richerson, G. B.; Stevens, C. F. *Proc. Natl. Acad. Sci. USA* **1990**, *87*, 5359.
- 141) Orci, L.; Perrelet, A.; Friend, D. S. *J. Cell Biol.* **1977**, *75*, 23.
- 142) Jankowski, J. A.; Schroeder, T. J.; Ciolkowski, E. L.; Wightman, R. M. *J. Biol. Chem.* **1993**, *268*, 14694.
- 143) Gold, G.; Grodsky, G.M. *Experientia* **1984**, *40*, 1105.
- 144) Hutton, J. C.; Peshavaria, M. *Biochem. J.* **1982**, *204*, 161.
- 145) Figlewicz, D. P.; Formby, B.; Hodgson, A. T.; Schmid, F. G.; Grodsky, G. M. *Diabetes* **1980**, *29*, 767.
- 146) Coore, H. G.; Hellman, B.; Taljedal, I. B. *Biochem. J.* **1969**, *111*, 107.

- 147) Dunn, L. A.; Holz, R. W. *J. Biol. Chem.* **1983**, 258, 4989.
- 148) Jankowski, J. A.; Schroeder, T. J.; Holz, R. W.; Wightman, R. M. *J. Biol. Chem.* **1992**, 267, 18329.
- 149) Colca, J. R.; Wolf, B. A.; Comens, P. G.; Mcdaniel, M. L. *Biochem. J.* **1985**, 228, 529.
- 150) Konrad, R. J.; Young, R. A.; Record, R. D.; Smith, R. M.; Butkerait, P.; Manning, D.; Jaret, L.; Wolf, B. A. *J. Biol. Chem.* **1995**, 270, 12869.
- 151) Grant, P. T.; Coombs, T. L.; Frank, B. H. *Biochem. J.* **1972**, 126, 433.
- 152) Cunningham, L. W.; Fischer, R. L.; Vestling, C. S. *J. Amer. Chem. Soc.* **1955**, 77, 5703.
- 153) Hutton, J. C.; Sener, A.; Herchuelz, A.; Vlaverde, I.; Boschero, A. C.; Malaisse, W. *J. Horm. Metab. Res.* **1980**, 12, 294.
- 154) Ammala, C.; Eliasson, L.; Bokvist, K.; Larsson, O.; Ashcroft, F. M.; Rorsman, P. *J. Physiol.* **1993**, 472, 665.
- 155) Wakasugi, H.; Kimura, T.; Haase, W.; Kribben, A.; Kaufmann, Schulz, I. *J. Membrane Biol.* **1982**, 65, 205.
- 156) Fernandez, J. M.; Villalon, M.; Verdugo, P. *Biophys. J.* **1991**, 59, 1022.
- 157) Jankowski, J.A.; Schroeder, T. J.; Ciolkowski, E. L.; Wightman, R. M. *J. Biol. Chem.* **1993**, 268, 14694.

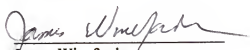
BIOGRAPHICAL SKETCH

Lan Huang was born May 19, 1966, in Niyiang, Jiangsu, P.R. China. She received a Bachelor of Science degree in chemistry from Nanjing University, P.R. China, in 1986. For a period of 3 years, she studied and worked as a research assistant in the Department of Chemistry at Nanjing University. She married Quan Cheng in September 1989. After her husband came to the University of Florida for graduate school in August of 1990, she came here to visit him 4 month later. Then she decided to continue her graduate study in the area of analytical chemistry. In August of 1991, she began her graduate study at the University of Florida Department of Chemistry and studied with Dr. Robert T. Kennedy. During the graduate study, her lovely daughter, Rebecca Cheng, was born in February 20, 1993, in Gainesville. She completed her research and obtained her Doctor of Philosophy degree in December of 1995.

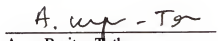
I certify that I have read this study and that in my opinion it conforms to acceptable standards of scholarly presentation and is fully adequate, in scope and quality, as a dissertation for the degree of Doctor of Philosophy.


Robert T. Kennedy, Chairman
Assistant Professor of Chemistry

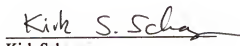
I certify that I have read this study and that in my opinion it conforms to acceptable standards of scholarly presentation and is fully adequate, in scope and quality, as a dissertation for the degree of Doctor of Philosophy.


James Winefordner
Graduate Research Professor of Chemistry


I certify that I have read this study and that in my opinion it conforms to acceptable standards of scholarly presentation and is fully adequate, in scope and quality, as a dissertation for the degree of Doctor of Philosophy.


Anna Brajter-Toth
Associate Professor of Chemistry

I certify that I have read this study and that in my opinion it conforms to acceptable standards of scholarly presentation and is fully adequate, in scope and quality, as a dissertation for the degree of Doctor of Philosophy.


Kirk Schanze
Associate Professor of Chemistry

I certify that I have read this study and that in my opinion it conforms to acceptable standards of scholarly presentation and is fully adequate, in scope and quality, as a dissertation for the degree of Doctor of Philosophy.


Mark Atkinson
Associate Professor of Pathology
and Laboratory Medicine

This dissertation was submitted to the Graduate Faculty of the Department of Chemistry in the College of Liberal Arts and Sciences and to the Graduate School and was accepted as partial fulfillment of the requirements for the degree of Doctor of Philosophy.

December 1995

Dean, Graduate School